



**University of Kerbala**  
**College of Science**  
**Department of Physics**

**Radiological and Toxicological Investigation of Biological  
Samples in Lung Cancer Patients**

A Thesis

Submitted to the Council of the College of Science, University of Kerbala in Partial  
Fulfilment of the Requirements for the Ph.D. Degree in Science of Physics

By

**Furqan Abbas Alwan**

Supervisors

**Prof Dr. Abdalsattar Kareem Hashim**  
**Prof Dr. Shaymaa Awad Kadhim**

**2022 A.D**

**1444 A.H**

بِسْمِ اللَّهِ الرَّحْمَنِ الرَّحِيمِ


أَلَمْ نَشْرَحْ لَكَ صَدْرَكَ ۙ ۝١  
وَوَضَعْنَا عَنكَ وِزْرَكَ ۙ ۝٢  
الَّذِي أَنْقَضَ ظَهْرَكَ ۙ ۝٣  
وَرَفَعْنَا لَكَ ذِكْرَكَ ۙ ۝٤  
فَإِنَّ مَعَ الْعُسْرِ يُسْرًا ۙ ۝٥  
إِنَّ مَعَ الْعُسْرِ يُسْرًا ۙ ۝٦  
فَإِذَا فَرَغْتَ فَانصَبْ ۙ ۝٧  
وَإِلَىٰ رَبِّكَ فَارْغَبْ ۙ ۝٨

صدق الله العلي العظيم

سورة الشرح

## Supervisors Certification

We certify that the preparation of this thesis, entitled “**Radiological and Toxicological Investigation of Biological Samples in Lung Cancer Patients**” was made under our supervision by (**Furqan Abbas Alwan**) at the Department of physics, College of the Science, University of Karbala in partial fulfillment of the requirements of doctor philosophy in Physics.

Signature: 

Name: Dr. Abdalsattar Kareem Hashim

Title: Professor

Address: Department of physics, College of Sciences, University of Kerbala

Date: 11/12/2022

Signature: 

Name: Dr. Shaymaa Awad Kadhim

Title: Professor

Address: Department of physics, College of Sciences, University of Kufa

Date: 20/12/2022

In view of the available recommendations, I forward this thesis for debate by the examining committee.

Signature: 

Name: Dr. Mohammed Abdulhussain Al-kaabi

Title: Assistant Professor

Head of Physics Department, College of Science

Date: 21/12/2022

# Acknowledgment

Sincere emotions and the kindest words radiate from my heart to the individuals responsible for my life's continuation and success. Those who stood with me during difficult times urged me to persevere and not give up. I present the most heartfelt thanks, and gratitude of the heart is overflowing with respect and appreciation to: -

- My supervisors, Prof. Dr. Abdalsattar Kareem Hashim and Prof. Dr. Shaymaa Awad Kadhim, for their efforts and guidance in completing the thesis on time.
- The staff of the Department of Physics who taught me at the undergraduate and postgraduate levels.
- The staff of the Imam Husain Center for Oncology and Hematology in Karbala city, Iraq.
- My family and everybody supported me.
- Dr. Mazin fadhil anad

## ***DEDICATION***

- To my dearest father and mother,
- To my husband
- To my uncles and aunts.
- My brothers and sisters.

I Dedicate to you my humble work.

Furqan



## **Abstract**

Lung cancer LC is one of the most dangerous cancers worldwide. Early diagnosis of the disease contributes to better treatment. Many genetic, environmental, and occupational factors are linked to the incidence of this disease.

The present study aims to use the clinical data of LC patients along with the spectroscopic criteria and biochemical parameters for potential use as diagnostic biomarkers for LC disease. The present study consists of statistical analysis and practical experiments on lung cancer patients.

The patient's medical reports and sera were collected for physical and chemical analysis using various spectroscopic techniques. One hundred and seventy lung cancer patients and 90 healthy subjects participated in the study. The separated sera from all samples were analyzed using various spectroscopic techniques, including Attenuated Total Reflection Fourier Transform Infrared Spectroscopy (ATR-FTIR), Atomic Absorption Spectroscopy (AAS), and solid-state nuclear track detector (SSNTD).

The statistical study results show that the highest value for the Lung cancer prevalence rate was recorded in the Hindia region at 66.16% and the lowest value in the Al-Khairat region at 16.04%. The highest values of all cases were in the city center (51.3%) and the lowest in the Al-Husaniyah region (13.1%). The number of Lung cancer patients has increased to 298, with a rate of 44.04 cases per 100,000 people, which indicates a serious lung cancer situation in Karbala city. FTIR analyses of sera showed that the absorbance of patients with lung cancer is greater than that of healthy people. In addition, it was found that some functional groups were lost from the spectra of patients, in addition to more spectral shifts in patients than the spectra of healthy people, which could be used in the early diagnosis of diseases. AAS spectroscopic results revealed a higher serum zinc than the healthy

females (1247.02 PPb) and the lowest level in the female group of patients (531.54 PPb). Serum copper was higher in the male patient's group (218.59 PPb) and the lowest in the group of healthy females (152.45 PPb). The highest levels of lead are in male patients (13.40 PPb) and the lowest in healthy males (5.38 PPb). Serum cadmium was the highest in female patients (123.74 PPb) and the lowest value recorded in healthy male subjects (14.02 PPb). The results of the SSNTD technique reported that the radiation obtained from the radon gas in the samples was higher in LC patients than in the controls.

The calculated uranium, radium, and radon levels in LC patients were higher than in the control group. From the measured parameters and clinical data results, it can be concluded that spectroscopic methods and biochemical changes in sera may potentially diagnose LC.



## *List of contents*

Chapter One " Introduction and Literature Review"		
	Abstract	II
	List of contents	IV
	List of figures	VIII
	List of tables	XI
	List of abbreviations and symbols	XIII
1.1	Introduction	1
1.2	Lung cancer	2
1.2.1	Symptoms	2
1.2.2	Types of lung cancer	3
1.2.3	Diagnostic of lung cancer	3
1.2.4	Risk factors of lung cancer	4
1.2.5	Treatment	4
1.2.5.1	Radiotherapy	4
1.2.5.2	Chemotherapy	4
1.2.5.3	Immunotherapy	5
1.3	Summary statistic 2020	5
1.4	Trace elements and cancer	6
1.4.1	Cadmium	7
1.4.2	Copper	7
1.4.3	Lead	8
1.4.4	Zinc	8
1.5	Radon	8
1.5.1	Decay of radium-226	9
1.6	Literature review	10
1.7	Objectives of the study	21
Chapter Two " Theoretical Part "		
2.1	Introduction	23
2.2	Blood	23
2.2.1	The circulatory system	24
2.2.2	The respiratory system	24
2.3	Vibrational spectroscopy	25
2.3.1	General principles of fourier transform spectroscopy	27

2.3.2	Attenuated total reflection technology	27
2.4	Atomic absorption spectroscopy	28
2.5	Alpha particle decay	29
2.5.1	Internal exposure to alpha radiation	30
2.5.2	Health effects of alpha radiation	31
2.6	Solid state nuclear track detectors SSNTD	32
2.6.1	Benefits of SSNTD	33
2.6.2	CR-39 detector	34
2.7	The chemical etching	35
2.8	Radon gas	36
2.8.1	Physical and chemical properties of radon	39
2.8.2	The relationship of radon to LC	40
<b>Chapter Three " Experimental Part"</b>		
3.1	Introduction	41
3.2	Study area	42
3.3	Sample preparation	43
3.4	FTIR spectrophotometry	43
3.5	Atomic absorption spectroscopy (AAS)	45
3.5.1	Apparatus	46
3.5.2	Chemical substances	46
3.5.3	Sample digestion	47
3.6	Solid state nuclear track detector CR-39	49
3.6.1	Sodium hydroxide solution (NaOH)	50
3.6.2	Water bath	51
3.6.3	Optical microscope	51
<b>Chapter Four," Results and Discussion"</b>		
4.1	Introduction	53
4.2	Statistical analysis	53
4.3	Result and discussion	54
4.3.1	Statistical treatment of theoretical data	54
4.3.2	Fourier transform infrared spectroscopy (FTIR)	61
4.3.3	Flameless atomic absorption spectroscopy (FAAS)	72
4.3.4	Correlation coefficient	78
4.3.5	Solid state nuclear track detector	84
4.3.6	Correlation between trace elements and uranium concentrations	97
<b>Chapter Five," Conclusion and Recomendations"</b>		

5.1	Conclusions	100
5.2	Recommendations	101
5.3	Future studies	101
References		102

## *List of figures*

<b><i>Chapter One " Introduction and Literature Review"</i></b>		
1.1	The lung cancer	2
1.2	The number of new cases, genders, and ages in 2020	5
1.3	The number of new cases, males, and ages in 2020	6
1.4	The number of new cases, females, and ages in 2020	6
1.5	The radium-226 decay chain	10
<b><i>Chapter Two " Theoretical Part "</i></b>		
2.1	Blood cells under the microscope	24
2.2	Typical stretching and bending vibrational modes	26
2.3	Comparison between infrared transmission spectroscopy and attenuated total reflection	28
2.4	The essential elements of an atomic absorption spectrometer are shown	29
2.5	Alpha-emitters entering the human body	31
2.6	The chemical form of the CR-39 detector	34
<b><i>Chapter Three " Experimental Part "</i></b>		
3.1	A flow chart of the main parts of the current study	41
3.2	Represents a map of Iraq, showing the location of the Tumor center in Karbala governorate	42
3.3	The centrifuge device	43
3.4	A flow chart explains the FTIR procedures	44
3.5	The FTIR device	44
3.6	A flow chart explains the FAAS procedures	45

3.7	Atomic absorption spectroscopy device	46
3.8	Image of the hood for discharging the fumes when preparing the samples	48
3.9	Filtering the samples using filter paper and adding deionized water	48
3.10	A flow chart explains the SSNTD procedures	50
3.11	Represents the water bath	51
3.12	Shows the density of alpha particle tracks at a 400 X optical microscope magnification on the detector surface	52
<b><i>Chapter Four, " Results and Discussion "</i></b>		
4.1	Percentage and prevalence rate for each region in the Karbala governorate between 2012 and 2021	55
4.2	Comparison of the Prevalence rate and the township for lung cancer patients in the Karbala governorate	57
4.3	Lung cancer cases are taken from the Imam Hussein Center in some governorates of Iraq	60
4.4	The relation between prevalence rate and count	61
4.5	Comparison between lung cancer patients (red) and healthy people (blue) by age groups (30-35)	64
4.6	Comparison between lung cancer patients (red) and healthy people (blue) by age groups (35-40).	64
4.7	Comparison between lung cancer patients (red) and healthy people (blue) by age groups (45-50)	65
4.8	Comparison between lung cancer patients (red) and healthy people (blue) by age groups (50-55).	65
4.9	Comparison between lung cancer patients (red) and healthy people (blue) by age groups (60-65)	66

4.10	Comparison between lung cancer patients (red) and healthy people (blue) by age groups (65-70)	66
4.11	Comparison between lung cancer patients (red) and healthy people (blue) by age groups (70-75)	67
4.12	Comparison between lung cancer patients (red) and healthy people (blue) by age groups (75-80)	67
4.13	Comparison between lung cancer patients (red) and healthy people (blue) by age groups (80-85)	68
4.14	Calibration of the atomic absorption system for copper	72
4.15	Calibration of the atomic absorption system for zinc	73
4.16	Calibration of the atomic absorption system for lead	73
4.17	Calibration of the atomic absorption system for cadmium	74
4.18	Comparison of serum concentrations of Zn, Cu, Pb, and Cd among the studied groups for two genders	76
4.19	Serum concentrations of Zinc, Copper for lung cancer patients and health for each group	80
4.20	Serum concentrations of lead, Cadmium for lung cancer patients and health for each group.	81
4.21	Radon concentrations for lung cancer patients and health for the female group	87
4.22	Activity concentration of radium for lung cancer patients and health for the female group	88
4.23	The concentration of uranium of radon concentration for lung cancer patients and health for the female group	89
4.24	The annual effective dose of radon concentration for lung cancer patients and health for the female group	89
4.25	Radon concentrations for lung cancer patients and health for the male group.	92

4.26	The activity concentration of radium for lung cancer patients and health for the male group	92
4.27	The concentration of uranium of radon concentration for lung cancer patients and health for the male group	94
4.28	The annual effective dose of radon concentration for lung cancer patients and health for the male group	94
4.29	The average of radon in air space constriction for lung cancer patients and healthy for two group	95
4.30	The average of uranium constriction for lung cancer patients and healthy for two group	96
4.31	Average uranium concentrations with minerals for health and patient of female	98
4.32	Average uranium concentrations with minerals for health and patients of male	99

## List of table

<b><i>Chapter Three " Experimental Part "</i></b>		
3.1	Concentrations of stock solutions and their commercial sources.	47
<b><i>Chapter Four," Results and Discussion "</i></b>		
4.1	the prevalence rate and the percentage of total cases according to age groups for some townships of Karbala Governorate	55
4.2	Cases of LC according to gender, age groups and prevalence rate for the township of Karbala governorate 2012-2021	56
4.3	Number of lung cancer cases according to the age group for a township in Karbala governorate during 2012-2021	58
4.4	Comparison of the number of cases for age groups between the living and the dead two between 2012 and 2021	59
4.5	Lung cancer cases are taken from the Imam Hussein Center in some governorates of Iraq	59
4.6	Age of lung cancer patients and healthy people	62
4.7	Frequency assignment of FTIR vibrational bands in human serum samples	62
4.8	FTIR spectral intensity ratio parameters results of healthy and lung cancer expressed as mean $\pm$ standard deviation.	70
4.9	The correlation factor between the studied ratios	71
4.10	The descriptive patient information and healthy samples	74
4.11	Comparison of the results of serum zinc, copper, lead, and cadmium between both sexes between healthy and patients groups	75
4.12	Comparison of the results statistically among samples of serum concentrations of zinc, copper, lead, and cadmium for healthy and patients females	77



4.13	Comparison of the results statistically between samples of serum concentrations Zn, Cu, Pb, and Cd for healthy and patients males	77
4.14	Correlation among samples of serum concentrations Zn, Cu, Pb, and Cd minerals in the healthy group	78
4.15	Correlation among samples of serum concentrations Zn, Cu, Pb, and Cd minerals in the LC group	79
4.16	Global comparison among mean serum zinc, copper, lead, and cadmium levels for patients and healthy	82
4.17	Radon, radium, and uranium concentrations in the female group's blood samples health	85
4.18	Radon, radium, and uranium concentration in blood samples patients for the female group	86
4.19	Radon, radium, and uranium concentration in blood samples health for the male group	90
4.20	Radon, radium, and uranium concentration in blood samples patients for the male group	91
4.21	The average radon in air space constriction for lung cancer patients and healthy for two group	94
4.22	The average uranium concentration for lung cancer patients and healthy for two group	95
4.23	Comparison between radon and uranium concentrations for blood samples of the present study with the other studies.	96
4.24	Average uranium concentrations with minerals for health and patient of female	97
4.25	Average uranium concentrations with minerals for health and patient of male	98

### *List of abbreviations and symbols*

<i>Abbreviation</i>	<i>Full phrase</i>
SCC	Squamous cell carcinoma
SCLC	Small-cell lung cancer
NSCLC	Non-small cell lung carcinoma
WHO	World health organization
ICRP	International commission on radiological protection.
IAEA	International atomic energy agency
EPA	United states environmental protection agency
MeV	Million electron volts
SSNTD	Solid state nuclear track detector
NaOH	Sodium hydroxide
Bq	Becquerel
Sv	Sievert
°C	Degree centigrade
K	Calibration factor
ppm	Parts per million
ppb	Parts per billion
L.C	Lung cancer
NF	Normal female
PF	patient female
NM	Normal male
PM	patient male
FTIR	Fourier transform infrared spectroscopy

# **Chapter one**

## **Introduction and Literature**

### **Review**

## Chapter one

### Introduction and Literature Review

#### 1.1 Introduction

Cancer is defined as a broad group of diseases involving uncontrolled cell growth, characterized by uncontrolled cell growth to become immortal, forming malignant tumors, and invading nearby body parts [1]. Cancer is the second leading cause of death worldwide after cardiovascular diseases [2]. Cancer may occur anywhere in the body. Lung cancer affects both men and females in high numbers. Lung cancer is one of the primary cancer diagnoses in the world and the number one cancer-related cause of death [3]. The survival time for LC is poor, with over 90% of patients dying within five years of diagnosis [4]. Finding a reliable approach to early diagnosis of LC is vital because the incidence and mortality of LC remain so high [5]. Lung cancer is divided into small cell LC (SCLC) and non-small cell LC (NSCLC), the latter standing for approximately 80% of all cases of these patients, 65% present in an advanced or metastasized state already at diagnosis, and only 26% have stage I disease and are potential candidates for surgery if fit for that [6]. Spectroscopy is emerging as a potential diagnostic tool in the medical field to provide information about the different chemical and morphological structures of healthy and pathological tissues [6, 7]. Blood is the chief circulatory medium of the human body and reflects the physiological and pathological changes in the tissues, which leads to changes in the various plasma and cellular constituents [7].

## 1.2 lung cancer

Lung cancer is a type of cancer that begins in the lungs, as shown in Figure 1.1. The lungs are two spongy organs in the chest that pull in oxygen and release carbon dioxide when exhaled. Lung cancer is the leading cause of cancer deaths worldwide [8]. People who smoke have an increased risk of LC, although LC can also occur in people who have never smoked. The risk of LC increases with the time you smoke and the number of cigarettes you smoke. If you quit smoking, even after smoking for many years, you can significantly reduce your chances of developing LC [9].

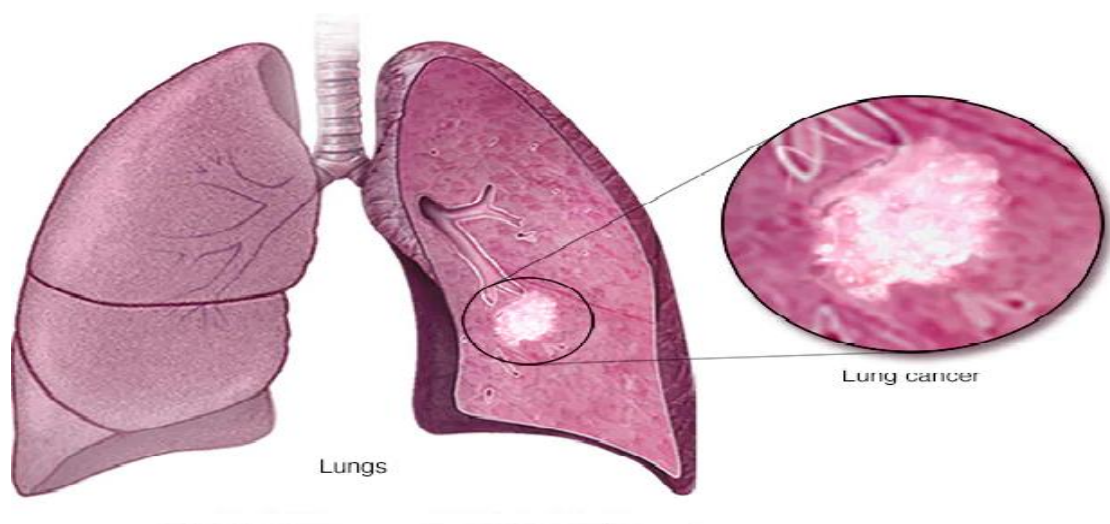


Figure 1.1. Lung cancer [10].

### 1.2.1 Symptoms

Lung cancer usually does not cause signs and symptoms in its early stages. Signs and symptoms of LC usually appear as the disease progresses [11-13]. LC signs and symptoms may include:

- 1- A new cough that does not go away.
- 2- Coughing up blood, even a small amount.
- 3- Shortness of breath.
- 4- Pain in chest.
- 5- Hoarseness.

6- Lose weight without trying.

7- Bone pain.

8- Headache.

### **1.2.2 Types of lung cancer**

Lung cancer divides into two main types based on the appearance of the cancer cells under a microscope.

The two main types of LC are:

A-Small cell LC: Small cell LC occurs almost exclusively in heavy smokers, and this type is less common than non-small cell LC.

B-Non-small cell LC: is an umbrella term for several types of LC, including squamous cell carcinoma, adenocarcinoma, and large cell carcinoma [14].

### **1.2.3 Diagnosis of lung cancer**

The patient is referred to the respiratory medicine clinic, which investigates suspected LC if primary NSCLC is suspected. The investigation's primary goals are to confirm the lesion's malignancy, gauge the disease's degree of dissemination, and coordinate with oncologists and thoracic surgeons to choose the most appropriate course of action [15].

### **1.2.4 Risk factors of lung cancer**

Several factors may increase the risk of developing LC. Some of these risk factors can be controlled; For example, by quitting smoking. However, other uncontrollable factors exist, such as genetic factors [16].

Among the risk factors for LC are:

1- Smoking. The risk of LC increases with the number of cigarettes you smoke daily and the number of years you smoke. However, quitting smoking at any age can greatly reduce your chances of developing LC.

- 2- The chances of developing LC are increased if a subject is exposed to second-hand smoke, even if they are non-smokers.
- 3- The previous radiotherapy increases the higher risk of developing LC.
- 4- The natural breakdown of uranium in soil, water, and rocks results in the production of radon, which eventually finds its way into the air of breath. Any building or home can build up dangerous levels of radon gas.
- 5- The risk of developing LC can increase if the subjects are exposed to asbestos at work and other carcinogens, including arsenic, chromium, and nickel.
- 6- A family history of LC increases the risk of having LC. in the future.

## **1.2.5 Treatment**

### **1.2.5.1 Radiotherapy**

Radiation therapy uses high-energy beams from sources such as X-rays and protons to kill cancer cells. During radiation therapy, patients lie on a table while a machine moves around their body that directs radiation to precise points on the patient's body [17].

### **1.2.5.2 Chemotherapy**

Chemotherapy uses drugs to kill cancer cells. One or more chemotherapy drugs may be given in two ways, either intravenously-through a vein in your arm—or orally or through the mouth. Typically, a combination of drugs is administered in a series of treatments spanning a few weeks or months with intervals in between to allow recovery [18].

### 1.2.5.3 Immunotherapy

The idea behind immunotherapy is to use your immune function to combat cancer. The immune system's ability to fight disease may not be sufficient to fight cancer because cancer cells produce proteins that help them conceal themselves from immune system cells. Patients with locally advanced lung malignancies and tumors that have migrated to other parts of the body are typically the only ones that can benefit from immunotherapy treatments [18].

### 1.3 Summary statistic 2020

The global cancer statistics in 2020 introduced the estimates of incidence and mortality worldwide for 36 cancers in 185 countries [19], where the number of new cases of LC for both genders is 11.4 %, as seen in Figure 1.2.

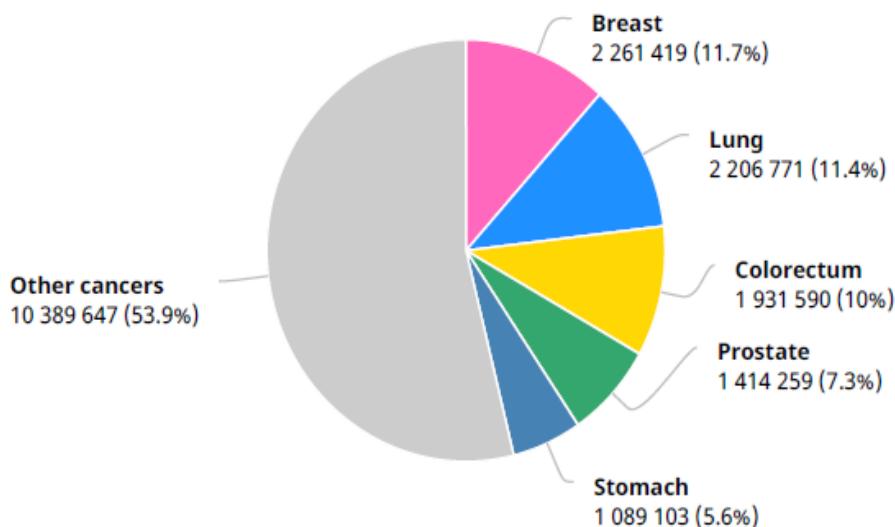


Figure 1.2. The number of new cases in 2020 for both genders, all ages [19].



While the number of new cases of LC in males is 14.3%, as seen in Figure 1.3

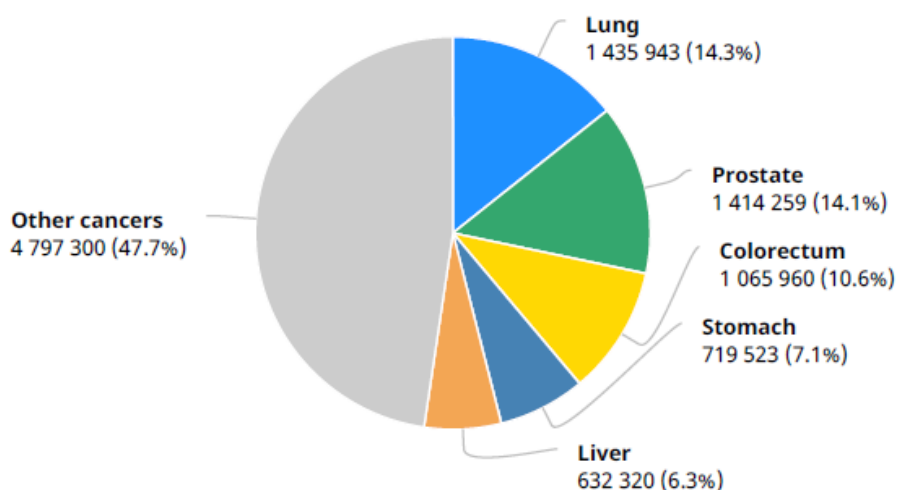


Figure 1.3. The number of new cases in 2020 for males of all ages [19].

While the number of new LC cases in females is 8.4%, as seen in Figure 1.4

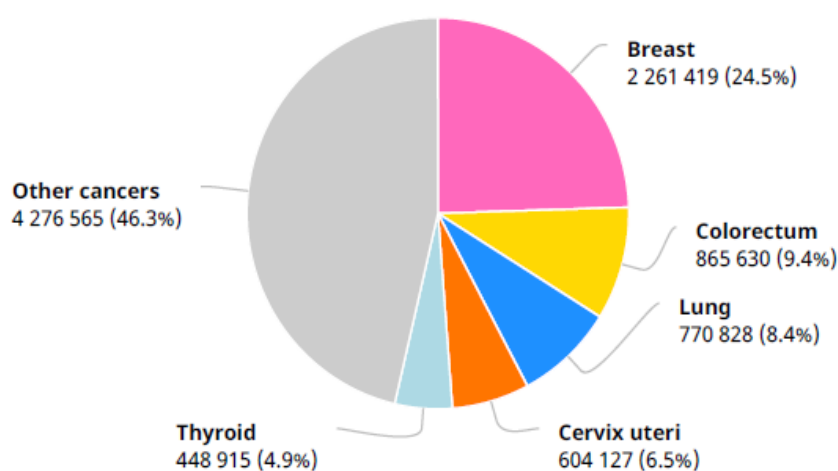


Figure 1.4. The number of new female cases in 2020 at all ages [19].

## 1.4 Trace elements and cancer

There has been a clear interest in recent years in the concentrations of trace elements and heavy metals present in humans and knowing whether the concentration of these elements changes with malignant diseases, i.e., the increase and decrease in the cause much damage such as toxicity [20-25].

The absence of trace elements in an organism causes death or severe malfunction since they are needed in very small amounts for life to continue. The concentration of trace elements in living tissues ranges between 0.01-100 mg/kg [26]. All the essential trace elements can harm humans and animals if they consume much food for a long period [27].

The primary distinction between heavy metals and trace elements is that trace elements are not harmful at low concentrations. Heavy metals are typically toxic at extremely low concentrations. Numerous trace elements are synthesized and deposited in human fluids and tissues, where they can perform various tasks based on their chemical makeup [28, 29]. Cadmium enters the environment due to human activities, especially industrial activities and waste disposal [30]. Here are some of the main functions of some trace elements.

### **1.4.1 Cadmium**

The main source of human exposure to cadmium (Cd) is food, and tobacco smoke is a significant source of cadmium toxicity, causing other problems such as cancer, cardiovascular disease, and hypertension. Cadmium is classified as a human carcinogen. Cadmium toxicity causes other problems such as cancer, cardiovascular disease, and hypertension. Cadmium is classified as a human carcinogen [31].

### **1.4.2 Copper**

Copper, an essential element in the functioning of numerous metalloproteinases and enzymes, depends on the presence of copper, which is also important for the regulation of gene expression and growth, defense, and bone strength. Copper deficiency leads to anemia, low blood cells, leukemia, neurological diseases, osteoporosis, and a disorder of the connective tissues. Excessive copper toxicity is extremely uncommon and typically results from industrial wastewater. It causes gastrointestinal problems. Also, in this case, toxicity can occur in certain diseases, such as Wilson's disease. Wilson reduces

copper excretion through the bile and accumulates in the liver, brain, and kidney [32].

### **1.4.3 Lead**

Lead (Pb) has long been known to be a toxic element. Various human activities cause an increase in lead levels until it reaches humans through food and drinking water. Exposure to lead in large quantities causes kidney failure, encephalopathy, neurophysiological defects, anemia, renal injury, hypertension, blood, and poisoning [33].

### **1.4.4 Zinc**

Zinc is an essential nutrient that is found in all tissues of the human body. A structural component of more than 300 enzymes, it is also necessary to metabolize macromolecules, nucleic acids, and other minerals [34]. Zinc has an important role in gene expression. About 10% of the proteins in the human genome have the potential to bind to zinc. Zinc deficiency is considered rare due to its frequent and near-ideal intake, but zinc deficiency generally affects it. Zinc comes in many forms: health, growth, and reproductive function. It is a disease inherited from zinc deficiency. Pollution results in increased exposure to zinc. The main symptoms of acute poisoning are nausea, vomiting, diarrhea, coma, and fever. Zinc is considered. Copper is mutually exclusive, competing for intestines absorption [35].

## **1.5 Radon**

A radioactive gas that causes cancer is radon-222. Although radon cannot be seen, tasted, or smelled, it may be a concern in your house. You run a greater chance of getting LC if you smoke and have high radon levels in your house [36]. Buildings can become contaminated with radon-222 gas from natural sources, especially in small spaces like basements and attics [37].

Additionally, some spring waters and hot springs contain it [38]. According to epidemiological data, there is a direct link between LC incidence and inhaling radon at high levels. As a result, radon is viewed as a serious contaminant that impacts indoor air quality across the globe. The United States Environmental Protection Agency (EPA) claims that, after smoking cigarettes, radon is the second leading factor in LC.

### **1.5.1 Decay of radium-226**

Radium-226, which naturally occurs in variable amounts in most types of granite and soil, is the source of radon. The decay chart for radium-226 is provided below. It depicts the numerous changes depicted in Figure 1.5. As a result of one by-product itself decaying to another element, which decays further until it eventually reaches a stable element, a chain of products is generated as a radioactive substance decomposes. In this instance, lead is the stable element. Radon-222 is the substance we are interested in that is caused by the decay of radium-226 around halfway down the chain. Due to its nature as a gas that may travel through atmospheric air, radon-222 poses a specific threat [39].

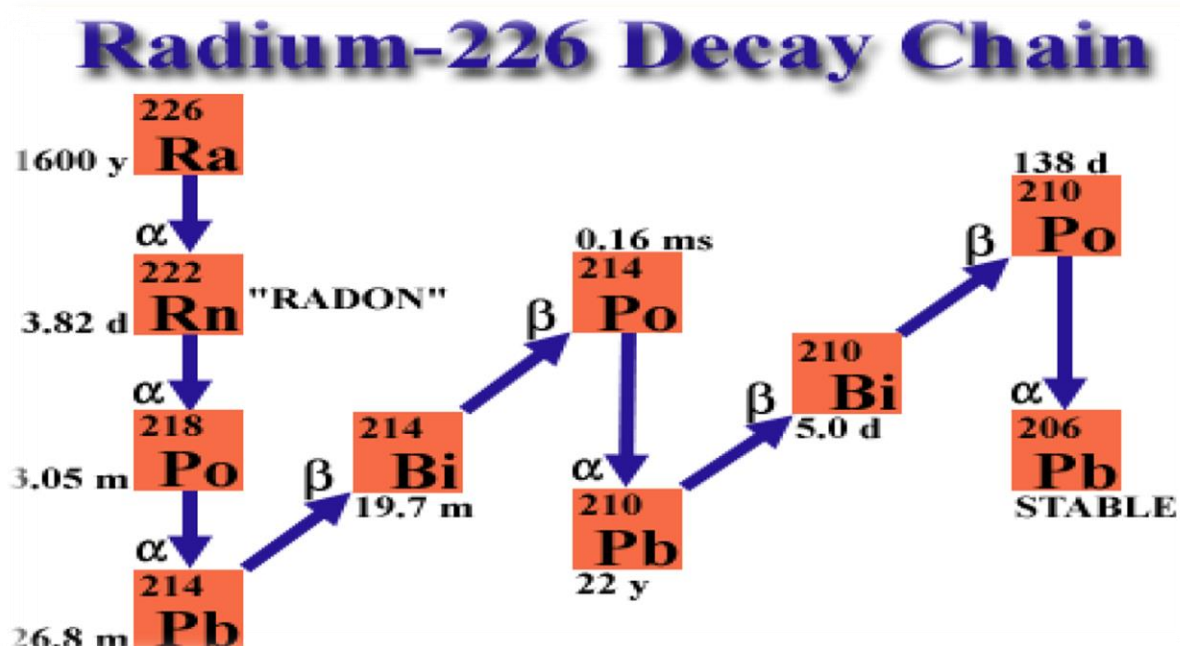


Figure 1.5. The radium-226 decay chain [40].

## 1.6 Literature review

There have been previous studies and research on LC disease. The important studies on this disease are reviewed in the following.

Statistical part				
Sq.	Authors	Ref.	Year	Research method
1.	Maleal et al.	[41]	2014	Investigate epidemiological and serological studies in a sample of Thi-Qar, Basrah, and Missan provinces south of Iraq. The sample blood included 32 patients diagnosed with prostate cancer, using the Minivace technology, where Basrah province recorded the highest percentage (75%) of prostate cancer in comparison with Thi-Qar (15.6%) and (9.3%) in Missan, and the

				results proved that there are significant differences in the distribution of this disease and that the level of prostate-specific antigen increases with age.
2.	Najmaddin et al.	[42]	2015	Evaluate the incidence rates of different types of cancer in Sulaymaleiyah from January 2006 to January 2014. The data were compared with those reported for other middle east countries. The registration of 8031 cases of various types of cancers during the eight years, and the study proved an increase in the annual incidence of cancerous diseases in all age groups from 38 to 61.7 cases per 100,000. In males, several types of cancers were diagnosed: lung, prostate, bladder, colon, and rectum.
3.	Ali et al.	[43]	2017	They investigated for cancers in an Iraqi city. This study included 12,000 samples of blood of patients suspected of having cancer in Karbala city, Iraq, between 2008 and 2015. Of these, 838 confirmed samples were studied, including 518 females and 320 males. In males, high prevalence and incidence rates were observed for bladder, gastro-oesophageal, colorectal, lymphoma, and prostate cancers. It was noted that most

				cancer cases were in the older age groups. The study also proved bladder cancer in males.
4.	Osmale et al.	[44]	2018	Evaluated prostate cancer studies from around the world and investigated the causes of differences among them. Prostate cancer incidence and mortality rates showed significant discrepancies between countries and ethnicities. Through the PSA test in blood samples, it was found that prostate cancer was more prevalent among men.
5.	Mary et al.	[45]	2019	Determine the underlying cause of death among Danish men with prostate cancer. The study included 15878 patients diagnosed with prostate cancer, where five categories of deaths were identified: 1) due to prostate cancer, 2) due to other cancers. 3) due to urinary tract cancer. 4) as a result of vascular cancer 5) Other possible causes of death. About 51.2% of deaths were due to prostate cancer, 17.0% to cardiovascular disease, and 16.7% to other causes. More than half of the deceased men in this study cohort died of their prostate cancer disease within a mean of 2.4 years of follow-up, and this death rate is likely to be overstated.

6.	Rafid et al.	[46]	2020	<p>This study aimed to report the incidence and pattern of various cancers and their distribution across various demographic groups in Basra, Iraq. The study included 2,163 cancer cases for adult males, females, and children. A total of 2,163 cancer cases were identified, of which 2,020 were in adults (93.4%), and 143 were in children (6.6%). Among adults, most cancers were found in females (59%). Patients' mean age at diagnosis was <math>51.4 \pm 19.6</math> years for adults and <math>6.4 \pm 4.23</math> years for children. Cancer incidence rates per 100,000 people increased with age. Breast cancer was the most frequently found in adult females, with an incidence rate of 60.64 per 100,000 people. The most common types of cancer found in adult males were urinary bladder, lung, and bronchus; leukemia was the most common cancer in children. The incidence of cancer per 100,000 people increased with age. This information will help healthcare providers to respond adequately to the demands of diagnosis, treatment, and palliative care for such patients.</p>
7.	Karwan et al.	[47]	2021	<p>This study assesses epidemiological estimates of cancer incidence and the projection of future cancer trends in the</p>



				<p>upcoming decade by analyzing the population-based cancer registry from 2013 to 2019 in both the Erbil and Duhok governorates. The total number of female cancer patients was higher in both governorates, and the total number of patients doubled from 2013 to 2019 in Erbil and Dohuk. Data analysis indicates an increased percentage of cancer patients from 2020 (107.4%) to 234.3% in 2030 in the Erbil governorate and from 106% to 163% in the Duhok governorate. Breast and LC in females have been ranked as one of the most common cancers in Erbil and Dohuk governorates since 2013.</p>
8.	Sylvia et al.	[48]	2022	<p>The relationship between smoking and body mass and their association with prostate cancer. The study involved 351,448 men with information on smoking at the time of diagnosis of prostate cancer. Smoking was associated with a lower risk of any PCa (HR 0.89, 95% CI 0.86–0.92), which was most pronounced for low-risk PCa (HR 0.74, 95% CI 0.69–0.79) and was restricted to PCa cases diagnosed in the prostate-specific antigen (PSA) era. Smoking was associated with a higher risk of PCa death in the full cohort (HR 1.10,</p>

				95% CI 1.02–1.18). Smokers have a higher risk of dying from prostate cancer, which further increases with obesity.
<b>FTIR Spectrophotometry</b>				
<b>9.</b>	Paul et al.	[4]	2010	They evaluated Fourier transform infrared spectroscopy (FTIR) as a high throughput and cost-effective method for identifying biochemical changes in sputum as biomarkers for detecting LC. The results showed that FTIR applied to sputum might have high sensitivity and specificity in diagnosing LC with the potential as a non-invasive, cost-effective, and high-throughput method for screening
<b>10.</b>	Xiaoliang et al.	[49]	2013	Examining reduced total reflection Fourier transform infrared FTIR spectroscopy could be a diagnostic tool for distinguishing malignant and non-malignant lungs. These measurements were made using FTIR on lung tissue samples from 30 people who had a pulmonary lobectomy. Sixty lung tissue samples were collected for FTIR spectroscopy. Before making a histologic diagnosis, samples were analyzed using FTIR spectroscopy. Each absorbent band's peaks, intensities, and full width at half maximum were measured, and relative

				intensity ratios were computed. Malignant and non-malignant tissues were separated using canonical discriminant analysis. According to the data, twenty-two indicators were substantially different between the malignant and non-malignant groups. In order to create discriminant functions, three independent factors—peak intensity at 1546 cm/s, intensity ratio at 1120 cm/s, and full width at half maximum at 1303 and 1240 cm/s were used. All discriminants had a sensitivity and specificity of 96.7%.
<b>11.</b>	Xin et al.	[5]	2014	compared serum from healthy people and those with LC using FTIR spectroscopy, the serum of patients and healthy individuals were compared using FTIR spectroscopy since serum might represent physiological and pathological changes in the human body. The ( $A_1/A_{11}$ ) ratio may help separate LC patients' serum from the serum of healthy individuals. Additionally, the curve-fitting results showed that serum from LC patients had lower $\alpha$ -helix/ $\beta$ -sheet ratios than serum from healthy individuals. These findings suggested that the serum IR spectrum might help identify LC

12.	Julian et al.	[50]	2016	The infrared spectroscopic blood test was used for non-small cell lung carcinoma and subtyped as pulmonary squamous cell carcinoma or Adenocarcinoma. A study was conducted on 161 patients with early cancer suspicion to identify and verify spectral biomarker candidate patterns for detecting non-small cell lung carcinoma (NSCLC). The FTIR spectra of blood samples revealed marker patterns for distinguishing cancer patients from clinically relevant disease control patients.
<b>Atomic Absorption Spectrophotometry</b>				
13.	Ufuk et al.	[51]	2010	measured serum levels of copper (Cu), lead (Pb), zinc (Zn), iron (Fe), cobalt (Co), cadmium (Cd), manganese (Mn), and magnesium in (LC) patients to assess the relationship between specific mineral, trace element, and heavy metal levels in these individuals (Mg). The findings suggested that patients with (LC) may be affected by these minerals
14.	Katarzyna et al.	[52]	2018	They stated that their goals were to analyze the correlations between serum and whole blood Cu and Zn levels and clinical, socioeconomic variables, and nutritional data, as well as to look into the link between

				Cu and Zn status and all-cause mortality in LC. Higher serum Cu levels, Cu/Zn ratios, and whole blood Zn levels were shown to be associated with a lower risk of death in LC patients
15.	Sookyung et al.	[53]	2019	They studied the prognostic value of ferritin to hemoglobin ratio in patients with advanced non-small cell LC. They found the ferritin to hemoglobin ratio, a potential parameter of tumor progression, was a significant prognostic factor for OS, with a direct correlation to survival time in patients with advanced NSCLC
16.	Katarzyna et al.	[54]	2021	They used atomic absorption spectrometry status to evaluate the disturbances in serum and whole blood Cu and Zn to assess the relationships between serum and whole blood Cu and Zn status, and clinical, sociodemographic, and nutritional data to investigate the association of Cu and Zn status with all-cause mortality in LC. Outcomes of a higher serum Cu level, Cu/Zn ratio, and whole blood Zn level were shown to affect all-cause mortality risk in LC patients negatively
17.	Atiyah et al.	[55]	2022	This study aimed to compare the concentrations of trace elements (Cu, Zn,

				<p>Ni) in females with breast cancer and LC and healthy females. Findings Serum Cu levels in females with LC and healthy females were significantly lower than in females with breast cancer. Furthermore, serum Cu levels in females with LC were significantly lower than in healthy females (<math>p &lt; 0.05</math>). The healthy female had the highest levels of zinc and nickel compared to the groups of a female with breast cancer and LC. Moreover, serum zinc and nickel levels were significantly higher in females with LC than in females with breast cancer. Conclusion Serum concentrations of trace elements increase in some groups and decrease in others, and there is a link between some elements that can be used as a means of early detection</p>
<b>Solid-state nuclear track detector</b>				
18.	Ansam et al.	[56]	2019	<p>measured the concentrations of Alpha particles in Blood samples of Leukemia patients in Babylon governorate Iraq by using a CR-39 nuclear track detector. The results showed that the blood sample for the leukemia patient in the city center had the highest amounts at <math>13.98 \pm 0.94 \text{ Bq/m}^3</math>. The lowest concentration, <math>5.24 \pm 0.54 \text{ Bq/m}^3</math>,</p>

				was found in Al-Mudhatia, while the average value was $7.79 \pm 0.51$ Bq/m <sup>3</sup> . The concentration of alpha particles released by radon, on the other hand, was higher in male blood samples than in female blood samples
19.	Fatima et al.	[57]	2020	measured the concentrations of radium and Uranium in blood samples of LC patients by using a CR-39 nuclear track detector in Iraq. The concentrations ranged between (0.1592 Bq / kg to 3.2278 Bq / kg) and (5.5671-112.8615 ppm)
20.	Tabarak et al.	[58]	2021	They collected serum samples from people with LC and healthy people in Babil Province. In these samples, alpha particle concentrations are measured using the CR-39 detector. The results indicated that people with LC had a higher concentration of alpha particles than healthy subjects, with mean concentrations of 19.223 and 1.789, respectively. Moreover, the result found that females had relatively higher radon gas concentrations compared to males, considering all measured samples (patients and healthy subjects)
21.	Rasha et al.	[59]	2022	this study was conducted on women with breast cancer to evaluate the Uranium

				<p>concentrations in their blood. The study aims to assess the concentration of uranium in the blood of Iraqi breast cancer women to establish reference values for the levels of toxic uranium in their blood and the possibility of getting breast cancer. The outcomes show elevated levels of uranium concentration in the blood of women with breast cancer, which was found to be <math>92 \pm 0.6 \text{ ngL}^{-1}</math> compared to the control group (<math>40 \pm 0.4 \text{ ngL}^{-1}</math>) and internationally published data. The results show that the uranium concentration in the blood of breast cancer women is higher than those in the control group and some of the globally published data.</p>
--	--	--	--	--

### 1.7 Objectives of the study

1. The present research will study LC in physical ways, such as infrared, atomic spectroscopy, and CR-39 NTD, to obtain a result that would be useful for the early detection of this disease.
2. The study also aimed to conduct a statistical study on LC cases to determine the number of cases in Karbala governorate, Iraq, and the regions with the highest prevalence of this disease in the governorate, during the past ten years.



3. The spectra obtained using the FTIR technique for absorbing the serum of LC patients will be used for comparing them with the serum of healthy people to obtain indicators that help us in early diagnosis.
4. Choosing a group of effect elements related to LC and measuring their concentrations using Flameless Atomic Absorption Spectroscopy (FAAS) in patients and comparing them with the control groups for both genders to find out the mechanism of the association between the decrease and increase of these concentrations and its effect on the occurrence or non-occurrence of this disease.
5. Also, to demonstrate whether the relationship between the radon and uranium concentration with the occurrence of LC is found.
6. Identify the relationship between the studied trace elements and uranium concentration, and search whether it behaves positively or revers.

# ***Chapter Two***

## ***Theoretical Part***

## Chapter Two

### Theoretical Part

#### 2.1 Introduction

This chapter includes descriptions of the background related to this study, such as the physical concepts and mathematical relationships.

#### 2.2 Blood

The transmission of radioactive elements inside the human body depends on our understanding of human physiology. The human body is made up of a variety of systems and organs in general. Each of them has a distinct purpose. The circulatory system pumps and distributes blood to the body; the respiratory system supplies oxygen to the body. Furthermore, the digestive system, which breaks down and absorbs food, is the three most crucial for understanding how radioactive material is distributed in the human body [60]. Blood is a unique form of connective tissue; it consists of three major cell types: erythrocytes (red blood cells), leukocytes (white blood cells), and platelets [61], as shown in Figure 2.1). Blood cells transport gases, nutrients, waste products, hormones, antibodies, chemicals, ions, and other substances in the plasma to and from different cells in the body [60]. The left pump of the heart pumps blood through the arteries into all body tissues. When the blood passes through the capillaries, an exchange occurs during which the oxygen and food transfer to the cells. The right pump of the heart pumps the blood through the pulmonary artery to the lungs, where the blood is oxidized and returned to the heart [60].

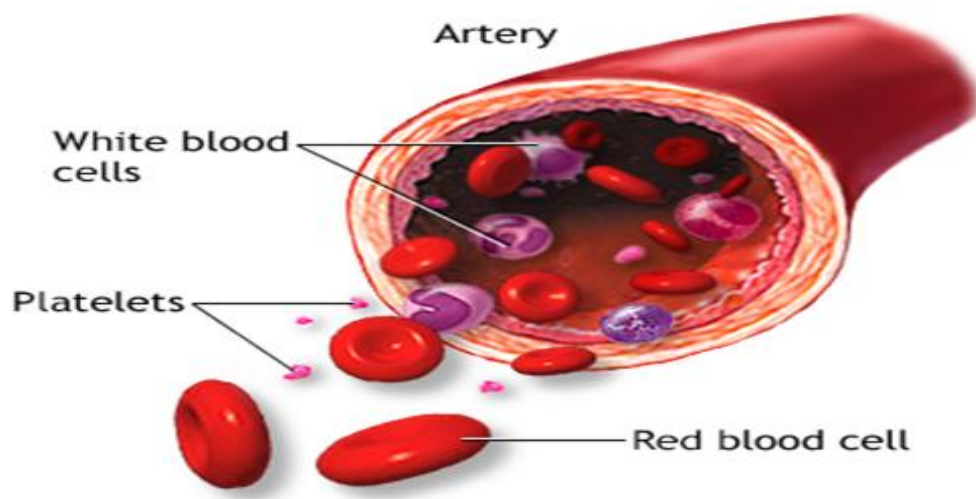


Figure 2.1. Blood cells under the microscope [60].

### 2.2.1 The circulatory system

The circulatory system, which consists of a closed loop of pipes, transports blood from the heart to every area of the body before returning to the heart. There is not only one blood circulatory system in the human body, but two are connected: The systemic circulation provides organs, tissues, and cells with blood to get oxygen and other vital substances. Pulmonary circulation is where the fresh oxygen we breathe enters the blood. At the same time, carbon dioxide is released from the blood [62, 63].

### 2.2.2 The respiratory system

When blood flows through the capillaries close to the alveoli, where oxygen is received to burn food and supply the cells, breathing occurs in the lungs [60]. The person inhales various chemicals, such as gas or airborne dust. If these compounds are gases, they enter the blood at variable rates with the air, depending on how quickly the blood is melting [64]. If these materials were in the form of dust, some of them would be inhaled, and some would be expelled [60]. The rate of melting determines how precipitants behave in the lungs. If they are quickly soluble, they are

absorbed quickly and flow with the blood. They could remain attached to the lungs for several months if they take a long time to dissolve. One of the primary entry points for radioactive elements into the body and the distribution of blood to various body organs is the respiratory system.

### **2.3 Vibrational spectroscopy**

Serum samples can interact with light in various ways, including absorption, scattering, and reflection. When a substance absorbs IR radiation, the chemical bonds begin to vibrate. Therefore, for infrared absorbance to occur, chemical bonds must be present. When the distance between two or more atoms within a molecule changes, a molecule will absorb energy. The vibrational energy is this [65]. Stretching and bending are the two atomic oscillations corresponding to the regular vibration modes. Stretching is a repetitive movement along the bond axis that might be symmetric or antisymmetric. The bending vibration happens when a group of atoms moves differently from the rest of the molecule or when the bond angle between two atoms changes. The terms "scissoring," "wagging," "rocking," and "twisting" refer to these movements. The modalities of stretching and bending are depicted in Figure 2.2. The molecule absorbs infrared energy in a specific manner [66]. The energy of the radiation should be the same as a transition between one of the discrete energy levels of the molecule.

Furthermore, the dipole moment should change. For instance, no infrared radiation is absorbed when two oxygen atoms in carbon dioxide move symmetrically in or out because the dipole moment remains constant. Therefore, the symmetric stretch is passive in the infrared [67].

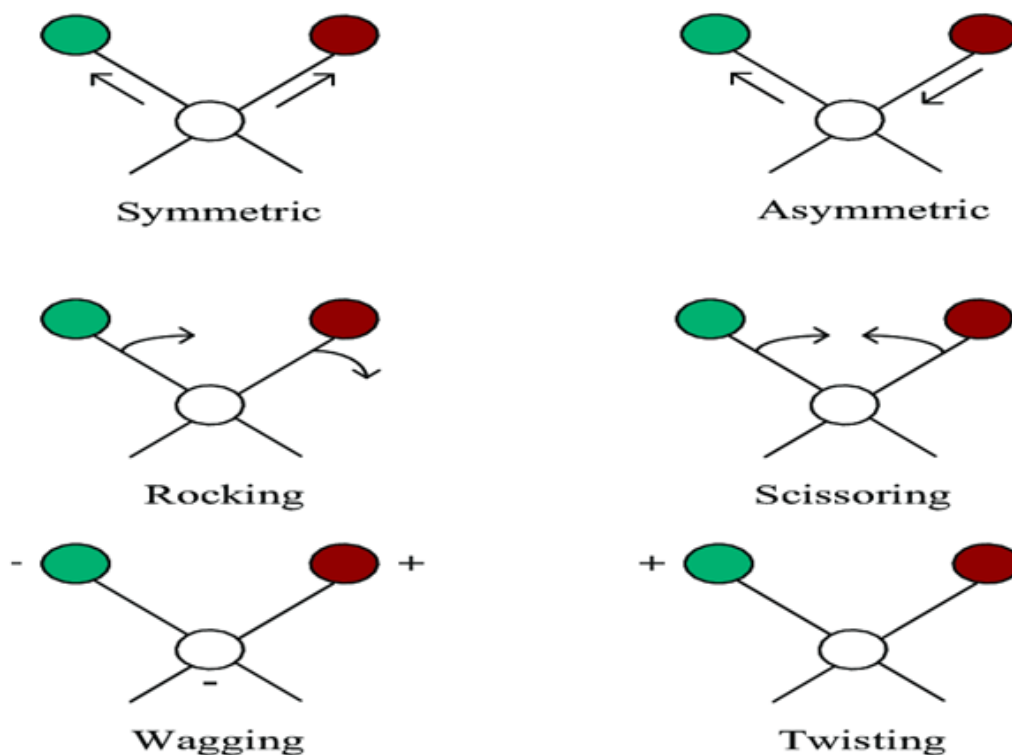


Figure 2.2. Typical stretching and bending vibrational modes [68].

However, when the oxygen both moves left or right, the antisymmetric stretch changes the dipole moment, and infrared radiation is absorbed in  $2350\text{ cm}^{-1}$ . The vibration of the diatomic molecule can be considered as two masses connected by a massless spring, which obeys Hooke's law. The displacement of the two atoms from the center of mass is given by [69].

$$\frac{\mu(d^2R)}{dt^2} = -KR \quad (2.1)$$

where  $\mu$  is the reduced mass and  $R$  is the total distance between the two atoms

$$\mu = \left( \frac{m_1 m_2}{m_1 + m_2} \right) \quad (2.2)$$

The energy levels are demonstrated via a quantum mechanical analysis to be supplied by

$$E_{vib} = hv (n + 1) \quad (2.3)$$

Where  $n$  is the principle quantum number, which can only have positive integer values, and  $h$  is Plank's constant. The energy difference between the molecules must be equivalent to the energy of the photon in order for them to absorb a photon and be stimulated to a higher vibrational state. This criterion might be met if the quantum number shifts by a factor of 1. The selection rule for molecular vibration refers to this circumstance.

### 2.3.1 General principles of Fourier transform spectroscopy

Infrared spectroscopy is a relatively old analytical technique with many applications. This technique is based on the vibrations of the atoms of a molecule. Every atom within a molecule oscillates around an equilibrium position, leading to induction changes in bond length and angle [70]. The range of the infrared region goes from 10 to about 10 000  $\text{cm}^{-1}$ . The IR window can be divided into three regions: near, mid, and far-infrared. In most infrared spectroscopic analyses, the mid-infrared region (4000-400  $\text{cm}^{-1}$ ) is used, especially on biological samples, as it fits the vibrational and rotational frequencies of organic molecules characterizing these samples [71].

### 2.3.2 Attenuated total reflection technology

In Attenuated total reflection (ATR), the IR radiation is directed into the ATR crystal containing a high refractive index medium (germanium, diamond), called an internal reflection element (IRE). Depending on its length, several internal reflections occur within the ATR crystal until the beam reaches the detector. The absorption comes from the interaction

between the sample and the electric part of the evanescent wave created by the internal reflections and present at the crystal sample interface [72].

The absorption arises if the sample is in intimate contact with the IRE. The evanescent wave is characterized by its amplitude, which falls exponentially with the distance to the interface. Compared with the transmission mode, it avoids any problem of signal saturation (deviation of the Beer-Lambert law) related to the thickness of the sample [73]. The Comparison between Transmission Infrared Spectroscopy and Attenuated Total Reflection ATR is represented in Figure 2.3.

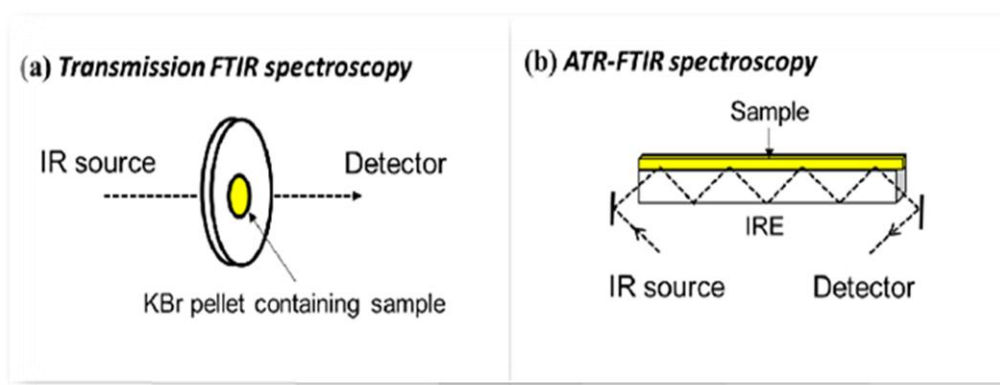


Figure 2.3. Comparison between infrared transmission spectroscopy and attenuated total reflection [74].

Coupling infrared spectroscopy with microscopy has led to the developing of a new technology called infrared micro-spectroscopy. It combines the high spatial resolution obtained by microscopy and the chemical data from IR spectroscopy [75, 76].

## 2.4 Atomic absorption spectroscopy

The fuel-oxidant flow, the flame, the lamp, which is either an HCL or an EDL, the sample in liquid form, the monochromatic, the amplifier, and the detector, as well as the readout device—which is typically a computer with software—are the fundamental requirements for flame



atomic absorption spectroscopy analysis [77]. The main parts of the AAS apparatus are shown in Figure (2.4).

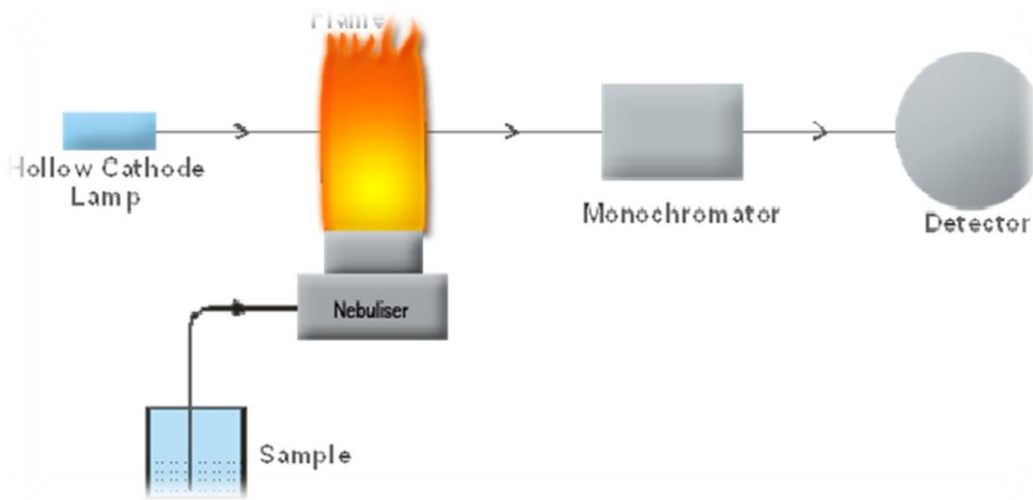


Figure 2.4. The essential elements of an atomic absorption spectrometer are shown [78].

The lamp functions as a radiation source by emitting the analytical element's distinctive sharp line spectra. The radiation source's emission beam is then modified, and the modulated signal travels through the atomic vapor, where the analyte atoms absorb radiation. The monochromator then chooses the appropriate spectral line, allowing the isolated analytic lines to fall onto the detector and provide the electric signal- a conversion of the light signal from that line. A selective amplifier amplifies the signal, and a computer or other readout device records the signal [79].

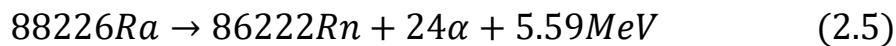
## 2.5 Alpha particle decay

Alpha decay consists of a nucleus with a high  $Z$  and mass number, which may emit two neutrons and two protons. The alpha particles helium-4 nuclei are positively charged. They have low penetrating power, and a piece of paper can stop alpha particles. Heavy nuclei can undergo

radioactive decay, known as alpha decay. The emission of alpha particles in heavy radionuclides results in two protons and two neutrons, out of which, in the process, energy is released [80].



An example is the alpha decay of  $^{226}\text{Ra}$  to the ground state of  $^{222}\text{Rn}$



### 2.5.1 Internal exposure to alpha radiation

In this section, we will show how the internal exposure of alpha particles occurs within the human body and how it reaches the blood. After that, we will discuss the sources of the emission of alpha particles and the physiology of the human body. Generally, explain radioactive materials' entry and transmission within the human body. Alpha-emitters such as U and Ra enter the organs across the gastrointestinal and respiratory systems through the food we consume, the water we drink, the air we breathe, and ingestion [60], as shown in Figure 2.5. These radioisotopes behave chemically and physiologically like calcium when we breathe in the radiation emitters; some are exhaled, while others remain in our lungs and go through the blood to the bone marrow.

If these minute amounts are taken through the mouth, they concentrate mostly on the kidney, bones, and liver. The food is digested before entering the bloodstream and moving to the body's organs. These minutes are stored inside the human body and emit low-level radiation radiated for a very long period, stimulating the bone marrow cells [81] and spreading cancer-related diseases. Radiation exposure and cancer

development have been linked in numerous studies [82, 83]. A few of these investigated related cancers, such as LC.

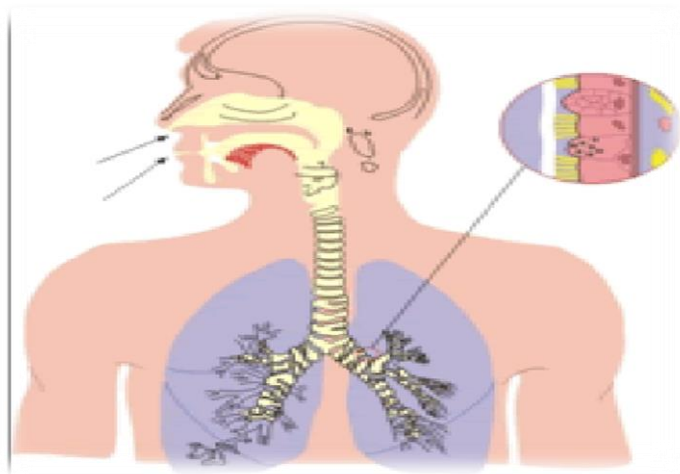


Figure 2.5. Alpha-emitters entering the human body [84].

## 2.5.2 Health effects of alpha particle

The health concerns associated with alpha particles depend on how they are exposed. Because alpha particles cannot penetrate the outer, dead layer of skin, external radiation often has less impact than internal exposure [85]. The radionuclides that generate alpha particles are extremely hazardous if consumed or inhaled because they release much energy quickly within living tissue[86]. Due to their size, the elements that produce alpha particles most frequently are uranium and radon. These slow-moving elements interact with atoms to ionize and excite them. Since collisions with the electrons that make up atoms and molecules result in ionizations, alpha particles rapidly lose energy when passing through a material. Alpha particles have an initial energy that ranges from 3 to 8 MeV [87]. There is less risk if the particle source is external to the body than if it is internal to the body, where all the energy is stored. Alpha particles are taken into the bloodstream when ingested and inhaled; in this situation, an

alpha particle may result in LC [85]. Alpha particle producing substances are among the most hazardous internal hazard sources for the reasons listed

1. Alpha particle levels in the human body are minimal; they do not surpass a few parts per millimeter.
2. The ability of alpha particles to ionize is high.
3. They boost this ionization's relative biological impact.
4. The span of all radioactive sources is their half-life for alpha.
5. It is challenging to remove the isotopes from the human body.

Finally, because alpha particles are biologically harmful, they are not used in vivo diagnostic research [88].

## **2.6 Solid-state nuclear track detectors SSNTD**

Solid-state detectors are used for accurate measurements of radiation energy. Although solid-state detectors are based on ionization, they are very different from ionization chambers, proportional counters, and Geiger counters. SSNTD is crucial for radon gas environmental detection and uranium exploration research. SSNTD is sensitive to alpha. However, SSNTDs are largely insensitive to beta and gamma rays. In other words, beta and gamma rays do not produce etchable individual tracks. The SSNTD also has the advantage of being mostly unaffected by humidity, low temperatures, moderate heating, and light. They, of course, do not require an energy source to be operated since their detecting property is an intrinsic quality of the material they are made of [89]. Such insulating substances produce a tiny damage trail along their path when a severely ionizing charged particle travels through them that is around 50 Å in diameter. Since it cannot be seen with the naked eye, this is known as a "Latent Track." With an electron microscope, this latent track can be seen. The precise type of physical and chemical alterations that take place at the

---

---

damage site depends on the particle's charge ( $Z$ ), velocity ( $v = v/c$ , where  $v$  is the particle velocity and  $c$  is the velocity of light), chemical makeup of the detector material, as well as external factors like temperature and pressure. Etching can be used to develop and extend these latent tracks so they can be seen under an optical microscope [90]. There are two types of SSNTD:

1. Organic detectors (polymers such CN-85, LR-115, CR-39, Lexan, Mikrofol, etc.).
2. Inorganic detectors (glasses or crystals).

### 2.6.1 Benefits of SSNTD

The key benefits of SSNTD are as follows [91]:

1. Relatively affordable.
2. They are insensitive to beta, gamma, and X-ray radiation but sensitive to radiation with high linear energy transfer (LET).
3. Developmental simplicity (there is no need for a dark room). In plain daylight, visible tracks are etched and created in polymers, mineral crystals, and glasses using specific chemicals (such as NaOH).
4. They provide a cumulative record over time and are integration devices.
5. Tracks left behind in meteorites, and geological materials from other planets can last for billions of years or longer.
6. Unlike electronic detectors like ionization chambers, they are passive and do not require power supplies.
7. Alpha particles and other lesser charged particles, such as fission fragments, can be differentiated from heavy charged particles.

8. They are small and durable and thus can be used in homes for indoor radon measurements.

### 2.6.2 CR-39 detector

CR-39 is a clear, stable plastic sensitive to the tracks of energetic protons, alpha particles, and heavier nuclei. After exposure, the tracks may be revealed by etching the material in solutions such as caustic alkalis. It was first discovered by Cartwright B.G. et al. (1978). CR-39's chemical name is polyallyl glycol carbonate (PADC); its element composition is  $(C_{12}H_{18}O_7)$ , or CR-39. It has a clear transparent rigid plastic of density  $1.31 \text{ g.cm}^{-3}$ , and its chemical structure consists of short polyallyle chains joined by links containing carbonate and die ethylene glycol groups into a dense three-dimensional network as shown in Figure 2.6) [92]. Among many known etched track detector materials, CR-39 is the most sensitive material capable of recording protons and alpha particles with a wide range of energies. Another advantage of it is the clarity of its surface after etching and the low background [93].

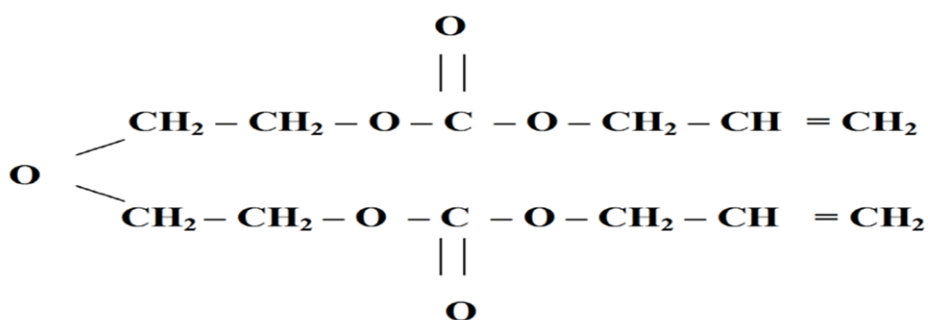


Figure 2.6. The chemical form of the CR-39 detector [94].

Its most important characteristics are:

1. Optically transparent.
2. Very sensitive.
3. Very symmetrical and homogeneous.
4. The presence of a non-solvent abrasive chemical.
5. This polymer is resistant to almost all solvents as well as heat resistant.

## 2.7 The chemical etching

Latent tracks, or radiation hazard trails, are created when ionizing particles pass through polymeric track detectors. The easiest way to see the tracks is to use a chemical solution to etch the (SSNTD) material, which preferentially attacks the damaged material and enlarges the original track to a size that can be seen under an optical microscope [94]. The chemical etching of plastic detectors is often done in a bath with a thermostat. The most popular etchant for plastics is an aqueous solution of sodium hydroxide (NaOH), with concentrations ranging from a molarity of 6.25 N and typical operating temperatures of 70 °C. The etching solution is typically poured into a sizable glass beaker and placed in the temperature-controlled bath. In order to prevent evaporation and the subsequent rise in the solute concentration of the etchant solution, hanging with a lid covers the top of the beaker [95]. For the etching procedure, a 6.25 normality NaOH solution was employed. The following formula is used to determine normality:

$$W = W_{eq} \times N \times V \quad (2.6)$$

W is the weight in grams of NaOH.

$W_{eq}$  is the equivalent weight of NaOH.

V is the volume of distilled water, where N is the normalcy. For chemical etching, 62.5 grams of NaOH and 250 ml of deionized water were used in the current investigation based on equation (2.6).

## 2.8 Radon gas

The main natural radiation source in human bodies is radon [96]. In the current study, blood samples were examined using SSNTD. This detector, a unique variation of NTD CR-39, has numerous advantageous characteristics, including strong visual clarity, stability under varying environmental conditions, and good sensitivity. Thus, the researchers recognized its utility. It is possible to quantify uranium in various settings, including the air, soil, and water, as well as on various biological samples, including blood and urine. Radioactive compounds can enter the body through food, inhalation, or skin absorption. The primary route of exposure to invasive radionuclides, including radon, is inhalation. The half-life of radon under alpha decay is 3.8 days. Because radon has a short half-life, the assessment will be done using biological samples such as serum, urine, and blood. The best sample to use to identify high uranium ingestion is urine. An alpha particle detector can be used for this procedure, particularly the CR-39 NTD. Blood samples are most commonly used in environmental toxicology [97]. In order for mensuration, radon concentrations should determine the diffusion constant (K) to the system using alpha particles, and the diffusion constant differs from one system to another depending on the geometric dimension of the diffusion chamber (radiation) [98].

It can also calculate the density of the track ( $\text{Tr.cm}^{-2}$ ) of the relationship [99]:

$$\text{Track Density } (\rho) = \frac{\text{Average number of total pits (Track)}}{\text{area of field view}} \quad (2.7)$$



After determining the calibration constant for the CR-39 detectors, radon concentrations ( $C_{Rn}^a$ ) in the aerobic gap can be measured at the top of the sample by binding it to the density of the atomic effects of alpha particles and the time the detectors are exposed as in the following relationship [99, 100].

$$C_{Rn}^a = \frac{\rho}{KT} \quad (2.8)$$

$C_{Rn}^a$  is the radon gas concentration in space ( $Bq.m^{-3}$ ).

Where  $\rho$  is the alpha track density due to radon ( $Track.Cm^{-2}$ ).

T represents the exposure time of the detectors, i.e., the period of storage of samples with detectors.

The dissolved radon concentrations ( $C_{Rn}^s$ ) in the samples can be expressed in terms of the radon concentrations emitted from the samples into the air surrounding the samples, as in the relationship below [99, 100].

$$C_{Rn}^s = \frac{C_{Rn}^a \cdot \lambda \cdot h \cdot T}{L} \quad (2.9)$$

Where  $C_{Rn}^s$  is the concentration of radon in the sample.

$\lambda$  is the constant of radon decay.

h is the distance between the detector and the top of the sample equal (4.5cm).

t is represents the exposure time of 90 days.

L is the sample's thickness, equal to 0.5cm.

It can calculate the activity of radon concertation from the relationship [100]:

$$C_{Rn}^{s,ac} = \frac{C_{Rn}^s \cdot L \cdot A}{M} \quad (2.10)$$

Where A is the sample's surface area, and M is the mass of the sample. The activity of radium concentration is represented in dry samples [98, 100]:

$$C_{Ra}^{s,ac} (Bq/kg) = \frac{C_{Rn}^a hA}{M} \quad (2.11)$$

The number of uranium atoms can be determined using the formula  $\lambda_U N_U = \lambda_{Rn} N_{Rn}$ , which represents the law of radiation equilibrium, the number of atoms of uranium is found  $N_U$  [100].

The weight of uranium in sample dry [101]:

$$W_U = \frac{N_U A_U}{N_a} \quad (2.12)$$

Where

$\lambda_U$  is the fixed uranium dissolution and amounts to  $4.9 \times 10^{-18} \text{ s}^{-1}$ .

$A_U$  is the mass number of uranium ( $^{238}\text{U}$ ).

$N_a$  is the number of Avogadro  $6.02 \times 10^{23} \text{ atom}$ .

Equation 2.13 represents uranium concentration [100]:

$$C_U = \frac{W_U}{w_s} \quad (2.13)$$

The annual effective dose (H) was calculated according to the formula

$$H (mSv/y) = C \times F \times O \times T \times D \quad (2.14)$$

Where C stands for the average radon concentration  $\text{Bq/m}^3$ , F is the equilibrium factor for indoor that is set as 0.4, O is the occupancy factor taken as 0.8, T is time in h in a year (8,760 hours/year), D is the dose conversion factor  $1.4 \times 10^{-8} \text{ Sv/Bq/m}^3 \text{ h}$  [102].

### 2.8.1 Physical and chemical properties of radon

radon is a radioactive gas that is tasteless, odorless, colorless, and inflammable. As a result, it is invisible to the human senses. It has a boiling temperature of  $-60.8 \text{ }^\circ\text{C}$  and a melting point of  $-70 \text{ }^\circ\text{C}$ . At  $9.96 \text{ kg.m}^{-3}$ ,

radon has the highest gas density and is roughly seven times heavier than air. There are three crucial isotopes of radon. These are:

(1)  $^{222}\text{Rn}$  (also known as radon, which is a member of the  $^{238}\text{U}$  decay series);

(2)  $^{220}\text{Rn}$  (also known as Thoron, which is a member of the  $^{232}\text{Th}$  decay series); and

(3)  $^{219}\text{Rn}$  (Called action, belongs to  $^{235}\text{U}$  decay series). According to science, the most common isotope of the atom radon,  $^{222}\text{Rn}$ , is radon [103]. The phrases radon and  $^{222}\text{Rn}$  are frequently used synonymously in the literature. This strategy was also used in the current work. The shortest half-life of  $^{219}\text{Rn}$ , which has an abundance of barely 0.7% in the earth's crust, is 4 seconds. Due to its extremely short half-life,  $^{219}\text{Rn}$  often vanishes shortly after the malefactor. Due to its short half-life of 55.5 seconds,  $^{220}\text{Rn}$  is likewise unable to go very far and is frequently removed from the monitoring system by adding filters or using other delaying strategies. The radon isotope  $^{222}\text{Rn}$  is the most significant one. It may travel considerable distances from its site of origin and has a half-life of 3.82 days [104]. Because of this, only  $^{222}\text{Rn}$  is typically considered when evaluating risk factors from radon exposure. radon has no sinks, and it is thought that very small amounts only reach the stratosphere [105]. As a result, radioactive decay was  $^{222}\text{Rn}$ 's only and final form of transition or deterioration.

### 2.8.2 The relationship of radon to LC

The health risk of radon is caused by exposure to its progeny or radon decay products (RDP), which are produced when radon decays. If radon gas is present, the decay products will become suspended in the air [106]. Because they are electrically charged, most will attach to dust particles or the surface of solid materials; some may remain unattached [107] and may be inhaled. Once deposited in the lungs, radon emits alpha radiation, which

irritates and can damage the living cells lining the lung. Because of their relatively short half-lives (less than half an hour), RDP mainly decays while still inside the lung. Two of these short-lived products, Polonium-218 and Polonium-214, emit alpha particles, whose energy dominates the dose to the lung and the associated risk of LC [108]. In the open air, the concentration of radon gas is very small and does not pose a health risk. However, in some confined spaces like basements and underground mines, radon can accumulate to relatively high levels and become a health hazard. The health effects of radon have been investigated for several decades [109]. Initially, investigations focused on underground miners exposed to high levels of radon in their occupational environment.

# ***Chapter Three***

## ***Experimental Part***

## Chapter Three

### Experimental Part

#### 3.1 Introduction

This chapter will explain how the blood samples are collected and prepared, the materials used, and the procedures for each of these techniques in our work. Each sample of blood serum samples was prepared in three different versions according to the chemicals used and the volume of the blood serum used in this study. The samples are in this study blood collected from different people in quantities sufficient for the research. These samples were taken from people with details such as; age, gender, site, and smoking. The study site was the Imam Husain Center for Oncology and Hematology, Karbala, Iraq. Figure 3.1 depicts the framework study.

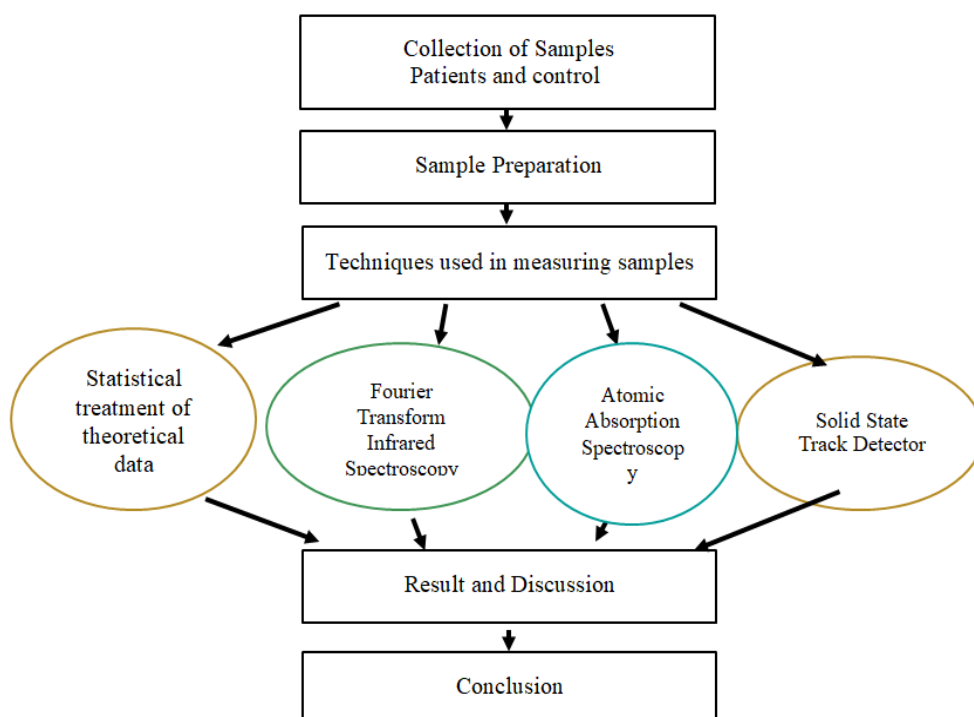


Figure 3.1. A flow chart of the main parts of the current study.

### 3.2 Study area

Karbala governorate was one of the nineteen governorates of Iraq, located in the middle Euphrates region, south of Baghdad, the capital. The governorate's population was 1,316,759 according to the 2021 census by the Central Statistical Organization (CSO). It was divided into seven administrative regions (Center of City, Al-Hur, Al-Husaniyah, Al-Hindiya, Al-Jadawal Al-Ghurb, Al- Khirat, and Ain Al-Tamur), as shown in Figure 3.2, where the population statistics were adopted to maintain the census for the year 2021.

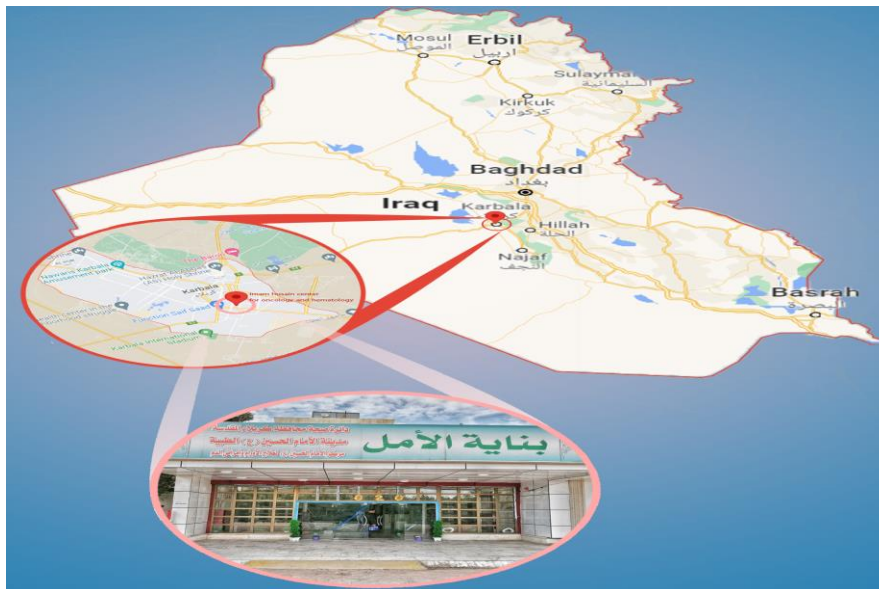


Figure 3.2. Represents a map of Iraq, showing the location of the Tumor center in Karbala governorate.

During the study period, data were collected from medical reports of LC patients and healthy people from the Imam Husain Center for Oncology and Hematology. This study has covered all LC patients from the governorate cases for different age groups. This study was conducted to calculate the prevalence rate of LC in the Karbala governorate.

### 3.3 Sample preparation

After collecting blood samples, they are placed in a Centrifuged device (ROTOFIX 32 A), Japan that rotates for 5 minutes to separate blood cells and suspended particles from the serum in Imam Husain Center for Oncology, and Hematology laboratory, as shown in Figure 3.3. The blood serum was transferred to neutral glass tubes and stored in a refrigerator prepared for measurement.



Figure 3.3. The centrifuge device.

### 3.4 FTIR Spectrophotometry

After collecting 55 blood samples of patients and 30 healthy people divided into nine categories by age groups (30-35), (35-40), (45-50), (50-55), (60-65), (65-70), (70-75), (75-80) and (80-85) so Figure 3.4 depicts the FTIR Procedures.



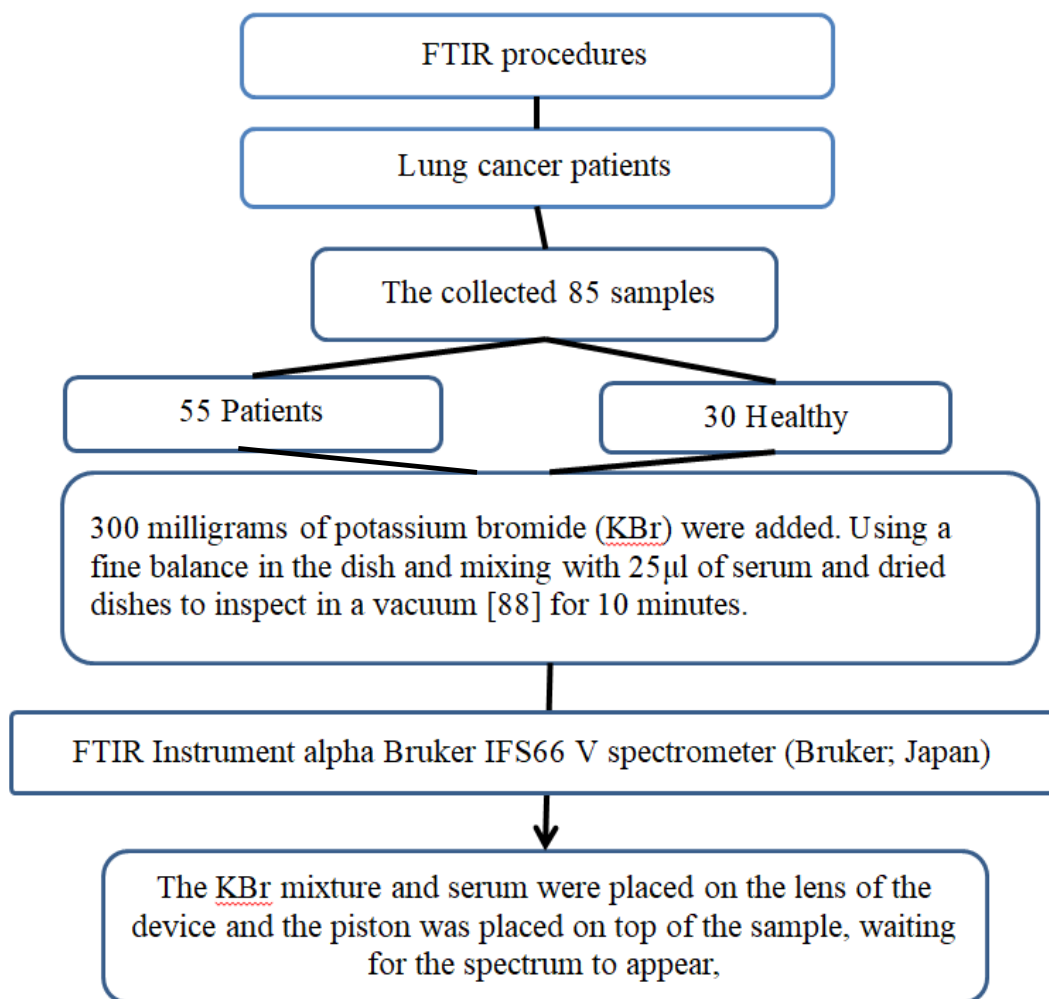


Figure 3.4. A flow chart explains the FTIR procedures.

Samples were measured in the Department of chemistry, College of Science, the University of Kufa, as shown in Figure 3.5, and a window-based data program processed the data.

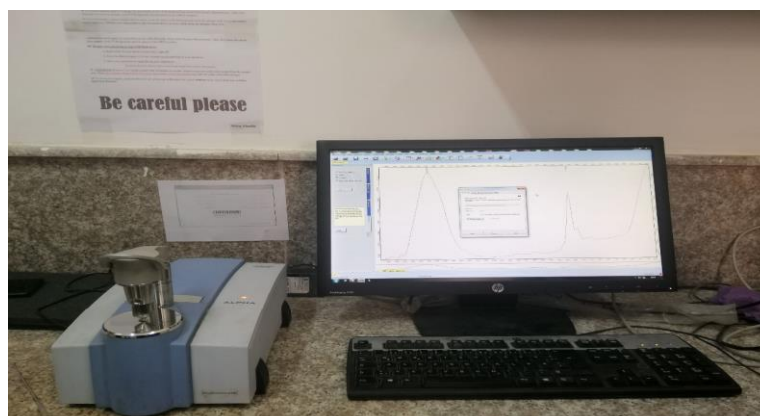


Figure 3.5. The FTIR device.

### 3.5 Atomic absorption spectroscopy (AAS)

Atomic absorption spectrophotometer was used to estimate trace elements level in the blood of all subjects. This part includes 65 samples collected from malignant LC patients who were 35 males and 30 females and 30 from healthy volunteers who were 20 males and 15 females. So Figure 3.6 depicts the FAAS procedures.

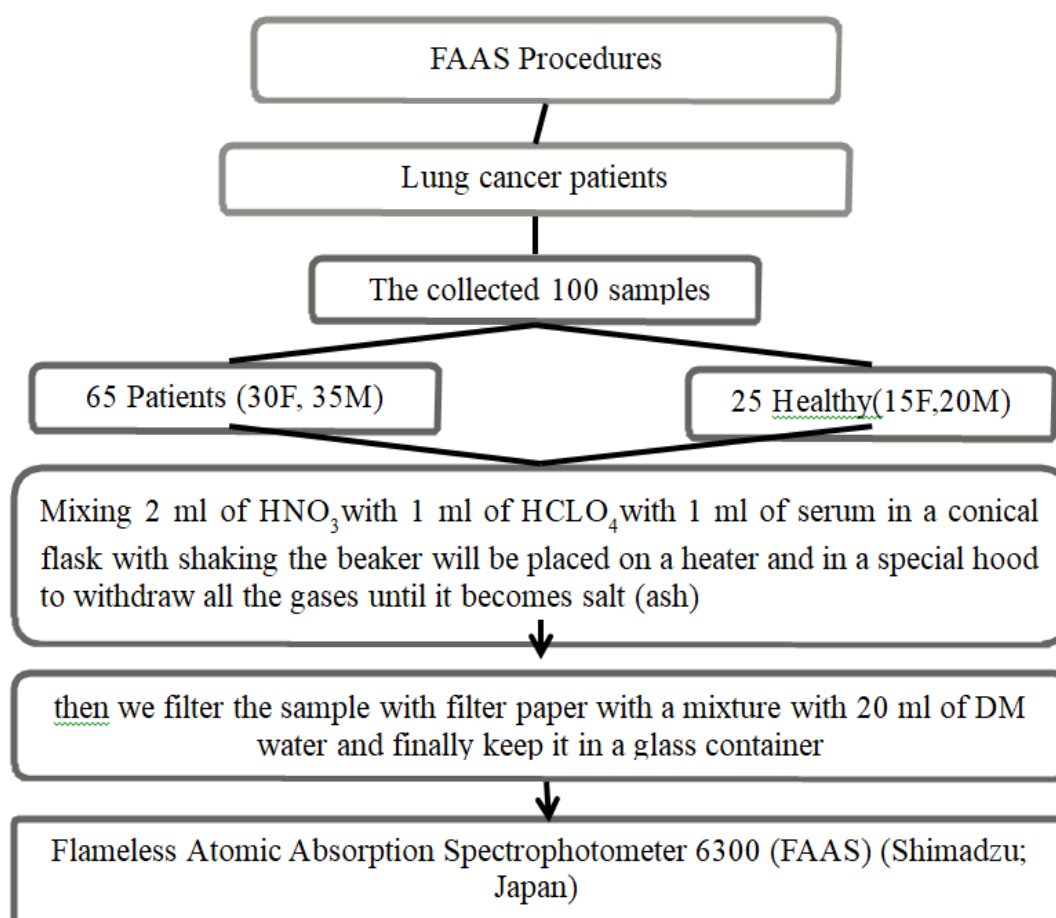


Figure 3.6. A flow chart explains the FAAS procedures.

Samples were measured using the Shimadzu AA-6300 Flame Atomic Absorption Spectrometer (FAAS) in the Biochemistry Laboratory, College of Medicine, University of Kerbala, as shown in Figure 3.7.



Figure 3.7. Atomic absorption spectroscopy device.

### 3.5.1 Apparatus

Flame Atomic Absorption Spectrometer (FAAS) was used to determine the levels of Cu, Zn, Cd, and Pb where the standard wavelength of (Cu, Zn, Cd, and Pb) was equal (283.3, 213.9, 228.8, and 283.3 nm respectively and practically wavelength of (Cu, Zn, Cd, and Pb) was equal (283.25, 213.75, 228.75 and 283.25 nm respectively, its width is 0.7 nm for all, and the flame type were Air-acetylene.

### 3.5.2 Chemical substances

All chemical substances used were of the highest purity (analytical reagent grade), obtained from Fluka and BDH companies. The standard stock solutions are listed in Table 3.1.

Table 3.1. Concentrations of stock solutions and their commercial sources.

No.	Chemical substances	Companies
1	HNO <sub>3</sub>	BDH, Turkey
2	HClO <sub>4</sub>	BDH, Turkey
3	Standard stock solutions(1000µg.ml <sup>-1</sup> )of Cu	Fluka, Switzerland
4	Standard stock solutions(1000µg.ml <sup>-1</sup> )of Zn	Fluka, Switzerland
5	Standard stock solutions(1000µg.ml <sup>-1</sup> )of Cd	Fluka, Switzerland
6	Standard stock solutions(1000µg.ml <sup>-1</sup> )of Pb	Fluka, Switzerland
7	Demineralized water / DM water	Prepared in the lab.

### 3.5.3 Sample digestion

This method mixed 500 ml of nitric acid HNO<sub>3</sub> with 250 ml of perchloric acid HClO<sub>4</sub> into a glass duct the size of 1000 ml. To digest the 1 ml serum sample, add 3 ml of the acid mixture in conical flasks with a volume of 20 ml and place them in the hood for digestion at 80 °C until the sample got dry, where the vapors resulting from heating the sample are expelled from a vacuum located in the hood in the Department of Environment, College of Science, the University of Kufa as shown in Figure 3.8.



Figure 3.8. Image of the hood for discharging the fumes when preparing the samples.

The samples were then transported after being cooled, diluted with 20 ml of deionized water, and filtered through 0.4  $\mu$ m of filter paper. The solution was placed in a glass bottle with a tight cap for storage, as shown in Figure 3.9. Samples were measured by a flame atomic absorption spectrophotometer (FAAS) type 7000A, Shimadzu, Japan.



Figure 3.9. Filtering the samples using filter paper and adding deionized water.

The results were obtained from the three measurement methods, and statistical analyses were carried out using the SPSS statistical software package (SPSS for Windows version 20, SPSS Inc., Chicago, Illinois,

USA). It is a statistical program used to conduct statistical analyses, and all tests deal with data statistically through its management and documentation and shows the relationship between independent and dependent variables in terms of their strength and weakness.

### **3.6 Solid state nuclear track detector CR-39**

The blood (5 ml) was dried, ground by pestle and mortar, and then stored in plastic containers with a total container height of 6 cm for four weeks to examine secular equilibrium between  $^{226}\text{Ra}$  and  $^{222}\text{Rn}$ . Then the covers were quickly replaced, with the specific Solid State Nuclear Track Detectors with code CR-39 were installed on the upper inner surface of the plastic container lid using double-sided adhesive. It was stored for 90 days. The container was covered with a tight lid with a diameter of 3.75 cm, and the height of the sample was 0.5 cm. We used a sensitive scale to weigh the samples, and their weight is 1 gram (5 ml = 1 gm), as shown in Figure (3.10). Solid-state nuclear track detectors product by TASTRAK (CR-39), as follows: TASTRAK Analysis System, Ltd., UK: America manufacture with code (LOT 64810987). A CR-39 detector sheet had dimensions of (2.5cm×2.5cm), and a thickness of 1mm. Where  $K = 0.28 \text{ Track.cm}^{-2} / \text{Bq.m}^{-3} \cdot \text{day}$  is calibration factor for CR-39 detectors [110].

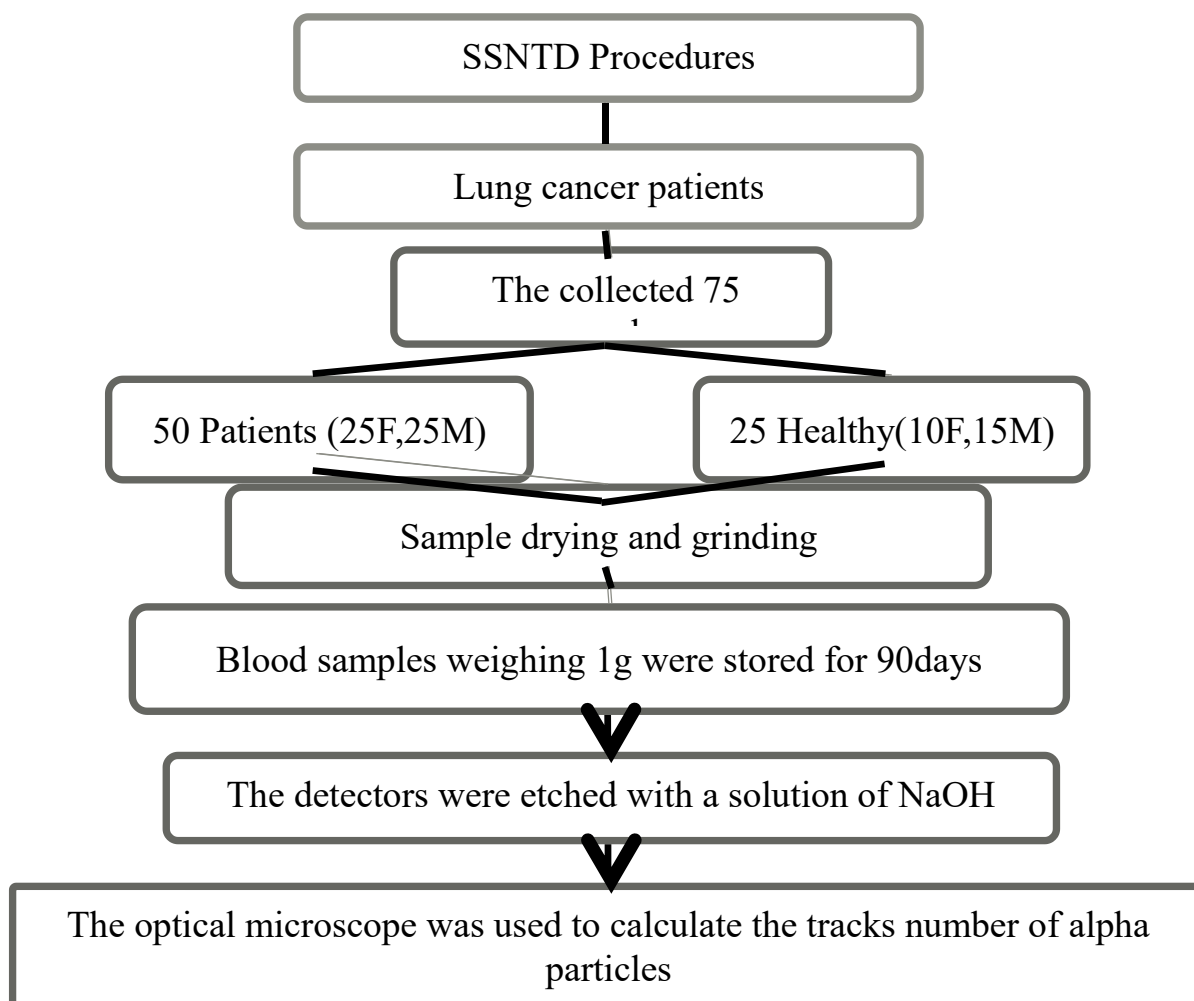


Figure 3.10. A flow chart explains the SSNTD procedures.

### 3.6.1 Sodium hydroxide solution

This solution was prepared by dissolving 62.5 g of sodium hydroxide NaOH granules in 250 ml of demineralized water in a Pyrex flask. This process was carried out using a Pyrex flask because dissolving sodium hydroxide NaOH in water usually releases heat, so it was carefully prepared. Chemical etching was carried out at a temperature of 70°C; the etching time was 6 hours [56].

### 3.6.2 Water bath.

The temperature of the chemical etching solution was regulated using a water bath (Clifton, England). The water bath includes a thermostat operating range of 20 °C to 110 °C in the Department of physics, College of Science, the University of Kufa, as shown in Figure 3.11. The temperature regulation accuracy was  $\pm 0.1$  °C. A chemical etching was carried out at 70°C, and demineralized water was used as a bath liquid.



Figure 3.11. Represents the water bath.

### 3.6.3 Optical microscope

An optical microscope (KRUSS-mbl 2000) was used with a magnification of 400X and a viewing area of 0.0676 cm<sup>2</sup>. This microscope was used to calculate the alpha particle caused by the fission of radon in blood samples in the CR-39 detector in the Department of physics, College of Science, the University of Karbala, as shown in Figure 3.12.



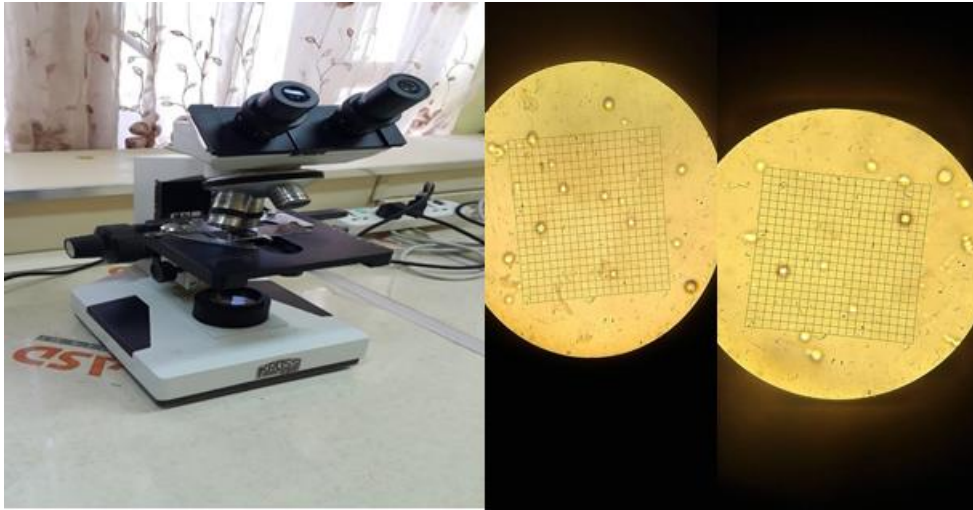


Figure 3.12. Shows the density of alpha particle tracks at a 400X optical microscope magnification on the detector surface.

***Chapter Four***  
***Results and Discussion***

---

---

## Chapter Four

### Results and Discussion

#### 4.1 Introduction

This section discusses the empirical results for theoretical statistics, Fourier transform infrared spectroscopy (FTIR), flameless atomic absorption spectroscopy (FAAS), and solid-state track detector. These results included prevalence and mortality rate and percentage. Analytical statistics, Correlation coefficient, employing the (FAAS) technique, and the part that explains the connection between the trace elements and uranium concentrations. This section incorporates Figures, Tables, and results that were utilized in discussing the outcomes obtained for the blood serum samples.

#### 4.2 Statistical analysis

The data were analyzed using the SPSS Version 20 software using statistical analysis (independent sample T-test, a nova test, Pearson correlation coefficient). Depending on whether the  $p < 0.05$ , the relationship between the concentration of groups is statistically significant; however, if it is larger than 0.05, it is not [111].

Correlation is an analytical statistic for estimating the probability of a linear society between two continuously moving variables. In conclusion, correlation factors determine the strength and direction of linear correlations between two variables. Pearson's correlation coefficient is utilized when two variables are regularly split.

## 4.3 Result and discussion

### 4.3.1 Statistical treatment of theoretical data

This part presents the statistical analysis of LC prevalence in Karbala/Iraq from 2012 to 2021. LC affects both men and females in large numbers. Iraq has recorded a rise in cancer patients with a high prevalence and mortality rate. The current study is a statistical and epidemiological one. Data on male and Female LC patients in Karbala governorate were collected from Al-Hussein Medical City during 2012-2021. The data was disaggregated by age, gender, and region.

Furthermore, the prevalence rate was determined for each district in the governorate. The prevalence and rate of change were also calculated. The significance of this statistic was studied using SPSS version 20, especially the chi-square test for statistical significance.

Data on patients with LC were obtained in cooperation with the imam Hussein Center for Cancerous Tumors staff, where data were collected for the years from 2012 to 2021, as shown in Table 4.1.

From Table 4.1, it was noticed that the total number of certain cases of LC during the past decade in separate areas of Karbala governorate reached 584, and the number of cases per 100,000 was 44.04 for the total number of categories (female and male) during that period. The City Center had the largest share of injuries, reaching 298, while the lowest number of patients was 10 in Al-Khairat and Ain Al-Tamur areas, as shown in Figure 4.2. The prevalence rate values, often referred to as the total number of cases in a specific period were extracted as [112], with the highest value of 66.16 in the Al-Hindiya region and the lowest value of 16.04 in the Al-Khairat region. The percentages recorded the highest value in the city's center, 51.37, and the lowest value in the Al-Husaniyah area, 13.1, as shown in Figure 4.1.

Table 4.1. The prevalence rate and the percentage of total cases according to age groups for some townships of Karbala Governorate.

Region	Karbala Population	Cases	Age Groups	Prevalence Rate (P.R)	Percentage %
Center of City	577543	298	20-90	51.6	51.37931
Al-Hur	260117	90	40-85	34.6	15.51724
Al-Husaniyah	165604	76	39-80	45.9	13.10345
Al-Hindiya	126986	84	38-84	66.16	14.48276
Al-Jadawal Al-Ghurb	93395	16	20-77	17.13	2.758621
Al-khairat	62339	10	49-75	16.04	1.724138
Ain Al-Tamur	30766	10	52-75	32.5	1.724138

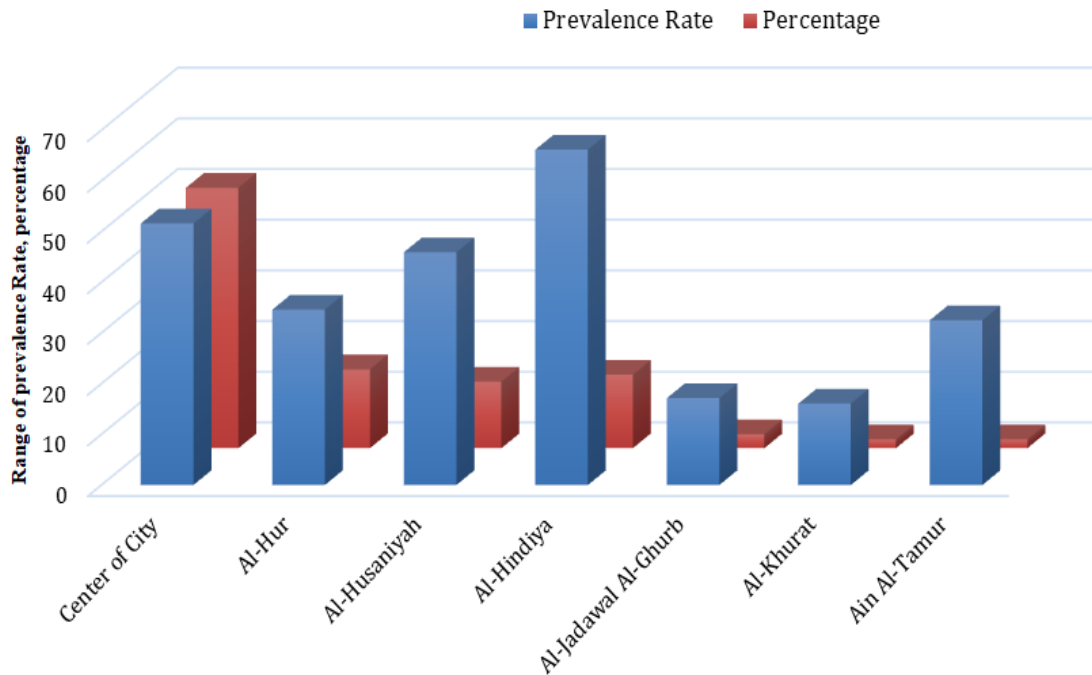


Figure 4.1. Percentage and prevalence rate for each region in the Karbala governorate between 2012 and 2021.

Tables 4.2 display the division of LC patients into two groups for males and females. The prevalence rate and percentage often referred to as dividing the number in the subgroup by the number in the entire group, then multiplied by 100, of both categories were calculated, depending on the age groups. It was noted that the highest prevalence rate in the Al-

Hussainiya area was 21.73 for female patients, and the Al-Hindiya area was 48.82 for male patients, as shown in Figure 4.2. At the same time, the lowest in the area of Al-Khairat was 3.2 for female patients, and in the Al-Jadawal Al-Ghurb was 11.77 for male patients. The percentage for the two categories was also calculated. It was the highest in the city center, reaching 53.73 and 49.61. The lowest in the area of Al-Khairat was 0.99 for female patients, and in the area of the Ain Al-Tamur, 1.82 for male patients.

Table 4.2. Cases of LC according to gender, age groups, and prevalence rate for the township of Karbala governorate 2012-2021.

Areas	Population	Female				Male			
		Cases	Age Groups	PR*	%**	Cases	Age Groups	PR*	%**
<b>Center of City</b>	577543	108	20-90	18.7	53.73	190	33-86	32.9	49.61
<b>Al-Hur</b>	260117	25	40-76	19.6	12.44	65	40-85	24.9	16.97
<b>Al-Husaniyah</b>	165604	36	39-75	21.73	17.91	40	40-80	24.15	10.45
<b>Al-Hindiya</b>	126986	22	38-84	17.32	10.95	62	42-80	48.82	16.19
<b>Al-Jadawal Al-Ghurb</b>	93395	5	38-73	5.35	2.49	11	20-77	11.77	2.87
<b>Al-khairat</b>	62339	2	60-71	3.2	0.99	8	49-75	12.83	2.09
<b>Ain Al-Tamur</b>	30766	3	54-73	9.75	1.49	7	52-75	22.75	1.83

\* *Prevalence Rate.*

\*\* *Percentage of the population from the total number of Karbala governorate population.*

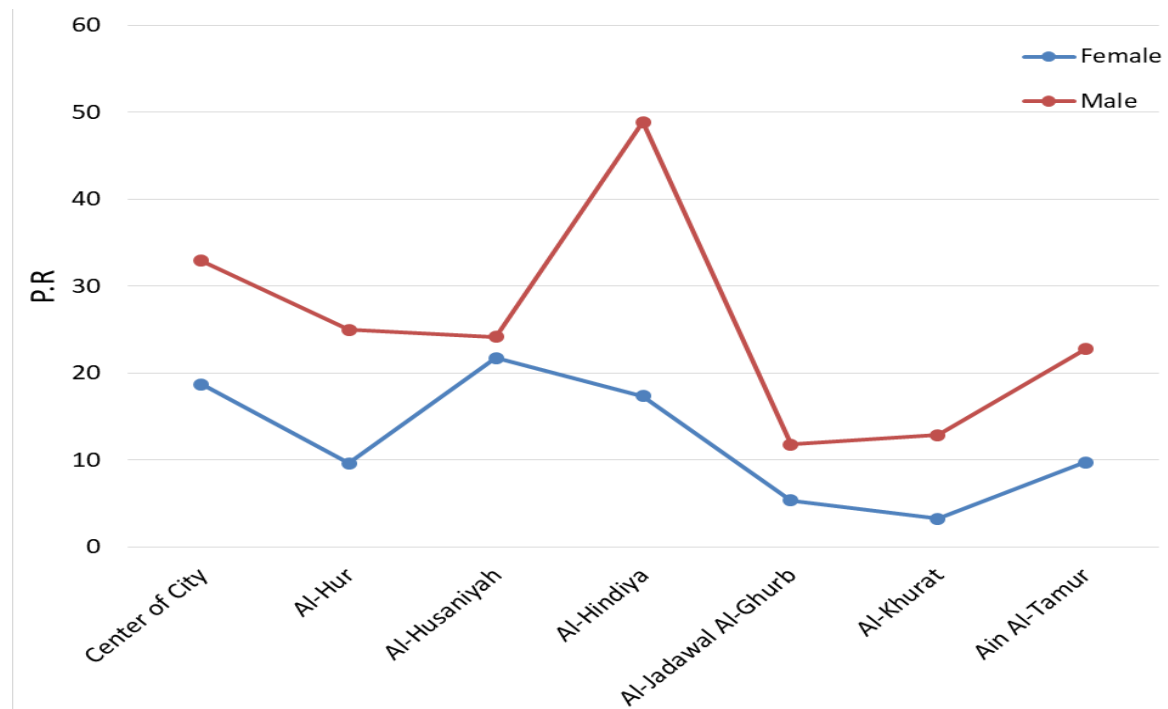


Figure 4.2. Comparison of the prevalence rate and the township for LC patients in the Karbala governorate.

From Table 4.3, it was shown that the total number of confirmed cases of LC during the past decade in the separate township in Karbala governorate reached 108 in the city center for females and 190 for males, while the lowest number of the patient was 3 for females and 8 for males in Al-Khairat.

Table 4.3. Number of lung cancer cases according to the age group for a township in Karbala governorate during 2012-2021.

Age group	City Center			Al-Hur		Al-husaunyah			Al-hindiya			jadwal Al-gharb			Al-khairat		Ain Al-tamr	
	W	M	total	W	M Total	W	M total	W	M total	W	M total	W	M total	W	M total	W	M total	
20-24	1	0	1	0	0	0	1	1	0	0	0	0	1	0	0	0	0	0
25-29	0	0	0	0	0	0	0	0	0	0	0	0	0	1	1	0	0	0
30-34	0	1	1	0	0	0	0	0	0	0	0	0	0	0	0	0	0	0
35-39	2	1	3	0	0	0	1	0	1	1	0	1	1	0	1	0	0	0
40-44	4	3	7	0	2	2	0	3	3	2	5	7	0	0	0	0	0	0
45-49	13	8	21	0	4	4	1	1	2	1	3	4	0	0	0	1	1	0
50-45	12	19	31	4	6	10	3	3	6	1	4	5	2	2	4	0	2	0
55-59	15	22	37	3	4	7	6	4	10	2	3	5	0	3	2	0	1	1
60-64	16	37	53	6	11	17	8	8	16	5	9	14	0	2	2	1	2	1
65-69	22	30	52	4	17	21	8	4	12	5	12	17	1	0	1	0	1	1
70-74	14	36	50	4	10	14	7	9	16	1	15	16	1	1	1	1	2	1
75-79	5	16	21	2	10	12	1	6	7	1	9	10	0	1	0	1	1	1
80-84	2	12	14	1	0	1	1	1	2	2	2	4	0	0	0	0	0	0
85-89	2	3	5	1	1	2	0	0	0	1	0	1	0	0	0	0	0	0
90<=	0	2	2	0	0	0	0	0	0	0	0	0	0	0	0	0	0	0
total	108	190	298	25	65	90	36	40	76	22	62	84	5	11	16	2	8	10

The results of Table 4.4 showed the comparison of the number of cases according to the age groups between the living and the dead during 2012-2021.



Table 4.4. Comparison of the number of cases according to the age groups between the living and the dead during 2012-2021.

Age group		<=36	37-46	47-56	57-66	67-76	77-86	≥ 87	Total
Year									
2012	Alive	0	3	9	12	14	3	0	41
	Dead	0	0	0	0	0	0	0	0
2021	Alive	2	3	15	25	20	3	1	68
	Dead	0	1	2	1	3	1	0	8

The results are comparable to other published works [14, 113]. From Table 4.4, the percentage change of the total cases of LC patients was 68. This means that there was an increase in the percentage change.

Table 4.5 shows a comparison of the number of cases for some Iraqi governorates near Karbala.

Table 4.5. Lung cancer cases in some governorates of Iraq.

Year	2012	2013	2014	2015	2016	2017	2018	2019	2020	2021	Total
Babylon	1	0	1	0	6	2	4	9	9	12	44
Baghdad	1	0	0	0	0	0	0	6	1	3	11
Dhi Qar	1	0	0	0	0	0	0	1	1	2	5
Najf	0	0	1	0	3	1	0	1	1	3	10
Anbar	0	0	1	0	0	0	0	0	0	0	1
Al.Diwanayah	0	0	0	0	1	0	0	0	1	1	3
Wasit	0	0	0	0	1	0	0	2	2	0	5
Muthanna	0	0	0	0	0	0	0	1	3	0	4
Dyala	0	0	0	0	0	0	0	1	1	0	2
Myesan	0	0	0	0	0	0	0	0	1	1	2
Mousal	0	0	0	0	0	0	0	0	0	2	2

Some governorates close to Karbala were also compared in terms of patients, where the highest number of LC patients was recorded in light of the studied data in the Babylon governorate and the lowest in the Anbar governorate, as shown in Figure 4.3.

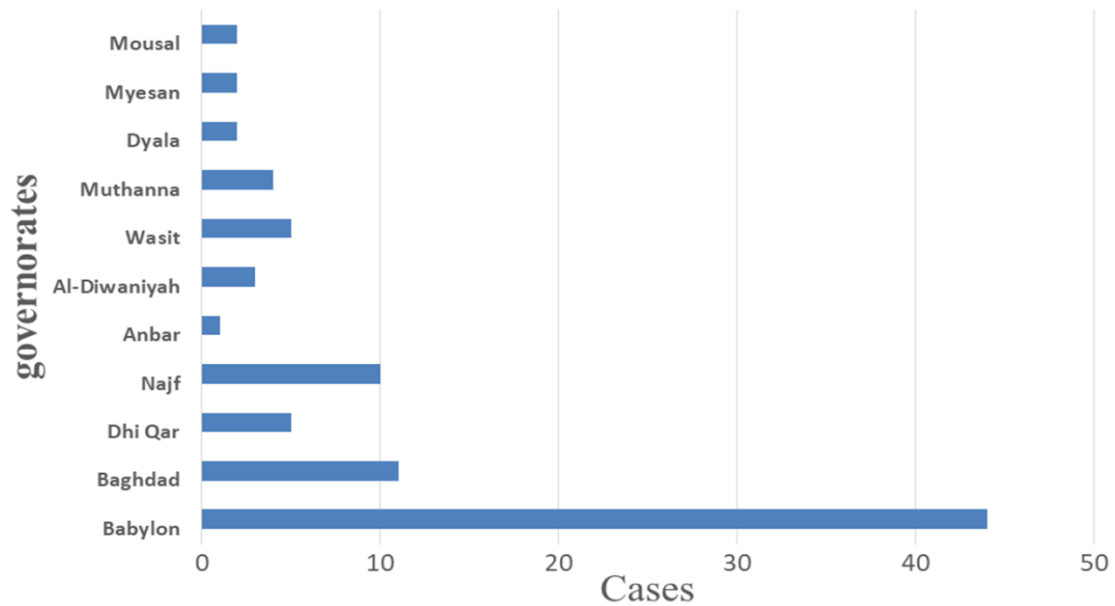


Figure 4.3. Lung cancer cases taken from the Imam Hussein Centre in some governorates of Iraq.

It was shown that the relationship between the prevalence rate in the city center was greater than in the governorate's other areas. Many factors led to an increase in the opportunities of LC, such as family history and genes, mutations in DNA, exposure to environmental toxins, like certain chemicals, carcinogens or radiation, smoking, and ultraviolet radiation that causes sunburn. The most important risk factor was age, clinical and experimental observations suggest that hormonal, genetic, and environmental factors may play a role in LC. Other factors associated with LC included an unhealthy diet (low fruit and vegetable intake, vitamins, and coffee), obesity and physical inactivity, indoor smoke from household use of solid fuels, infections, and hyperglycemia. When factors take into account age, gender and category, there are differences as in Table 4-1 (age groups, percentage, and the number of cases) the relationship was weak, positive and negative was weak and had no statistical significance between the age groups and the prevalence factor as well as with the number of cases, while the positive and strong positive relationship with the ratios

were shown in Figure 4.4. while the Pearson chi-square was 0.42 with  $p=0.2$ . Therefore, there is no statistical significance.

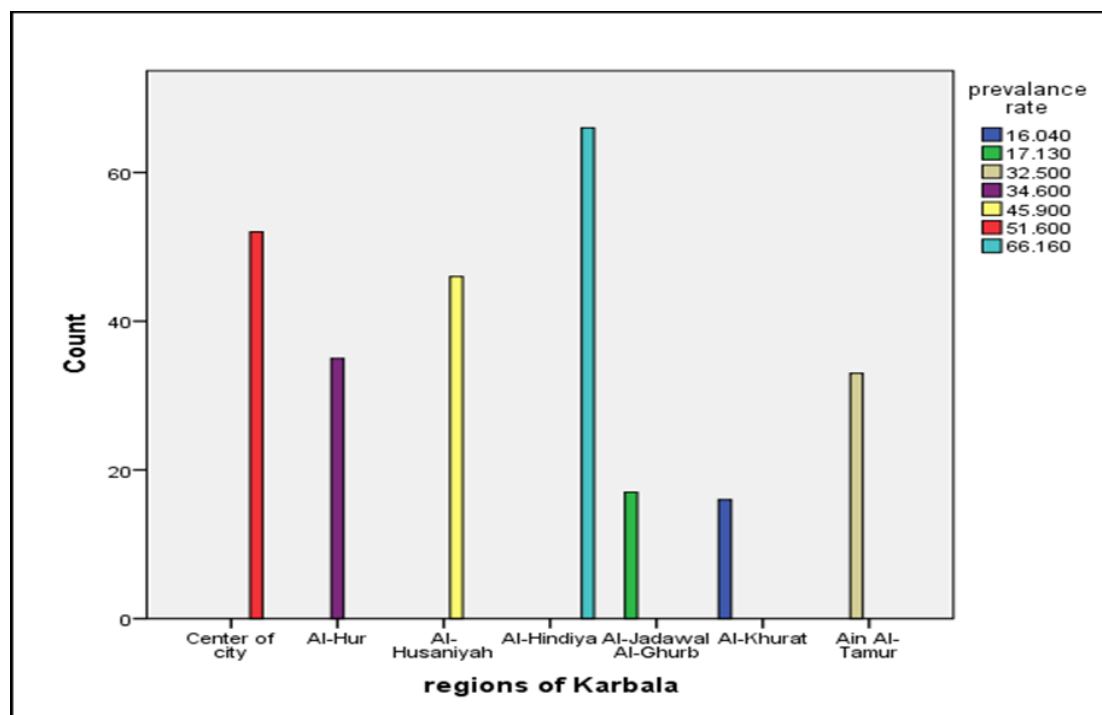


Figure 4.4. The relation between prevalence rate and number.

#### 4.3.2 Fourier transform infrared spectroscopy (FTIR).

This part included the FTIR technique employed to evaluate serum samples from (LC) patients and health. Blood samples were taken from 30 healthy adults and 55 LC patients from the Imam Hussain cancer center. All FTIR-ATR spectra were baseline adjusted and normalized to get accurate data. The study included two groups, the healthy group and the patient group, where the average age for each group was calculated, as shown in Table 4.6. In addition, the function groups analyzed of the cancer patients.

Table 4.6. Age of lung cancer patients and healthy people.

Group	Number	Mean± Std. Deviation
Healthy people	30	58.566±13.748 years
Lung cancer patients	55	58.490±14.006 years

Serum's FTIR-ATR spectra revealed details about biomolecules, such as functional groups, structure, bond types, and reactions. Biomarkers, or disease. Related molecular alterations in bodily fluids and key tissues, such as blood, were critical in aiding screening and diagnosis so that treatments might begin as soon as feasible. The group frequency of the major elements of LC indicated in Table 4.8 was used to assign suitable vibrational bands to absorption bands of spectra. By using FTIR, which was first characterized by the spectral of the normal case and LC represented in Table 4.7, the FTIR absorption overlay spectra of normal and LC were divided into nine categories in Figures 4.5 and 4.13 by the following:

Table 4.7. Frequency assignment of FTIR vibrational bands in human serum samples.

Sq.	Vibrational band (cm <sup>-1</sup> ) Human serum (stander)	Vibrational band(cm <sup>-1</sup> ) lung cancer (present study)	Assignment [5]	Component group [5]
1.	3280	3293	H–O–H stretching The amide A band	Amino acid (amide A)
2.	2957	2958	CH <sub>3</sub> asymmetric and symmetric stretching	Fatty acid/ lipids
3.	2920	2931	Asymmetric CH <sub>2</sub> stretching	Fatty acid/ lipids
4.	1635	1650	The amide I and amide II bands (proteins)	amide II
5.	1453	1451	CH <sub>2</sub> deformation CH <sub>2</sub> scissoring	Amino acid
6.	1396	1399	CH <sub>3</sub> bending C=O stretch of COO <sup>-</sup>	Amide I
7.	1311	1313	The amide III band CH <sub>2</sub> twist	Cyclopropane
8.	1170	1169	C–O (H) stretching in proteins Ester C–O asymmetric stretch	Amide IV Amino acid

A strong peak at 3293 cm<sup>-1</sup> indicates the presence of the crystallization water that connects the blood molecules in the solid state. The wave number of the functional groups is reported previously as the

following: OH<sup>-</sup> (3262 cm<sup>-1</sup>), -NH<sub>2</sub> (1542 cm<sup>-1</sup>), and C=O (1642 cm<sup>-1</sup>) [114]. The characteristic peaks at 1170 cm<sup>-1</sup> (stretching band of C-O) [115]. The amide peak is also previously found to appear at approximately the same peak at 1648 cm<sup>-1</sup> [115, 116]. These peaks belong to the functional groups of amino acids, either from the free amino acids or those involved in the protein structure [117]. As the proteins are the highest substances in the serum after water, most of the dried serum are proteins, and the present functional groups in the FTIR belong to the amino acids in the protein structure, especially albumin and immunoglobulins [118, 119]. Previous work showed that the contributions of proteins to FTIR spectra are in the frequency range of 3400–3030 cm<sup>-1</sup>, 1720–1480 cm<sup>-1</sup>, and 1301–1229 cm<sup>-1</sup>. These can be briefly described as 3280 cm<sup>-1</sup> (H-O-H stretching), 2957 cm<sup>-1</sup> (asymmetric CH<sub>3</sub> stretching), 2920 cm<sup>-1</sup> (asymmetric CH<sub>2</sub> stretching), 2872 cm<sup>-1</sup> (symmetric CH<sub>3</sub> stretching), 1650 cm<sup>-1</sup> (amide I of proteins), 1536 cm<sup>-1</sup> (amide II of proteins), 1453 cm<sup>-1</sup> (CH<sub>2</sub> scissoring), 1394 cm<sup>-1</sup> (C=O stretch of COO<sup>-</sup>), 1242 cm<sup>-1</sup> (asymmetric PO<sub>2</sub> stretch), 1171 cm<sup>-1</sup> (ester C–O symmetric stretches) and 1080 cm<sup>-1</sup> (CO stretch) [117]. Our results are approximately the same as in our study, with a difference that belongs to the presence of cancer.

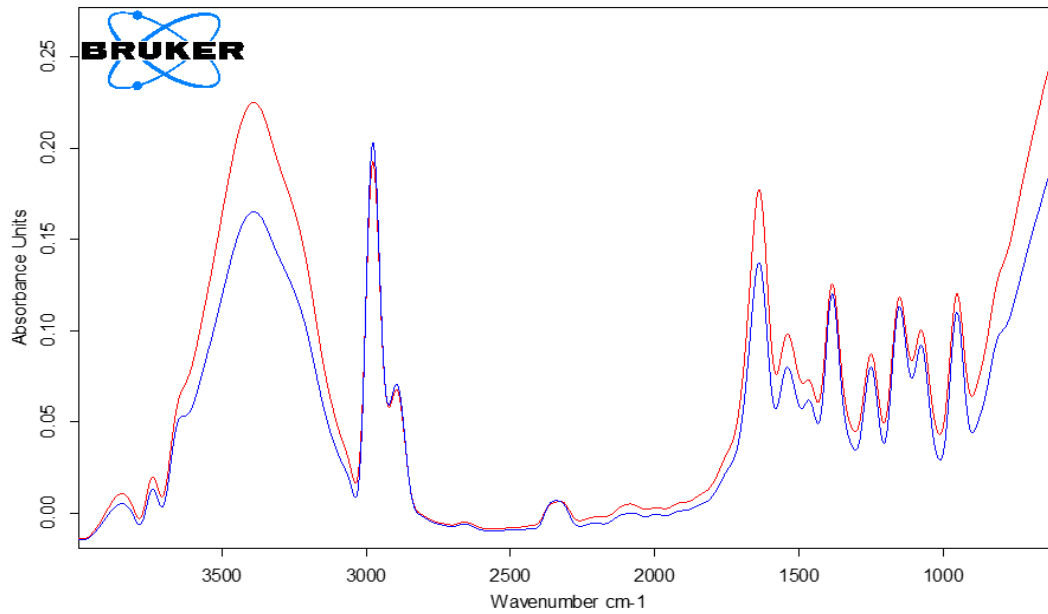


Figure 4.5. Comparison between lung cancer patients (red) and healthy people (blue) by age groups (30-35).

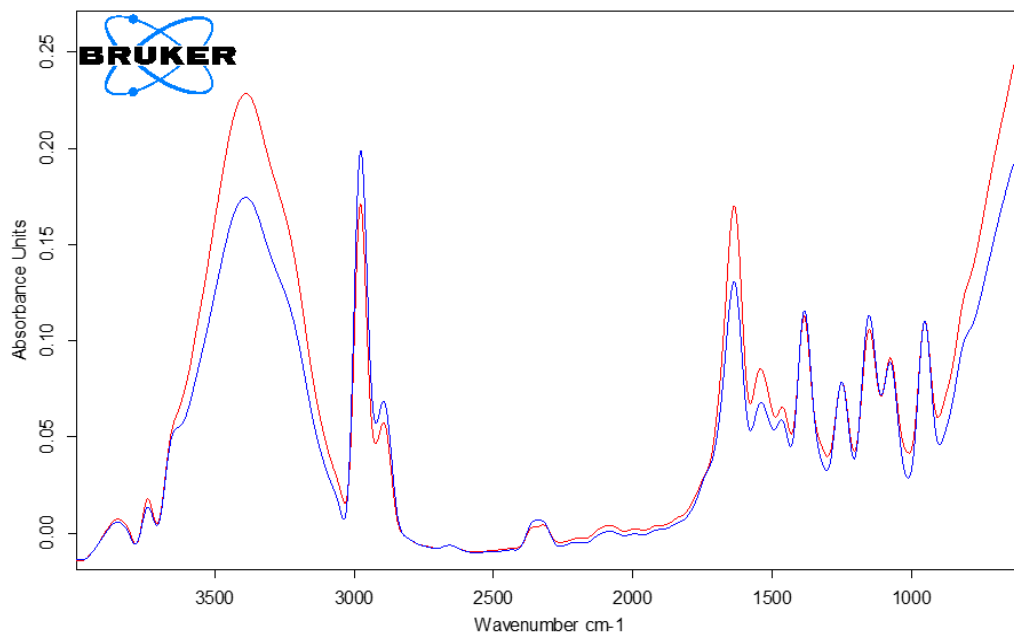


Figure 4.6. Comparison between lung cancer patients (red) and healthy people (blue) by age groups (35-40).

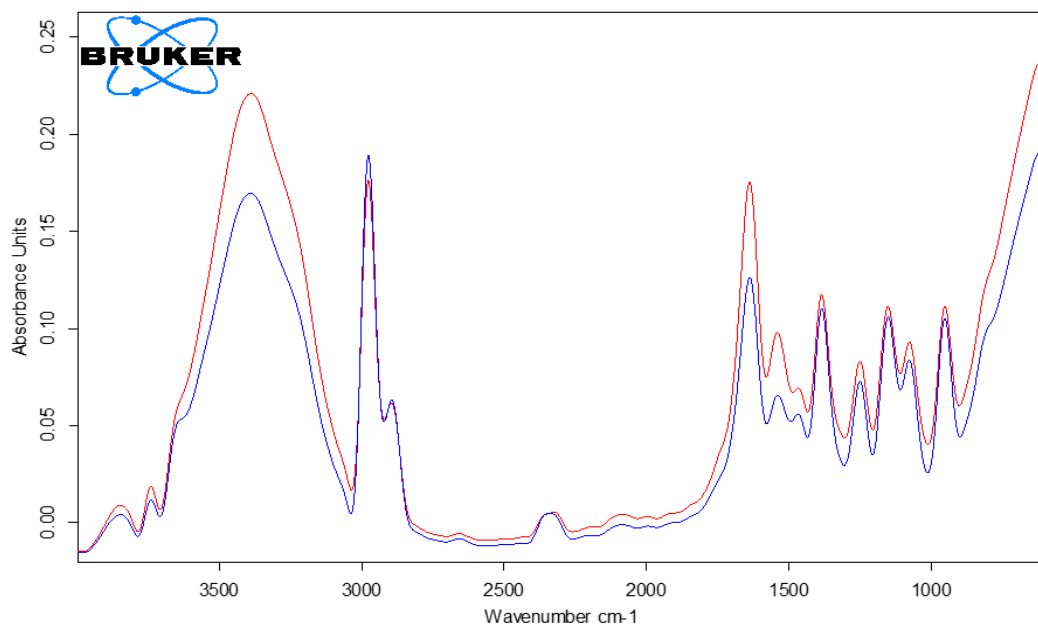


Figure 4.7. Comparison between lung cancer patients (red) and healthy people (blue) by age groups (45-50).

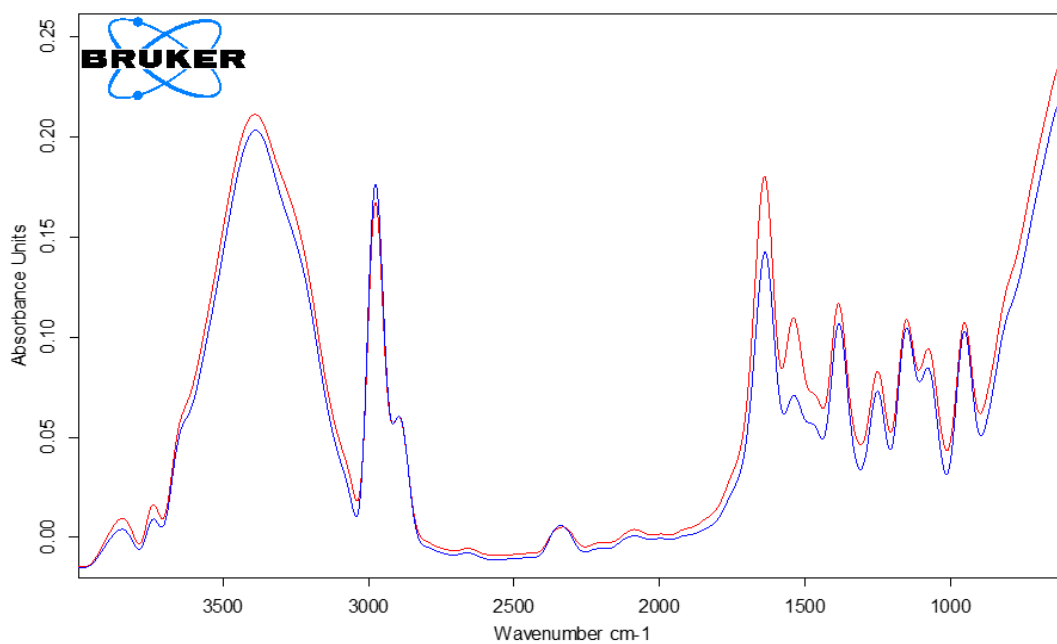


Figure 4.8. Comparison between lung cancer patients (red) and healthy people (blue) by age groups (50-55).

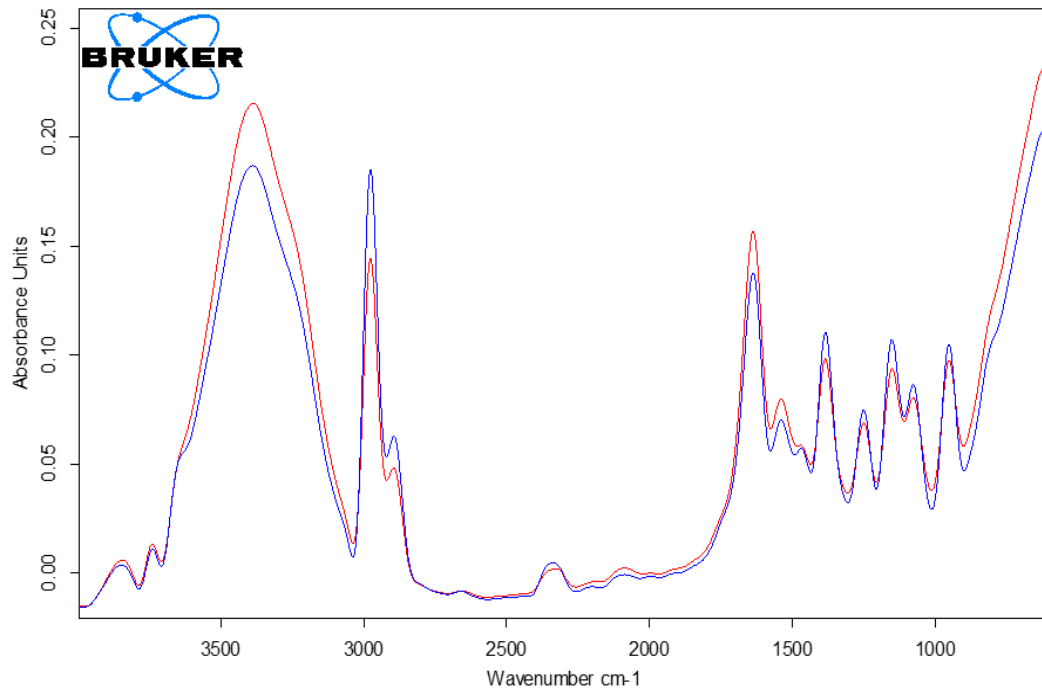


Figure 4.9. Comparison between lung cancer patients (red) and healthy people (blue) by age groups (60-65).

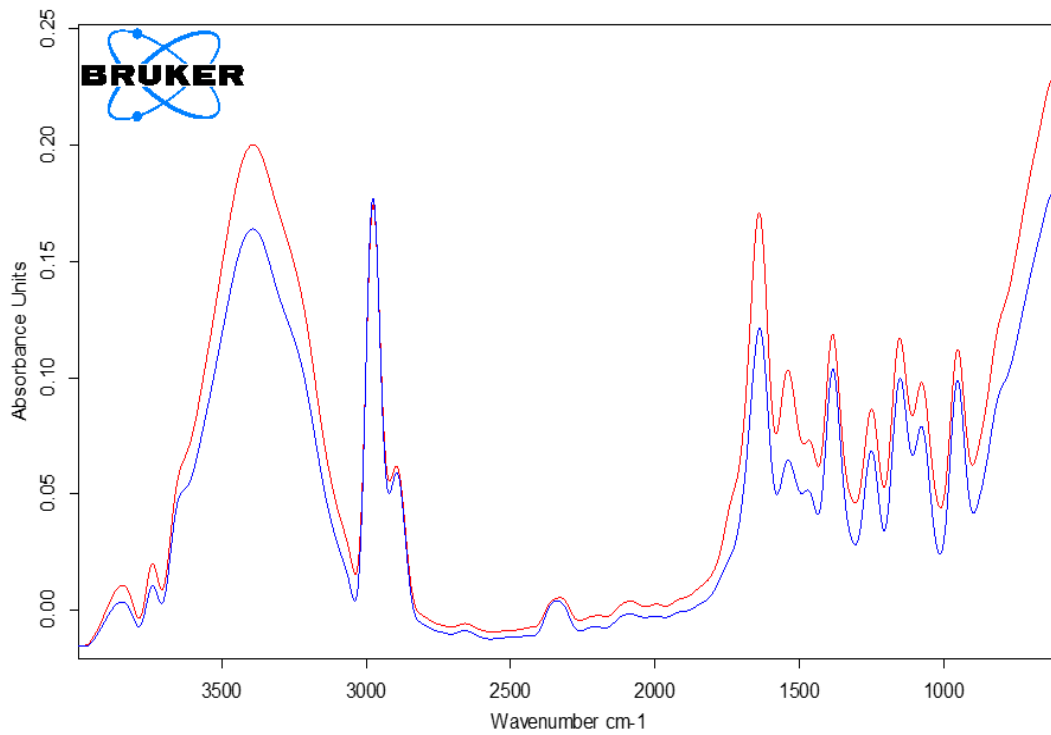


Figure 4.10. Comparison between lung cancer patients (red) and healthy people (blue) by age groups (65-70).



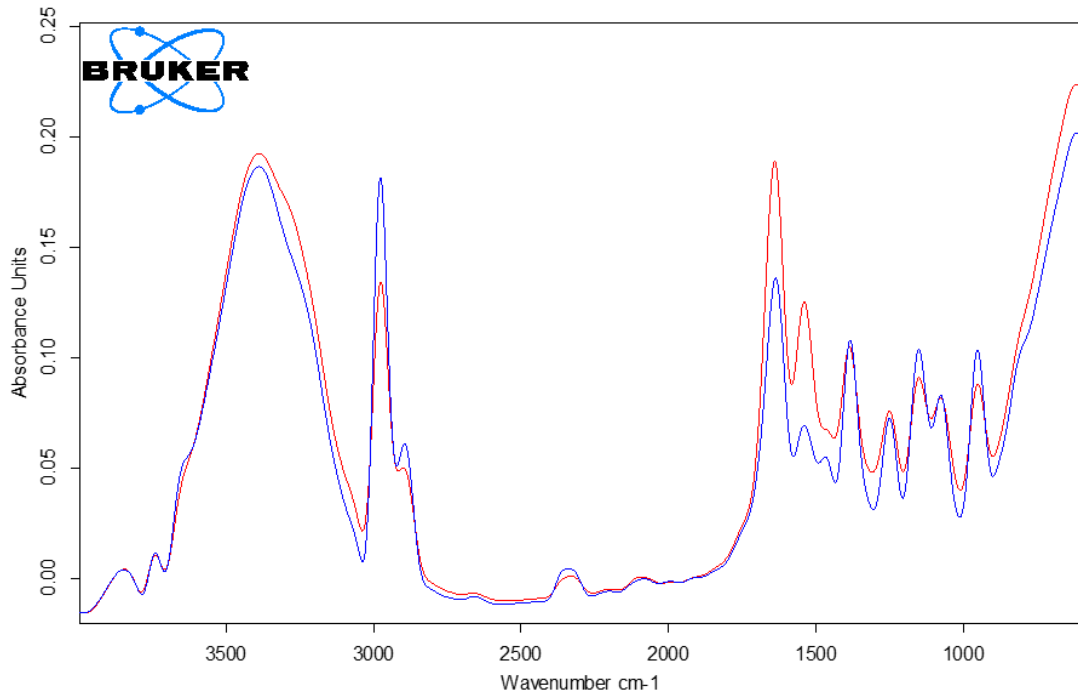


Figure 4.11. Comparison between lung cancer patients (red) and healthy people (blue) by age groups (70-75).

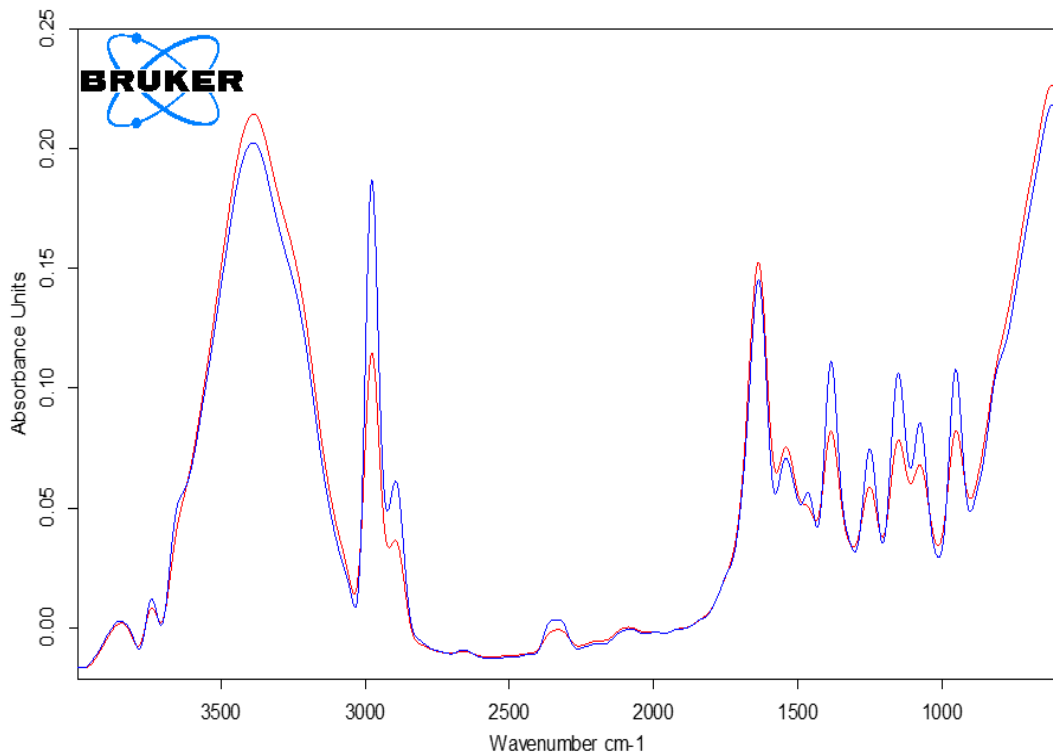


Figure 4.12. Comparison between lung cancer patients (red) and healthy people (blue) by age groups (75-80).

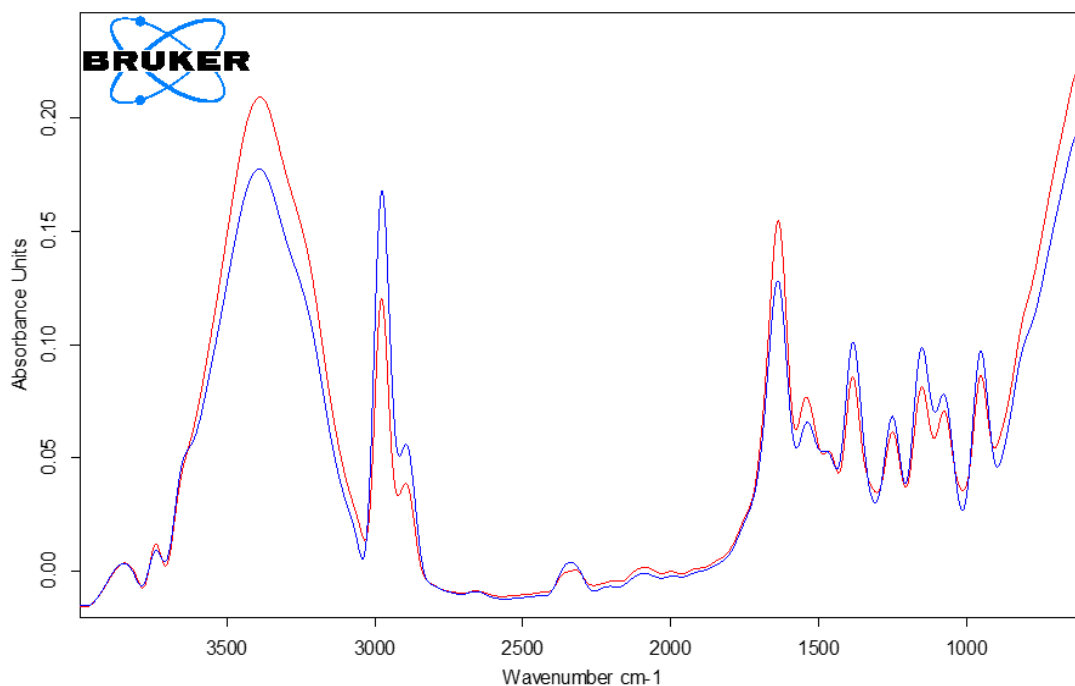


Figure 4.13. Comparison between lung cancer patients (red) and healthy people (blue) by age groups (80-85).

From Table 4.8, these results obtained using the independent sampling test are documented,  $p$ -value, mean  $\pm$  standard deviation. It shows that  $R_1$ (lipids/proteins) mean  $\pm$  standard deviation was  $0.778 \pm 0.369$  for LC patients while  $1.833 \pm 0.254$  for control groups, the ( $P$  value) of ( $R_1 = < 0.001$   $P$  less than 0.05) showing that the ratios were much larger for healthy persons than LC patients.  $R_2$ (proteins /proteins) may represent changes or variations in the structure and composition of proteins. The band frequency of about  $1651 \text{ cm}^{-1}$  is the amide I (proteins) [5], where the mean  $\pm$  standard deviation was  $2.014 \pm 0.308$  for LC patients when  $1.887 \pm 0.232$  for control groups, also indicating the composition of N–H bending also C–N stretching increasing in comparison to the amount of carbonyl stretching in the proteins of LC patient's serum. The  $p$ -value of ( $R_2 = < 0.001$ ,  $p < 0.05$ ) shows that the ratios were much larger for LC patients than normal. The band frequency of about  $1079 \text{ cm}^{-1}$  is  $\text{PO}_2^-$  Nucleic acids are stretched symmetrically,  $R_3$ (nucleic acids /proteins) can

evaluate the DNA levels [120], the mean  $\pm$  standard deviation was  $0.858 \pm 0.160$  for LC patients while  $1.315 \pm 0.071$  for control groups indicating the DNA amount decreased in LC patient's serum. The drop in DNA content might be linked to LC cell necrosis and apoptosis and DNA produced by LC cells [121]. These results were not in agreement with Wang's findings [122]. The p-value of ( $R_3 < 0.001$ ,  $p < 0.05$ ) shows that the ratios were much larger for healthy persons than LC patients. The band frequency of about  $1242 \text{ cm}^{-1}$  is  $\text{PO}^{2-}$ . Nucleic acids are stretched symmetrically, and  $R_4$  (nucleic acids / nucleic acids) can indicate structural changes of nucleic acids [5], the mean  $\pm$  standard deviation was  $1.157 \pm 0.124$  for LC patients when  $1.210 \pm 0.063$  for control groups. The p-value of ( $R_4 = 0.010$ ,  $p < 0.05$ ) shows that the ratios were much larger for healthy persons than LC patients. The band frequency about  $1169 \text{ cm}^{-1}$  threonine, tyrosine, and serine C-O (H) groups of protein residues make significant contributions to [134],  $R_5$  (nucleic acids / proteins) may be used to determine the relative amount of nucleic acids in a sample [5]. The mean  $\pm$  standard deviation was  $1.040 \pm 0.090$  for LC patients while  $0.989 \pm 0.032$  for normal groups, demonstrating that the serum of LC patients contained more nucleic acids than usual. The  $R_5 < 0.001$  ( $p < 0.05$ ) shows that the ratios were much larger for LC patients than normal. We know  $1106$  is due to the different C-O stretching vibrations of C-O-H and C-O-C bonds. The peaks at  $1057 \text{ cm}^{-1}$  wavenumbers correspond to C-O stretching (C-O symmetric stretching of glucose region) [123], in (carbohydrates). The mean  $\pm$  std. deviation of  $R_6$  (nucleic acids / nucleic acids) was ( $0.915 \pm 0.085$ ) for LC patient when ( $0.876 \pm 0.031$ ) for control groups. The p-value of ( $R_6 = 0.003$ ,  $p < 0.05$ ) shows that the ratios were much larger for LC patients than normal. Then  $1257 \text{ cm}^{-1}$  is due to  $\text{PO}^{2-}$ . Antisymmetric [124]. The peaks at  $1006 \text{ cm}^{-1}$  represented the glucose absorption features (carbohydrates). The mean  $\pm$  standard deviation of  $R_7$  (nucleic acids /

nucleic acids) was  $1.533 \pm 0.616$  for LC patients and  $2.202 \pm 0.224$  for healthy groups.  $1506 \text{ cm}^{-1}$  corresponding N-H in-plane bending vibration strongly coupled to C-N stretching vibration of protein [125]. The peaks at  $1057 \text{ cm}^{-1}$  wavenumbers correspond to C-O stretching (C-O symmetric stretching. of glucose region) in carbohydrates. The  $R_7 = < 0.001$  ( $p < 0.05$ ) showing that the ratios were much larger for healthy persons than LC patients. The mean of  $R_8$  (proteins / nucleic acids) was  $1.245 \pm 0.276$  for LC patients when  $1.068 \pm 0.1003$  for control groups. The P value of ( $R_8 = < 0.001$ ,  $p < 0.05$ ), showing that the ratios were much larger for LC patients than normal. The band frequency about  $1655 \text{ cm}^{-1}$  ( $\alpha$ -helix) and  $1685 \text{ cm}^{-1}$  ( $\beta$ -sheet) is the amide I (proteins), additionally, the relevant amount of  $\alpha$ -helix high in LC patient's serum. and  $R_9$  ( $\alpha$ -helix /  $\beta$ -sheet) can display the alterations of proteins components and structures [126], the results was  $1.854 \pm 0.170$  for LC patients when  $1.663 \pm 0.128$  for normal groups, recommending the amount of N-H bending and C-N stretching greater in comparison to the proteins' carbonyl stretching content of LC patients serum. The  $R_9 = < 0.001$  ( $p < 0.05$ ), showing that the ratios were much larger for LC patients than normal.

Table 4.8. FTIR spectral intensity ratio parameters results of healthy and lung cancer expressed as mean  $\pm$  standard deviation.

Ratios $\text{cm}^{-1}$	lung cancer patient (mean $\pm$ Std. Deviation)	Healthy person (mean $\pm$ Std. Deviation)	P-value
<b>R<sub>1</sub>(2959/1544)</b>	$0.778 \pm 0.3696$	$1.833 \pm 0.254$	$< 0.001$
<b>R<sub>2</sub>(1651/1544)</b>	$2.014 \pm 0.308$	$1.887 \pm 0.232$	0.036
<b>R<sub>3</sub>(1079/1544)</b>	$0.858 \pm 0.160$	$1.315 \pm 0.071$	$< 0.001$
<b>R<sub>4</sub>(1079/1242)</b>	$1.157 \pm 0.124$	$1.218 \pm 0.063$	0.010
<b>R<sub>5</sub>(1079/1169)</b>	$1.040 \pm 0.090$	$0.989 \pm 0.032$	$< 0.001$
<b>R<sub>6</sub>(1106/1057)</b>	$0.915 \pm 0.085$	$0.876 \pm 0.031$	0.003
<b>R<sub>7</sub>(1257/1006)</b>	$1.533 \pm 0.616$	$2.202 \pm 0.224$	$< 0.001$
<b>R<sub>8</sub>(1506/1057)</b>	$1.245 \pm 0.276$	$1.068 \pm 0.100$	$< 0.001$
<b>R<sub>9</sub>(<math>\alpha</math>-helix/ <math>\beta</math>-sheet)</b>	$1.854 \pm 0.170$	$1.663 \pm 0.128$	$< 0.001$

From Table 4.9, the results of the Pearson factor were documented to find out the strength of the relationship among the studied ratios of the two groups of LC and healthy people. Pearson's correlation was high, positive or negative, and statistically significant between R<sub>2</sub> and R<sub>9</sub>, R<sub>4</sub> and R<sub>6</sub>. Pearson's correlation was moderate, whether positive or negative and statistically significant between R<sub>1</sub> and (R<sub>3</sub>, R<sub>7</sub>), R<sub>4</sub> and (R<sub>5</sub>), R<sub>2</sub> and (R<sub>7</sub>, R<sub>8</sub>), R<sub>3</sub> and (R<sub>8</sub>), R<sub>8</sub> and (R<sub>9</sub>). However, Pearson's correlation was low, whether positive or negative, and statistically significant between R<sub>1</sub> and R<sub>4</sub>, R<sub>5</sub> and (R<sub>9</sub>), R<sub>1</sub> and (R<sub>9</sub>), R<sub>5</sub> and (R<sub>6</sub>), R<sub>7</sub> and (R<sub>9</sub>). Finally, Pearson's correlation was negligible, whether positive or negative, was not statistically significant between R<sub>1</sub> and R<sub>5</sub>, R<sub>8</sub>), likewise R<sub>2</sub> and (R<sub>3</sub>, R<sub>4</sub>, R<sub>5</sub>, R<sub>6</sub>), R<sub>3</sub> and (R<sub>4</sub>, R<sub>6</sub>, R<sub>7</sub>), R<sub>4</sub> and (R<sub>7</sub>, R<sub>9</sub>), R<sub>5</sub> and (R<sub>7</sub>, R<sub>8</sub>) R<sub>6</sub> and (R<sub>7</sub>, R<sub>9</sub>), R<sub>7</sub> and (R<sub>8</sub>), and statistically significant between R<sub>3</sub> and (R<sub>9</sub>), also R<sub>4</sub> and (R<sub>8</sub>).

Table 4.9. The correlation factor between the studied ratios.

		R <sub>1</sub>	R <sub>2</sub>	R <sub>3</sub>	R <sub>4</sub>	R <sub>5</sub>	R <sub>6</sub>	R <sub>7</sub>	R <sub>8</sub>	R <sub>9</sub>
<b>R<sub>1</sub>(2959/1544)</b>	P. C	1	0.361**	0.655**	0.354**	-0.187-	-0.477- **	0.522**	0.025	-0.351- **
	(p-value)		0.007	<0.001	0.008	0.172	<0.001	<0.001	0.855	0.009
<b>R<sub>2</sub>(1651/1544)</b>	P. C		1	0.039	-0.006-	0.232	0.198	-0.551- **	-0.658**	0.733**
	(p-value)			0.778	0.965	0.089	0.148	<0.001	<0.001	<0.001
<b>R<sub>3</sub>(1079/1544)</b>	P. C			1	-0.113-	-0.304-*	0.223	0.251	-0.559- **	-0.268-*
	(p-value)				0.411	0.024	0.102	0.065	<0.001	0.048
<b>R<sub>4</sub>(1079/1242)</b>	P. C				1	.703**	-0.897- **	0.132	0.287*	0.144
	(p-value)					<0.001	<0.001	0.338	0.034	0.294
<b>R<sub>5</sub>(1079/1169)</b>	P. C					1	-0.456- **	-0.127-	0.016	0.488**
	(p-value)						<0.001	0.356	0.910	<0.001
<b>R<sub>6</sub>(1106/1057)</b>	P. C						1	-0.218-	-0.485- **	-0.041-
	(p-value)							0.109	<0.001	0.768
<b>R<sub>7</sub>(1257/1006)</b>	P. C							1	0.259	-0.447- **
	(p-value)								0.056	0.001
<b>R<sub>8</sub>(1506/1057)</b>	P. C								1	-0.515- **

	(p-value)									<0.001
<b>R<math>\rho</math>(<math>\alpha</math>-helix/ <math>\beta</math>-sheet)</b>	P. C									1
	(p-value)									
** Correlation is significant at the 0.01 level (2- tailed).										
* Correlation is significant at the 0.05 level (2- tailed).										
*** Pearson Correlation=P.C										

### 4.3.3 Flameless atomic absorption spectroscopy (FAAS).

This part includes 65 samples from malignant (LC) patients and 35 from healthy volunteers from the Imam Hussein Center for Cancerous Tumours in Karbala Governorate. They are non-smokers and have no family history questions presented to patients). Also, they live exclusively in the Karbala governorate. The blood serum was also digested to obtain the four concentrations of copper, zinc, lead, and cadmium. Also, it aims to contribute to an accurate conception of the possibility of monitoring one of the types of malignant diseases by linking the concentration of some trace minerals in the serum and access to early detection where diluted concentrations were made for each element to calibrate the device for each element separately as shown in the Figure 4.14 to 4.17.

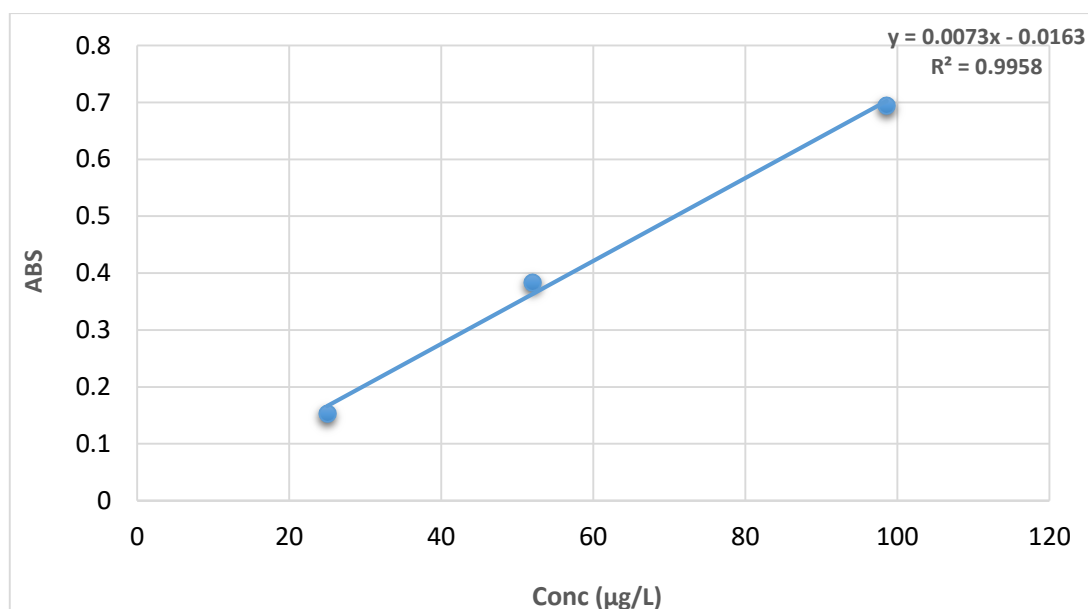


Figure 4.14. Calibration of the atomic absorption system for copper.

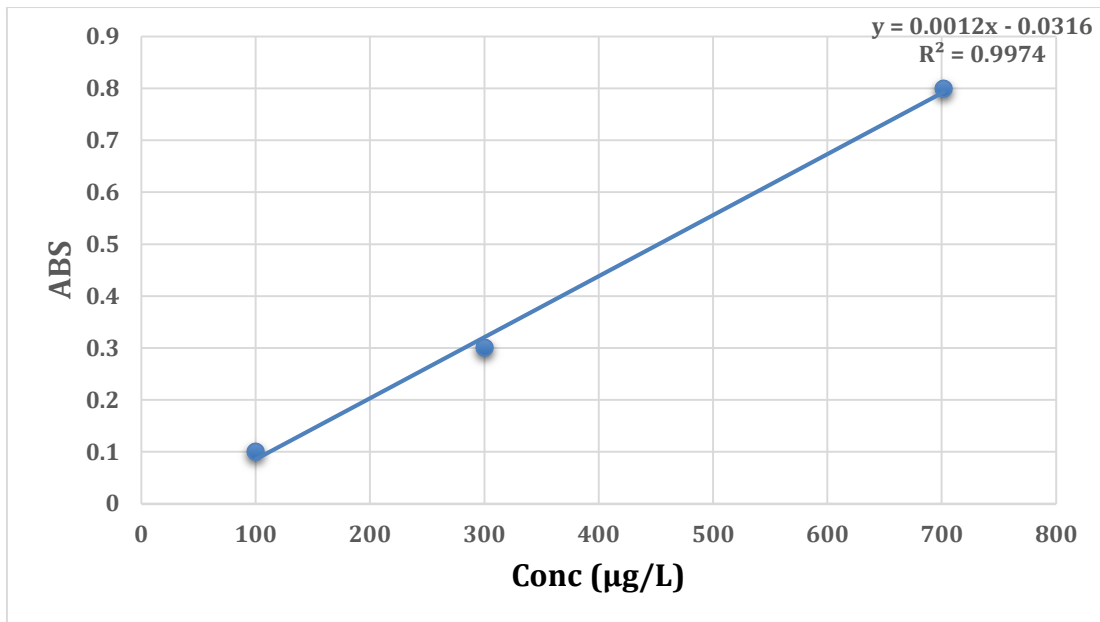


Figure 4.15. Calibration of the atomic absorption system for zinc.

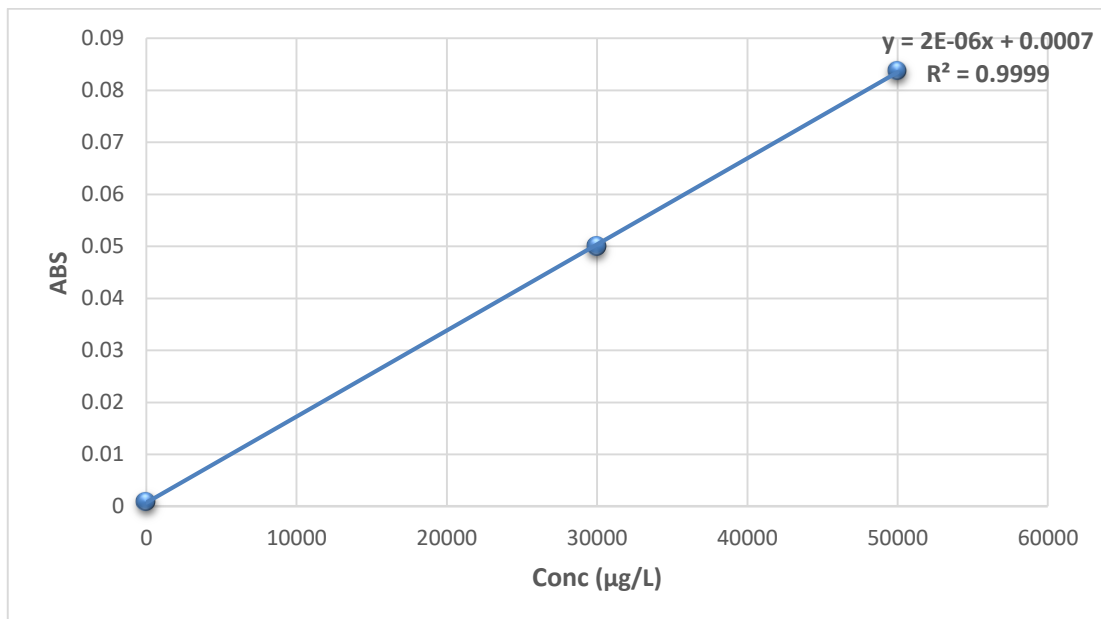


Figure 4.16. Calibration of the atomic absorption system for lead.

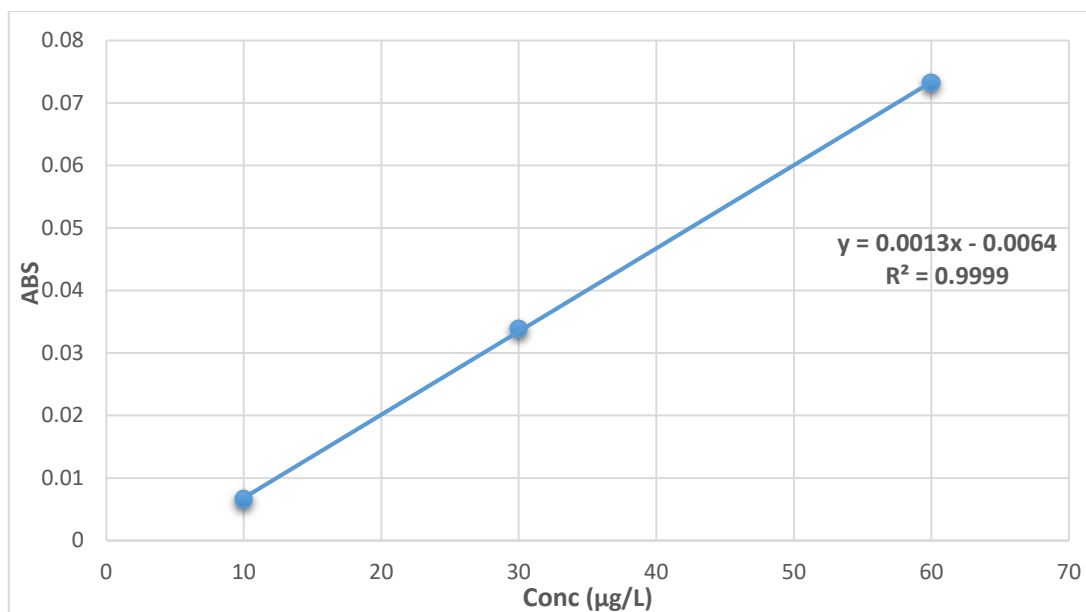


Figure 4.17. Calibration of the atomic absorption system for cadmium.

The study included the healthy and patient groups for each gender. The average age and p-value for each group were calculated as shown in the descriptive table below.

In Table 4.10, the average age mean in the healthy group male and the patient's male group were 65.70 and 59.08 years old, respectively. While the results of the female group, the patients group, and the normal group were 59.80 and 47.26 years old, respectively.

Tables 4.10. The descriptive lung cancer (LC) patient information and healthy samples.

<b>Gender</b>	<b>Group</b>	<b>No</b>	<b>Age(Mean ±SD. Deviation)</b>	<b>p-value</b>
<b>Male</b>	Healthy people	20	65.70 ±12.34 years	0.05
	LC patients	35	59.08 ±11.43 years	
<b>Female</b>	Healthy people	15	47.26 ± 7.29 years	<0.001
	LC patients	30	59.80 ±11.82 years	



From Table 4.11, the range of normal serum levels of Copper and Zinc (75-145, 66-110)  $\mu\text{g/L}$  [127, 128], lead (1-5  $\mu\text{g/L}$ ), and cadmium (5-50  $\text{ng/mL}$ ) [26, 129].

Table 4.11. Comparison of the results of serum zinc, copper, lead, and cadmium between both sexes between healthy and patients groups.

Minerals	Gender	Group	No.	Mean $\pm$ SD. Deviation	P-value
<b>Zn(<math>\mu\text{g/L}</math>)</b>	M	Healthy people	20	1247.02 $\pm$ 937.06	<0.001
		LC patients	35	666.75 $\pm$ 385.18	
	F	healthy people	15	1588.83 $\pm$ 604.25	<0.001
		LC patients	30	531.54 $\pm$ 301.22	
<b>Cu(<math>\mu\text{g/L}</math>)</b>	M	Healthy people	20	155.61 $\pm$ 93.71	0.01
		LC patients	35	218.59 $\pm$ 62.40	
	F	Healthy people	15	152.45 $\pm$ 67.01	0.31
		LC patients	30	176.46 $\pm$ 86.35	
<b>Pb(<math>\mu\text{g/L}</math>)</b>	M	Healthy people	20	5.38 $\pm$ 9.20	0.02
		LC patients	35	13.40 $\pm$ 15.91	
	F	Healthy people	15	8.30 $\pm$ 7.94	0.46
		LC patients	30	10.28 $\pm$ 9.24	
<b>Cd(<math>\mu\text{g/L}</math>)</b>	M	Healthy people	20	14.02 $\pm$ 21.68	<0.001
		LC patients	35	60.87 $\pm$ 20.70	
	F	Healthy people	15	21.41 $\pm$ 15.45	<0.001
		LC patients	30	123.74 $\pm$ 71.91	

It was noticed that the concentration values mean of serum zinc were the highest in the healthy group female and the lowest in the LC patients

female group, while the results of the average values of serum copper showed the highest in the LC patients male group and the lowest in the healthy people female group. The concentration values mean of serum lead were the highest in the LC patients male and the lowest in the healthy people male group. Finally, the average values of serum cadmium showed the highest in the LC patients female group and the lowest in the healthy male group. The  $p < 0.05$  means the relation between the concentration of groups is statistically significant. Figure 4.18 compares Zn, Cu, Pb, and Cd serum concentrations between healthy (male+ female) and LC patients [130, 131].

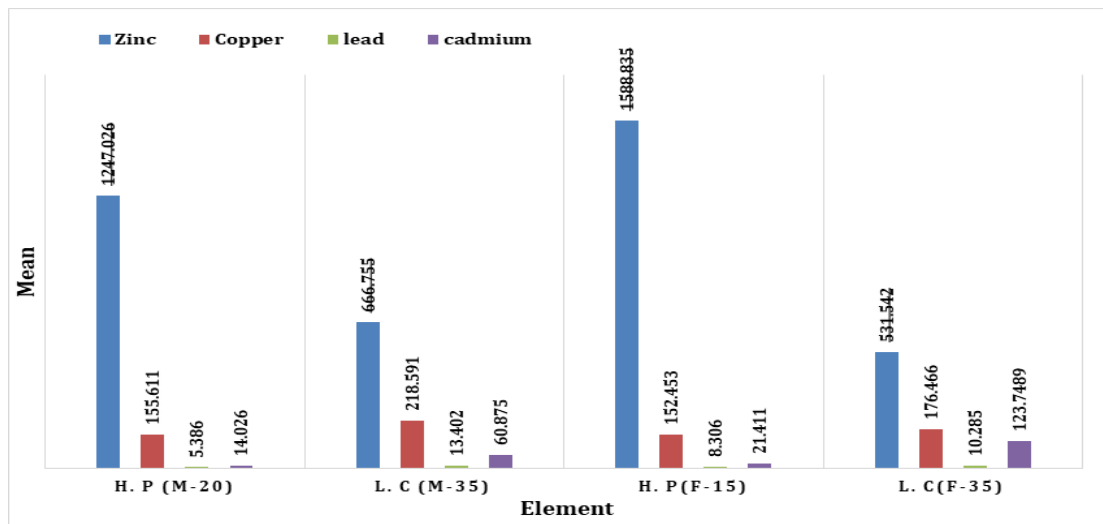


Figure 4-18. Comparison of serum concentrations of Zn, Cu, Pb, and Cd among the studied groups for two genders.

Tables 4.12 and 4.13 compare the results statistically between samples of serum concentrations of zinc, copper, lead, and cadmium for each group of healthy patients using the ANOVA test. For the female patient's group, the Pb level measured compared to the healthy group was lower, and this difference was statistically significant ( $p < 0.05$ ). Serum Zn level was considerably lower with LC patients than normal Cd level was significantly higher than healthy patients. Cu level was considerably low

in the serum of the LC group than healthy. However, for the male patient's group, serum Pb levels were equal in the LC group and healthy.

Table 4.12. Comparison of the results statistically among samples of serum concentrations of zinc, copper, lead, and cadmium for healthy and patients females.

Group	Minerals	No.	Mean	Std. Deviation	Min.	Max.	Sig.
Healthy	Pb( $\mu\text{g/L}$ )	15	8.30	7.94	0.04	25.82	<0.001
	Zn( $\mu\text{g/L}$ )	15	1588.83	604.25	874.81	3537.34	
	Cd( $\mu\text{g/L}$ )	15	21.41	15.45	1	46.21	
	Cu( $\mu\text{g/L}$ )	15	152.45	67.01	64.35	257.97	
LC	Pb( $\mu\text{g/L}$ )	30	10.28	9.24	0.07	41.65	
	Zn( $\mu\text{g/L}$ )	30	531.54	301.22	167.64	1615.50	
	Cd( $\mu\text{g/L}$ )	30	123.74	71.91	10.08	284.82	
	Cu( $\mu\text{g/L}$ )	30	176.46	86.35	0	358.82	

Table 4.13. Comparison of the results statistically between samples of serum concentrations Zn, Cu, Pb, and Cd for healthy and patients males.

Group	Minerals	No.	Mean	Std. Deviation	Min.	Max.	Sig.
Healthy	Pb( $\mu\text{g/L}$ )	20	5.22	8.99	0.04	36.81	<0.001
	Zn( $\mu\text{g/L}$ )	20	1247.02	937.06	620.29	5129.99	
	Cd( $\mu\text{g/L}$ )	20	14.02	21.68	1	80.65	
	Cu( $\mu\text{g/L}$ )	20	155.61	93.71	46.26	329.24	
LC	Pb( $\mu\text{g/L}$ )	35	13.40	15.916	0.04	73.11	
	Zn( $\mu\text{g/L}$ )	35	666.75	385.18	294.14	2129.11	
	Cd( $\mu\text{g/L}$ )	35	60.87	20.70	11.76	98.30	
	Cu( $\mu\text{g/L}$ )	35	218.59	62.40	52.95	371.36	

Zn value was lower in LC than in healthy controls, while serum Cd and Cu levels were also higher in the LC group than healthy, where the  $p < 0.05$  means the relation between the groups' concentration is statistically

significant. The mean concentration for the female patient's Pb, Cd, and Cu in the serum of LC patients was greater than in the healthy, but the correlation was significant ( $p < 0.05$ ), as seen in Table 4.12. The mean concentration for the male patient's group of Pb, Cd in the serum of LC patients was higher than in the healthy, but the correlation was significant ( $p < 0.05$ ), as seen in Table 4.13. These results were reported previously in LC patients [142].

#### 4.3.4 Correlation coefficients

Pearson's correlation coefficients were calculated in serum samples from LC patients and healthy persons for the four trace elements (Zn, Cu, Pb, and Cd). the healthy group is in Table 4.14.

Table 4.14. Correlation among samples of serum concentrations Zn, Cu, Pb, and Cd minerals in the healthy group.

		Female			Male		
		Pb	Zn	Cd	Pb	Zn	Cd
Pb	P*	1			1		
	r**						
Zn	P*	0.05	1		<0.001	1	
	r**	0.80			0.98		
Cd	P*	-0.04	-0.13	1	-0.10	-0.52	1
	r**	0.83	0.57		0.71	0.04	
Cu	P*	0.61	-0.19	0.21	-0.08	0.45	-0.33
	r**	<0.001	0.40	0.37		0.08	0.22

\*: Probability.

\*\* : Correlation coefficient.

Cd levels were negatively correlated with Pb and Zn values. The values of Cu and Zn, and Cd were negatively correlated. Zn and Pb levels. Pb and Zn levels, as well as Cu and Zn levels, showed a positive association. Cd levels were negatively correlated with Pb and Zn values. Cu levels were negatively correlated with Pb and Cd values. Zn and Pb levels, as well as Cu and Pb levels, were positively correlated.

In Table 4.15, the LC female group was negatively associated with Pb levels, while Cu, Pb, and Cd levels had a positive correlation. Cd levels were negatively correlated with Pb and Zn values. Cd levels were negatively correlated with Pb and Zn values. The amounts of Cu and Zn were negatively correlated. There was a positive link between the Cd and Pb, Cd level, and the Cu and Pb, Cd level.

Table 4.15. Correlation among samples of serum concentrations Zn, Cu, Pb, and Cd minerals in the LC group.

		Female			Male		
		Pb	Zn	Cd	Pb	Zn	Cd
Pb	r	1			1		
	p						
Zn	r	-0.23	1		-0.13	1	
	p	0.20			0.44		
Cd	r	-0.10	-0.04	1	<0.001	-0.26	
	p	0.58	0.79		0.95	0.12	
Cu	r	0.30	-0.13	0.02	0.02	-0.23	<0.001
	p	0.10	0.49	0.89	0.86	0.18	0.99

In Table 4.15, the LC male group. The levels of Pb and Zn were inversely correlated. Cd and Zn levels did not correlate well with one another. Cu and Zn levels exhibited a negative connection [131]

From Figure 4.19, the findings of this investigation revealed that serum copper and zinc levels did not differ substantially between male and female LC patients and healthy people.

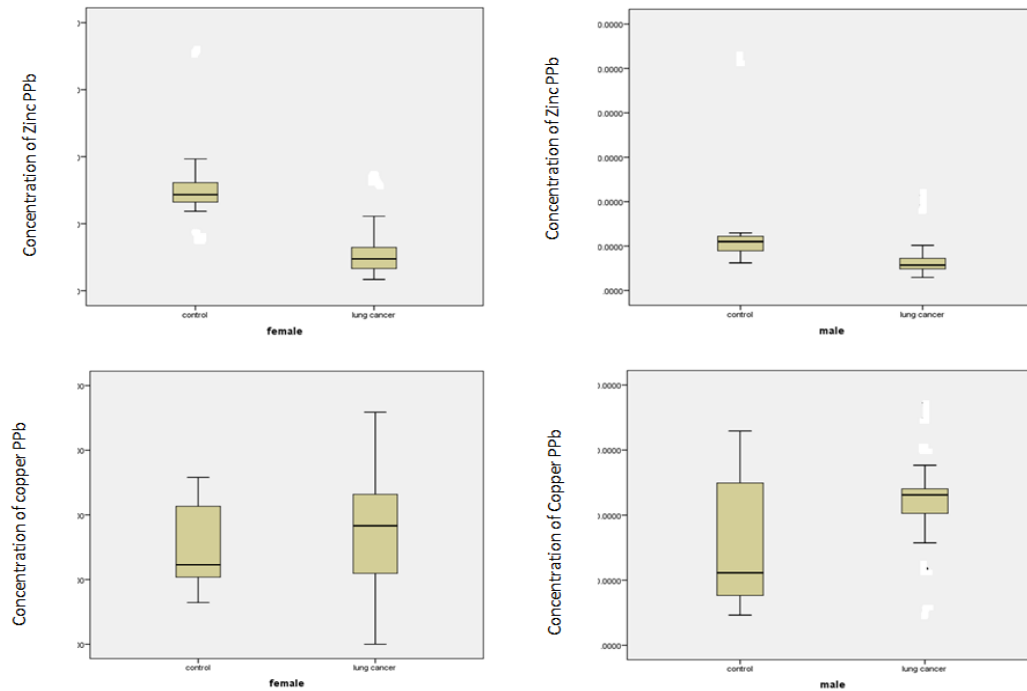


Figure 4.19. Serum concentrations of Zinc, Copper for lung cancer patients and health for each group.

From Figure 4.20, The findings of this investigation revealed that serum lead and Cadmium levels did not differ substantially between male and female LC patients and healthy people. These results were reported previously [131, 132]. Serum zinc was lower, while serum Cu levels and serum Cu/Zn ratios were higher in LC patients compared to the control group [132]. In a meta-analysis, the pooled results showed sufficient evidence approving the association between serum zinc levels and LC risk [133]. Furthermore, the serum zinc levels in LC were significantly lower than in controls.

Meanwhile, consistent results were obtained both in European populations and Asian populations. This meta-analysis suggested that serum zinc levels were significantly lower in lung cancer patients than in controls [133]. The reason may be due to the fact that cancer cells may consume zinc in the circulation to maintain cancer growth and maintain its membrane integrity [134]. Zhang et al. performed a meta-analysis using 33

articles to explore the association between serum copper levels and the risk of lung cancer [130]. Results from their study suggested that serum copper levels were higher in lung cancer than that in controls. Copper and zinc are closely related trace elements in cell proliferation, growth, gene expression, apoptosis, and other processes. These two trace elements are necessary for superoxide dismutase's proper activity due to their integral role as cofactors or ions stabilizing the molecular structure [135]. Zinc deficiency may have adverse events, especially on immune function[136]. Gómez et al. studied the association of zinc and its role in lung cancer [137]. In general, the zinc microenvironment may play a key role in oxidative stress, apoptosis, and/or cell signalling alterations that influence the behavior of cancer cells [137], which may play a role in preventing lung cancer. These studies support the hypothesis that disturbed redox status in lung cancer patients is linked with alterations in trace element status regarding Zn and Cu.

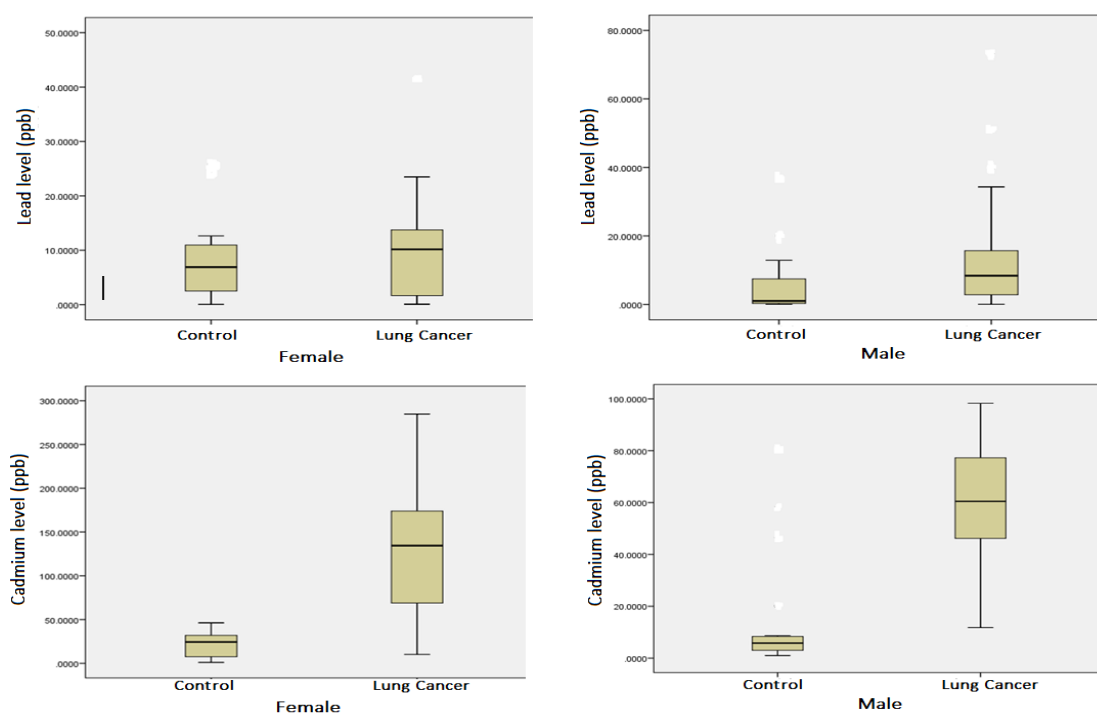


Figure 4.20. Serum concentrations of lead, Cadmium for lung cancer patients and health for each group.

This study concluded that the level of Pb in patients and the healthy group was higher than acceptable limits [138]. Heavy metals such as cadmium, lead, arsenic, and mercury play an important carcinogenic role, especially in lung cancer [139]. Previous studies found that cadmium is associated with the risk of lung cancer [140]. Cadmium and cadmium compounds are known to be human carcinogens based on findings of increased risk of lung cancer and pancreatic cancer among exposed workers [141]. There is an increase in the LC in persons exposed to cadmium more than in the nonexposed population [142, 143]. Recently, it is Cadmium level has been strongly associated with the occurrence of lung cancer, and blood cadmium level may be a valuable marker for the early detection of lung cancers [144]

By comparing our results, we can see that the values are similar to some studies but not to others, which is normal due to differences in the geology of the area of residence, the type of food consumed, the use of nutritional supplements or therapeutic supplements, as well as the nature of people's work, all of which cause changes in element concentrations as shown in Table 4.16.

Table 4.16. Global comparison among mean serum zinc, copper, lead, and cadmium levels for patients and healthy.

No.	Country	Mean			Type	Reference
			Patients	Healthy people		
1.	China	Cu	1.607ppm	1.404 ppm	Lung cancer	[145]
		Zn	0.460 ppm	0.525 ppm		
2.	China	Cu	1.151 ppm	1.068 ppm	Lung cancer	[146]
		Zn	0.812 ppm	1.039 ppm		
3.	China	Cu	1.508 ppm	1.403 ppm	Lung cancer	[147]
		Zn	0.797 ppm	0.908 ppm		
4.	China	Cu	1.379 ppm	1.093 ppm	Lung cancer	[148]
		Zn	0.726 ppm	0.876 ppm		
5.	Poland	Cu	1.455 ppm	0.953ppm	Lung cancer	[149]
		Zn	0.785 ppm	0.903 ppm		
6.	China	Cu	1.04 ppm	0.77 ppm	Lung cancer	[150]



		Zn	0.74 ppm	1.83 ppm		
7.	China	Cu	1.207 ppm	0.948 ppm	Lung cancer	[51]
		Zn	1.159 ppm	1.149 ppm		
8.	Turkey	Cu	0.977 ppm	1.748 ppm	Lung cancer	[130]
		Zn	0.539 ppm	2.051 ppm		
9.	China	Cu	1.471 ppm	0.923 ppm	Lung cancer	[151]
		Zn	0.594 ppm	1.075 ppm		
10.	China	Cu	1.624 ppm	1.285 ppm	Lung cancer	[147]
		Zn	0.673 ppm	1.27 ppm		
11.	Iraq Karbala M F	Cu	2.186 ppm 1.765 ppm	1.556 ppm 1.525 ppm	Lung cancer	current study
		Zn	0.667 ppm 0.532 ppm	1.247 ppm 1.589 ppm		
12.	Iran	Pb	5.546 ppb	4.927 ppb	prostate	[26]
		Cd	2.642 ppb	0.52 ppb		
13.	Iraq	Pb	12.993 ppb	12.249 ppb	breast	[152]
		Cd	0.7 ppb	0.7 ppb		
14.	Taiwan	Pb	2.25 ppb	1.13 ppb	breast	[153]
15.	Yuzuncu Yil	Pb	17.88 ppb	2.68 ppb	Colon	[154]
		Cd	1.832 ppb	0.27 ppb		
16.	Yuzuncu Yil	Pb	2.227 ppb	0.641 ppb	lung	[27]
		Cd	0.35 ppb	0.25 ppb		
17.	Turkey	Pb	22.27 ppb	6.41 ppb	[150]	[155]
		Cd	0.313 ppb	4.88 ppb		
18.	Pakistan	Pb	12.73 ppb	5.38 ppb	Colorectal	[156]
		Cd	0.563 ppb	0.264 ppb		
19.	Yuzuncu Yil	Pb	17.88 ppb	2.68 ppb	Colon	[154]
		Cd	1.832 ppb	0.27 ppb		
20.	Cu		0.75-1.45 ppm	Ranges for the trace elements		[127, 128]
	Zn		0.66-1.10 ppm			
21.	Pb		1-5 ppb	Ranges for the trace elements		[26, 129]
	Cd		0.5-5.0 ppb			
22.	Iraq Karbala (M+F)	Pb	13.402 ppb 10.285 ppb	5.385 ppb 8.306 ppb	lung	Current study
		Cd	6.088 ppb 12.375 ppb	1.4025 ppb 2.1411 ppb		

The results indicated an increase in the serum Cd level in the Iraqi LC patients compared with the cancer patients from other countries. Higher

Cd levels have been reported previously in healthy Iraqis [157] and LC patients from different countries [140, 144]. Cadmium is released into the environment through human activities, particularly industrial operations and waste disposal [29]. Therefore, attention should be focused on the sources of pollution in Karbala city. By comparing our results with previous work performed on LC patients in Karbala city [34], the same results were obtained, indicating the trend of the effect of higher heavy metals in the serum of LC patients. Serum lead, cadmium, and copper were higher in lung cancer patients than in healthy subjects in Karbala city [34].

#### **4.3.5 Solid state nuclear track detector**

This part includes alpha emitters ( $^{222}\text{Rn}$ ,  $^{226}\text{Ra}$ , and  $^{238}\text{U}$ ) using a CR-39 detector measured in blood samples taken from the Imam Hussein center for malignant tumors in Karbala. Our results were consistent with several studies [58, 100, 102, 158, 159].

The concentration of radon and the density of the track in the blood samples of LC patients and the normal group for females were found using equations 2.7 and 2.8, as presented in Tables 4.17 and 4.18 and Figure 4.21.

Table 4.17. Radon, radium, and uranium concentrations in the female group's blood samples health.

Code samples	$\rho$ (Track/cm <sup>2</sup> )	$C_{Rn}^a$ (Bq/m <sup>3</sup> )	$C_{Rn}^s$ (Bq/m <sup>3</sup> )	$C_{Rn}^s$ (Bq/kg)	$C_{Ra}^{s,ac}$ (Bq/kg)	$C_U$ (ppm)	H(msv/y)
<b>NF1</b>	897.478	35.614	6395.812	35.320	2.305	2.801	1.398
<b>NF2</b>	721.999	28.651	5145.272	28.414	1.854	2.253	1.124
<b>NF3</b>	217.196	8.619	1547.830	8.548	0.558	0.678	0.338
<b>NF4</b>	481.616	19.112	3432	18.954	1.237	1.503	0.750
<b>NF5</b>	503.251	19.970	3586.380	19.805	1.292	1.571	0.784
<b>NF6</b>	589.788	23.404	4203.085	23.211	1.514	1.841	0.918
<b>NF7</b>	173.927	6.902	1239.478	6.845	0.447	0.543	0.271
<b>NF8</b>	241.234	9.573	1719.137	9.494	0.619	0.753	0.376
<b>NF9</b>	262.868	10.431	1873.313	10.345	0.675	0.820	0.409
<b>NF10</b>	306.137	12.148	2181.665	12.048	0.786	0.955	0.477
<b>Min</b>	173.927	6.902	1239.478	6.845	0.447	0.543	0.271
<b>Max</b>	897.478	35.614	6395.812	35.32	2.305	2.801	1.398
<b>Average</b>	439.549	17.442	3132.397	17.298	1.128	1.371	0.684

Table 4.18. Radon, radium, and uranium concentration in blood samples patients for the female group.

Code samples	$\rho$ (Track/cm <sup>2</sup> )	$C_{Rn}^a$ (Bq/m <sup>3</sup> )	$C_{Rn}^s$ (Bq/m <sup>3</sup> )	$C_{Rn}^s$ (Bq/kg)	$C_{Ra}^{s,ac}$ (Bq/kg)	$C_U$ (ppm)	H(msv/y)
<b>PF1</b>	3436.006	136.349	24486.450	135.222	8.823	10.723	5.351
<b>PF2</b>	1926.333	76.442	13727.880	75.810	4.946	6.012	3.000
<b>PF3</b>	1616.226	64.136	11517.920	63.606	4.150	5.044	2.517
<b>PF4</b>	2012.875	79.876	14344.610	79.216	5.169	6.282	3.135
<b>PF5</b>	1224.398	48.587	8725.584	48.186	3.144	3.821	1.907
<b>PF6</b>	2407.121	95.521	17154.180	94.731	6.181	7.512	3.749
<b>PF7</b>	1291.705	51.258	9205.242	50.834	3.317	4.031	2.012
<b>PF8</b>	4224.497	167.639	30105.570	166.253	10.848	13.184	6.579
<b>PF9</b>	2539.337	100.767	18096.410	99.934	6.521	7.925	3.955
<b>PF10</b>	1729.211	68.619	12323.100	68.052	4.440	5.397	2.693
<b>PF11</b>	2320.579	92.086	16537.440	91.325	5.959	7.242	3.614
<b>PF12</b>	854.209	33.897	6087.459	33.617	2.193	2.666	1.330
<b>PF13</b>	1094.591	43.436	7800.526	43.077	2.811	3.416	1.705
<b>PF14</b>	2058.550	81.688	14670.110	81.013	5.286	6.424	3.206
<b>PF15</b>	1467.184	58.222	10455.780	57.740	3.767	4.579	2.285
<b>PF16</b>	854.209	33.897	6087.459	33.617	2.193	2.666	1.330
<b>PF17</b>	2231.634	88.557	15903.580	87.825	5.730	6.965	3.475
<b>PF18</b>	2779.731	110.307	19809.550	109.395	7.138	8.675	4.329
<b>PF19</b>	3282.154	130.244	23390.040	129.167	8.428	10.243	5.111
<b>PF20</b>	984.015	39.048	7012.516	38.725	2.527	3.071	1.532
<b>PF21</b>	1904.698	75.583	13573.700	74.958	4.891	5.944	2.966
<b>PF22</b>	3873.522	153.711	27604.380	152.440	9.947	12.089	6.032
<b>PF23</b>	3565.818	141.501	25411.550	140.331	9.156	11.128	5.553
<b>PF24</b>	3592.261	142.550	25600.000	141.372	9.224	11.211	5.594
<b>NF25</b>	765.268	30.368	5453.625	30.117	1.965	2.388	1.192
<b>Min</b>	765.268	30.368	5453.625	30.117	1.965	2.388	1.192
<b>Max</b>	4224.497	167.639	30105.57	166.253	10.848	13.184	6.579
<b>Average</b>	2161.445	85.771	15403.39	85.062	5.550	6.745	3.366

Where the lowest concentration of radon in the air, the samples were (NF7, 6.902 (Bq/m<sup>3</sup>)). While the highest concentration was (PF8, 167.639 (Bq/m<sup>3</sup>)) as in

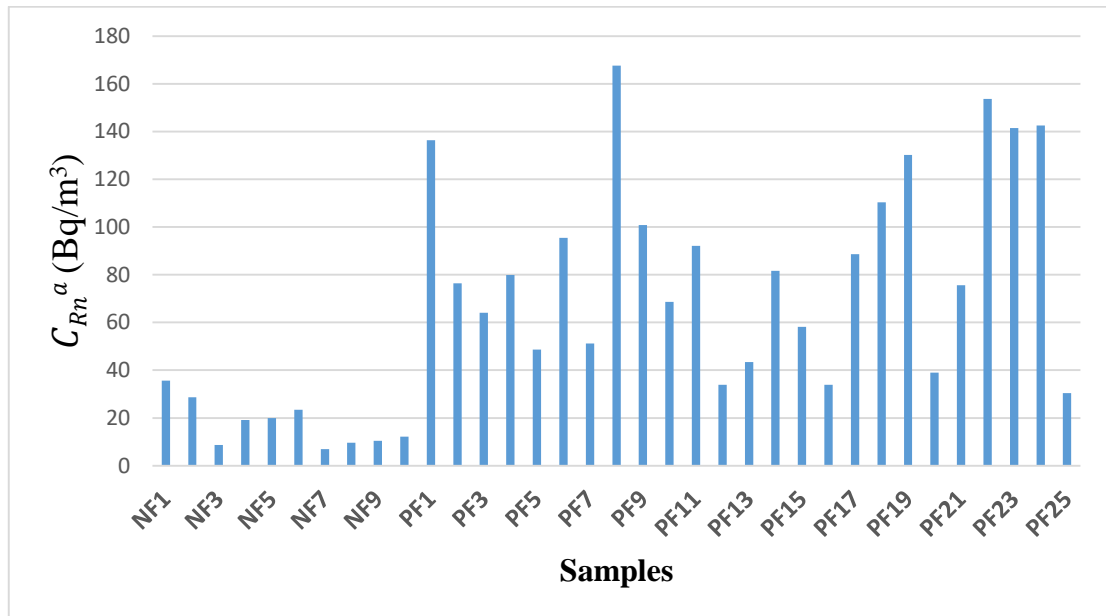


Figure 4.21. Radon concentrations for lung cancer patients and health for the female group.

It has been reported that radiation is higher in LC patients than in healthy controls [160, 161]. There is a huge risk of LC in any state of using radiation, especially in the screening for cancer [161] and after radiotherapy [162].

The activity of radium concentration in the blood samples of LC patients and the healthy group for females was found by using equation 2.11. The lowest activity concentration of radium in the samples was (NF7, 0.447 (Bq/kg)). At the same time, the highest concentration was (PF8, 10.848 (Bq/kg)), as in Table 4.17, 4.18, and Figure 4.22.

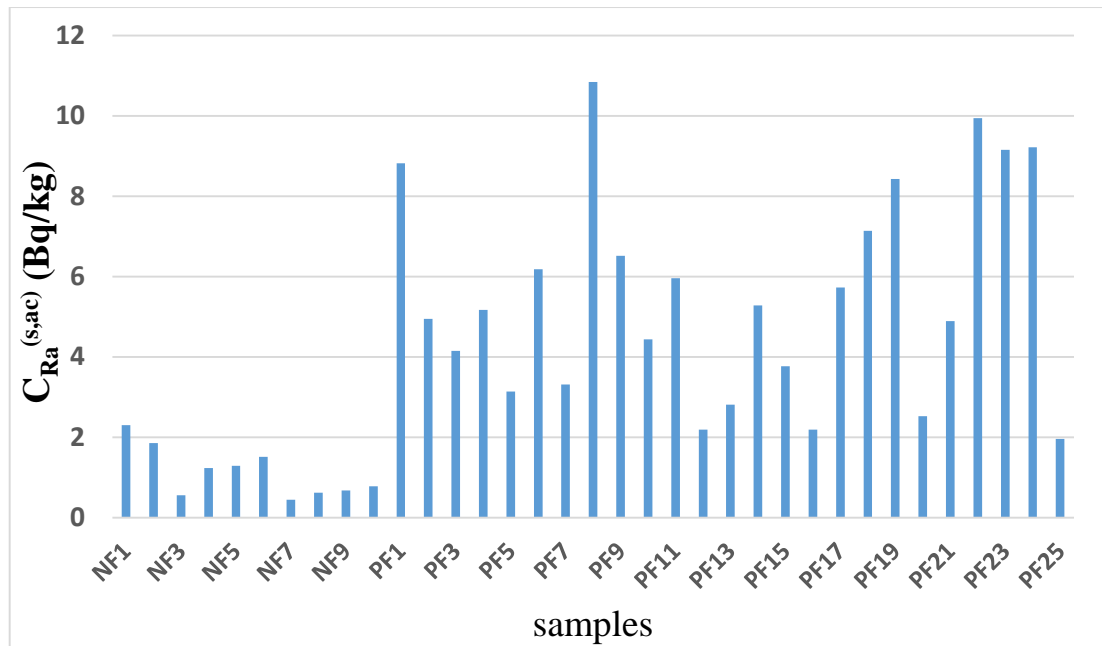


Figure 4.22. The activity concentration of radium for lung cancer patients and health for the female group.

The concentration of uranium and the annual effective dose of radon in the blood samples of LC patients and the health group for females was found using equations 2.13 and 2.14, where the lowest concentration of uranium in the sample was (NF7, 0.543 ppm). In contrast, the highest concentration was (PF8, 13.184 (ppm)), where the lowest concentration of the annual effective dose of radon in the sample was (NF7, 0.271 msv/y), while the highest concentration was (PF8, 6.579 (msv/y), Where was noticed that the average of the annual effective dose of patients is three times greater than the average of healthy people as in Tables 4.17 and 4.18 and Figure 4.23 and 4.24.

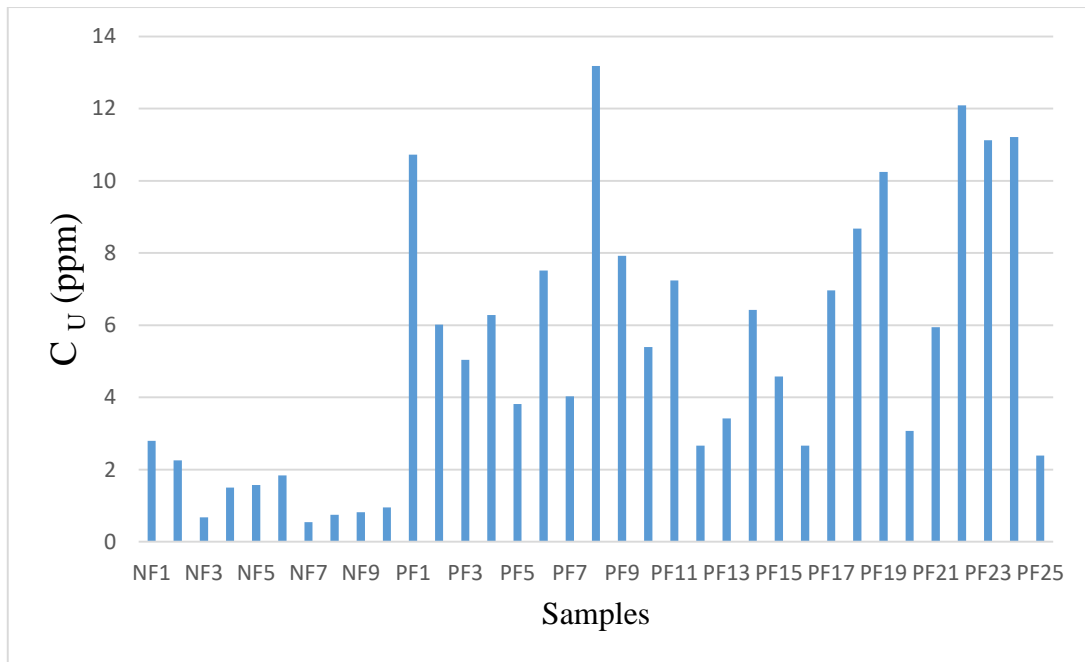


Figure 4.23. Uranium concentrations in lung cancer patients and healthy female groups.

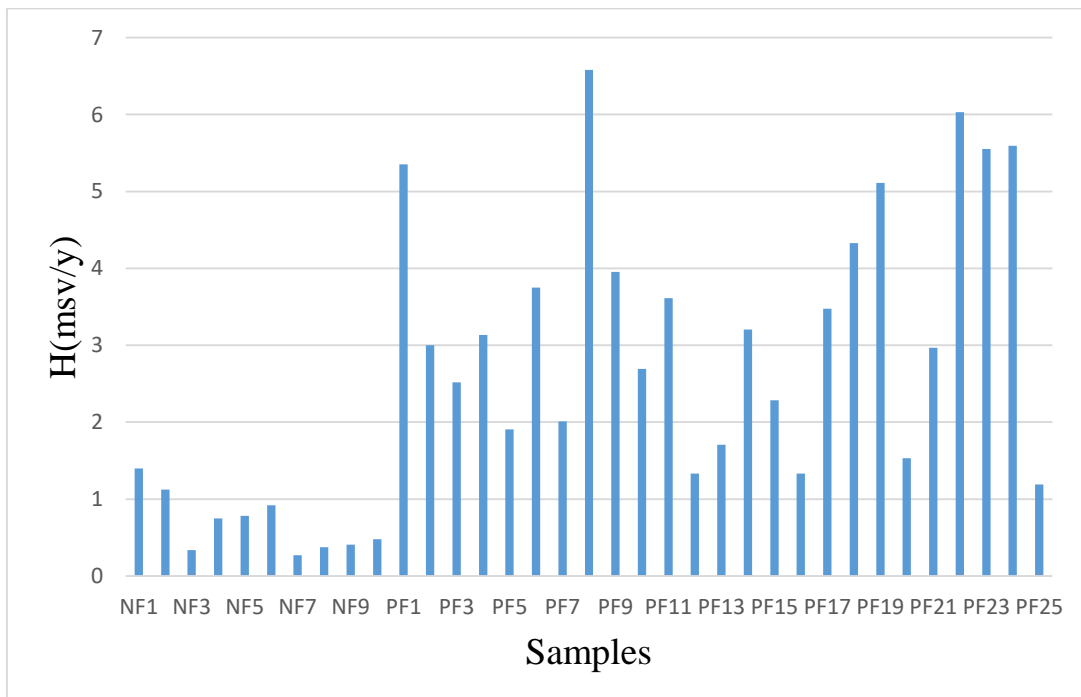


Figure 4.24. The annual effective dose of radon concentration for lung cancer patients and healthy female group.

In Tables 4.19 and 4.20, where the lowest concentration of radon in the samples was (NM15, 4.326 (Bq/m<sup>3</sup>), while the highest concentration was (PM16, 200.550 (Bq/m<sup>3</sup>), as and Figure 4.25.

Table 4.19. Radon, radium, and uranium concentration in blood samples health for the male group.

Code samples	$\rho$ (Track/cm <sup>2</sup> )	$C_{Rn}^a$ (Bq/m <sup>3</sup> )	$C_{Rn}^s$ (Bq/m <sup>3</sup> )	$C_{Rn}^s$ (Bq/kg)	$C_{Ra}^{s,ac}$ (Bq/kg)	$C_U$ (ppm)	H(msv/y)
<b>NM1</b>	546.520	21.687	3894.733	21.508	1.403	1.706	0.851
<b>NM2</b>	459.982	18.253	3278.028	18.102	1.181	1.436	0.716
<b>NM3</b>	503.251	19.970	3586.380	19.805	1.292	1.571	0.784
<b>NM4</b>	219.600	8.714	1564.961	8.642	0.564	0.685	0.342
<b>NM5</b>	284.503	11.290	2027.489	11.196	0.731	0.888	0.443
<b>NM6</b>	306.137	12.148	2181.665	12.048	0.786	0.955	0.477
<b>NM7</b>	546.520	21.687	3894.733	21.508	1.403	1.706	0.851
<b>NM8</b>	524.885	20.829	3740.557	20.657	1.348	1.638	0.817
<b>NM9</b>	589.788	23.404	4203.085	23.211	1.514	1.841	0.918
<b>NM10</b>	524.885	20.829	3740.557	20.657	1.348	1.638	0.817
<b>NM11</b>	284.503	11.290	2027.489	11.196	0.731	0.888	0.443
<b>NM12</b>	546.520	21.687	3894.733	21.508	1.403	1.706	0.851
<b>NM13</b>	327.772	13.007	2335.841	12.899	0.842	1.023	0.510
<b>NM14</b>	171.532	6.806	1222.347	6.750	0.440	0.535	0.267
<b>NM15</b>	109.024	4.326	776.949	4.291	0.280	0.340	0.170
<b>Min</b>	109.024	4.326	776.949	4.291	0.28	0.34	0.17
<b>Max</b>	589.788	23.404	4203.085	23.211	1.514	1.841	0.918
<b>Average</b>	396.361	15.728	2824.636	15.598	1.034	1.237	0.6171



Table 4.20. Radon, radium, and uranium concentration in blood samples patients for the male group.

Code samples	$\rho$ (Track/cm <sup>2</sup> )	$C_{Rn}^a$ (Bq/m <sup>3</sup> )	$C_{Rn}^s$ (Bq/m <sup>3</sup> )	$C_{Rn}^s$ (Bq/kg)	$C_{Ra}^{s,ac}$ (Bq/kg)	$C_U$ (ppm)	H(msv/y)
<b>PM1</b>	1794.117	71.195	12785.650	70.607	4.607	5.599	2.794
<b>PM2</b>	1969.604	78.159	14036.250	77.513	5.058	6.147	3.067
<b>PM3</b>	2012.875	79.876	14344.610	79.216	5.169	6.282	3.135
<b>PM4</b>	2407.121	95.521	17154.180	94.731	6.181	7.512	3.749
<b>PM5</b>	2539.337	100.767	18096.410	99.934	6.521	7.925	3.955
<b>PM6</b>	2058.550	81.688	14670.110	81.013	5.286	6.424	3.206
<b>PM7</b>	2253.269	89.415	16057.760	88.676	5.786	7.032	3.509
<b>PM8</b>	3128.302	124.139	22293.620	123.113	8.033	9.763	4.872
<b>PM9</b>	2428.756	96.379	17308.360	95.582	6.237	7.580	3.782
<b>PM10</b>	1553.723	61.656	11072.500	61.146	3.990	4.849	2.420
<b>PM11</b>	2560.973	101.626	18250.590	100.786	6.576	7.992	3.988
<b>PM12</b>	2779.731	110.307	19809.550	109.395	7.138	8.675	4.329
<b>PM13</b>	2823.002	112.024	20117.920	111.098	7.249	8.810	4.396
<b>PM14</b>	3173.977	125.951	22619.120	124.910	8.150	9.906	4.943
<b>PM15</b>	2779.731	110.307	19809.550	109.395	7.138	8.675	4.329
<b>PM16</b>	5053.854	200.550	36015.930	198.892	12.977	15.772	7.871
<b>PM17</b>	3500.912	138.925	24949.000	137.777	8.990	10.926	5.452
<b>PM18</b>	1837.388	72.912	13094.010	72.309	4.718	5.734	2.861
<b>PM19</b>	2142.688	85.027	15269.710	84.324	5.502	6.687	3.337
<b>PM20</b>	3479.277	138.067	24794.820	136.925	8.934	10.858	5.418
<b>PM21</b>	3128.302	124.139	22293.620	123.113	8.033	9.763	4.872
<b>PM22</b>	3414.370	135.491	24332.270	134.371	8.767	10.656	5.317
<b>PM23</b>	3260.518	129.386	23235.850	128.316	8.372	10.176	5.078
<b>PM24</b>	2274.904	90.274	16211.940	89.528	5.842	7.100	3.543
<b>PM25</b>	1532.088	60.797	10918.320	60.294	3.934	4.781	2.386
<b>Min</b>	1532.088	60.797	10918.32	60.294	3.934	4.781	2.386
<b>Max</b>	5053.854	200.55	36015.93	198.892	12.977	15.772	7.871
<b>Average</b>	2635.495	104.583	18781.67	103.718	6.767	8.224	4.104

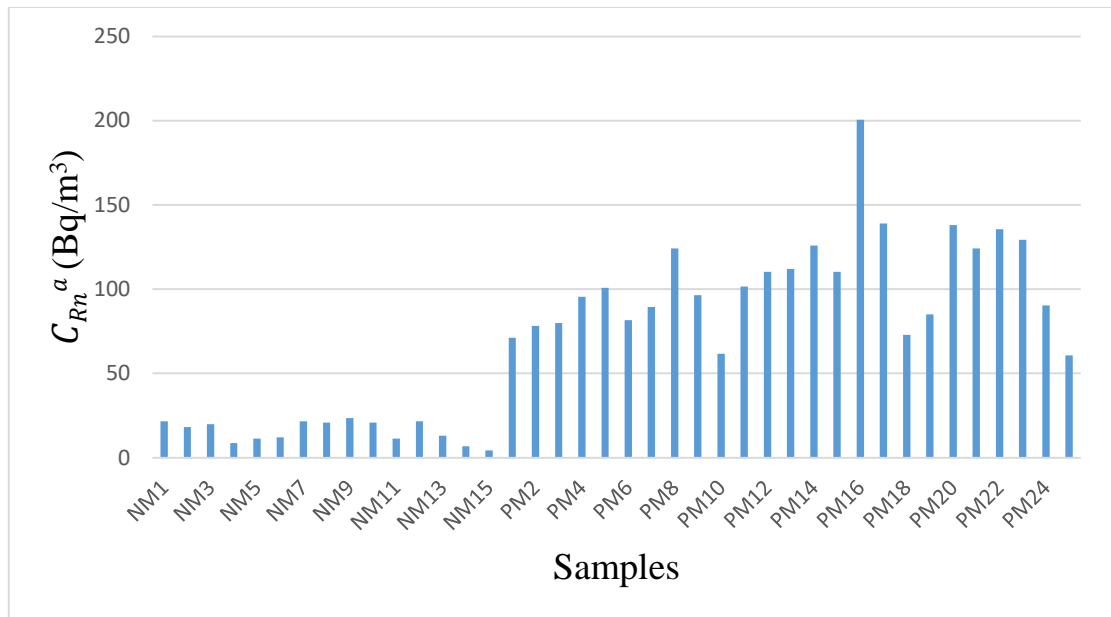


Figure 4.25. Radon concentrations for lung cancer patients and health for the male group.

The lowest activity of radium concentration was found in the sample NM15 (0.280 Bq/kg), while the highest concentration was found in the sample PM16 (12.977 Bq/kg), as in Tables 4.19 and 4.20 and Figure 4.26.

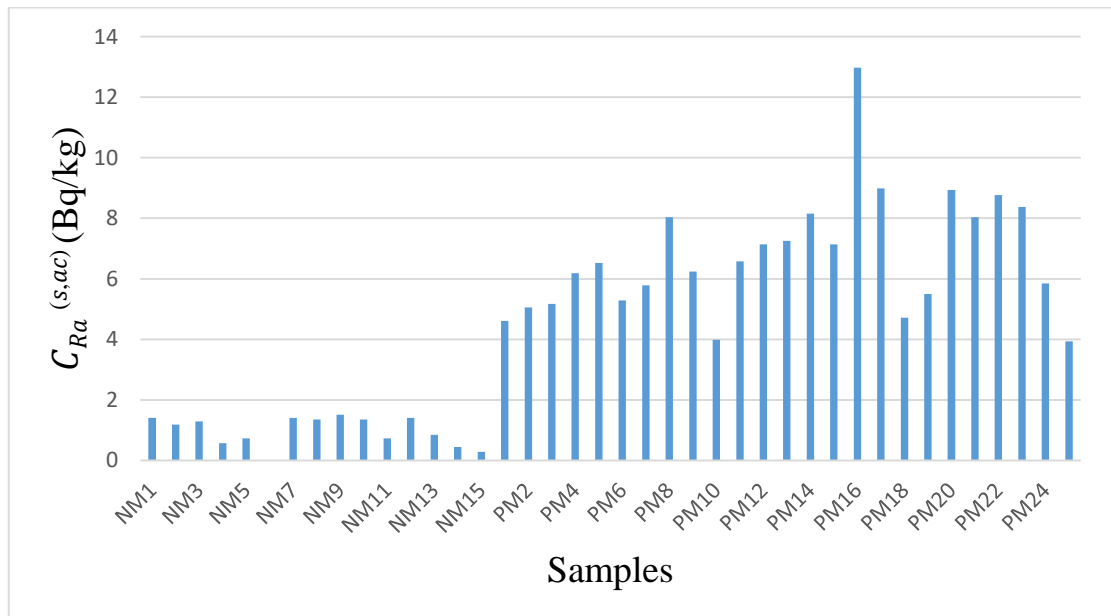


Figure 4.26. The activity concentration of radium for lung cancer patients and health for the male group.

Where the lowest concentration of uranium in the samples was (NM15, 0.340 (ppm), while the highest concentration was (PM16, 15.772 (ppm), and the lowest concentration of the annual effective dose of radon in the samples was (NM15, 0.170 (msv/y). At the same time, the highest concentration was (PM16, 7.871 (msv/y).

There is an increase in the uranium level with the increase in the LC incidence, where there is a high uranium level in the sera of the mining workers compared with the general male population [163]. The increase in the exposure to radiation by the workers explained this. Epidemiological studies of underground miners demonstrate that radon decay product exposures significantly increase lung cancer risk [164, 165].

The average annual effective dose of patients is four times greater than that of healthy people, as in Tables 4.19 and 4.20 and Figures 4.27 and 4.28.

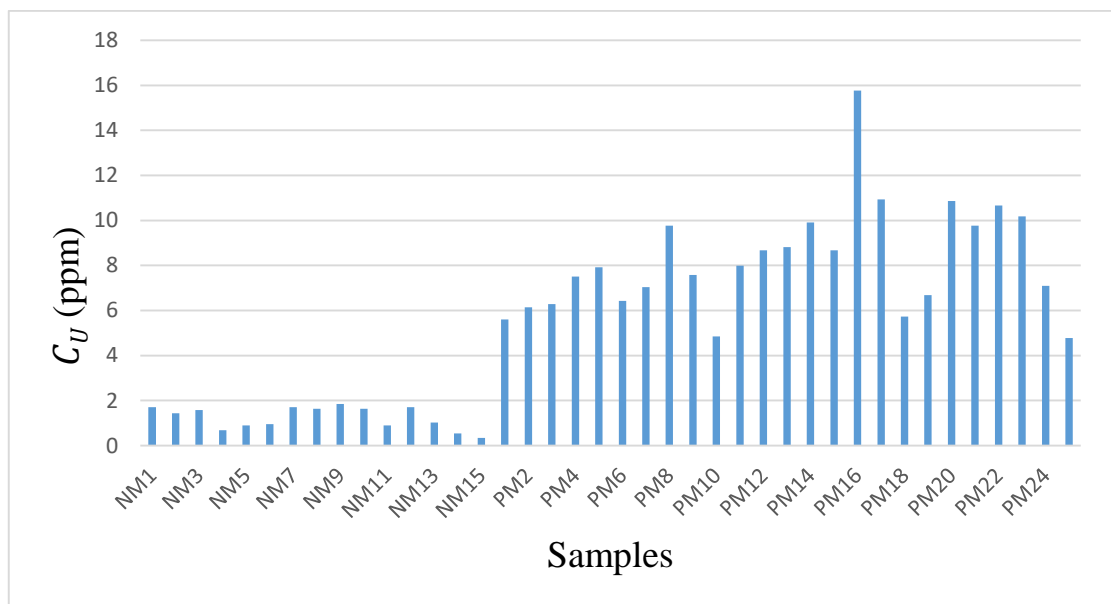


Figure 4.27. Uranium concentration in lung cancer patients and healthy males.

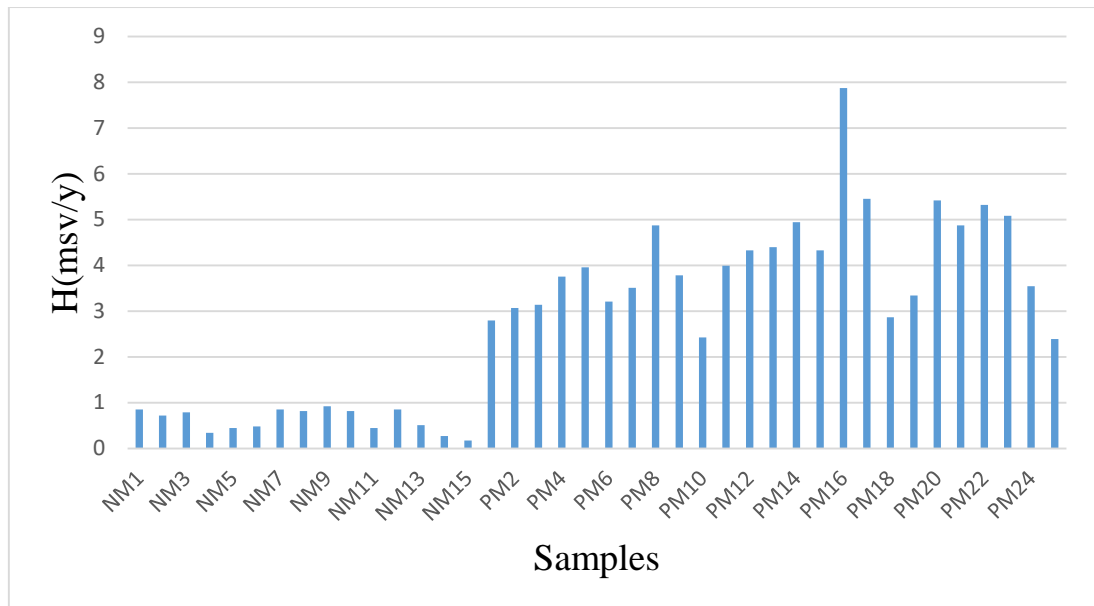


Figure 4.28. The annual effective dose of radon concentration for lung cancer patients and health for the male group.

The average of radon in air space in the healthy female was 17.442 Bq/m<sup>3</sup>, greater than the average of the healthy male, while the average radon in air space concentration in the patient male was the highest (104.583 Bq/m<sup>3</sup>) than the female, as in Table 4.21 and Figure 4.29.

Table 4.21. The average of radon in air space concentration for lung cancer patients and healthy for two groups.

Avg. C <sup>a</sup> R <sub>n</sub> (Bq/m <sup>3</sup> )		
	Females	Males
<b>Average N</b>	17.442	15.728
<b>Average P</b>	85.771	104.583

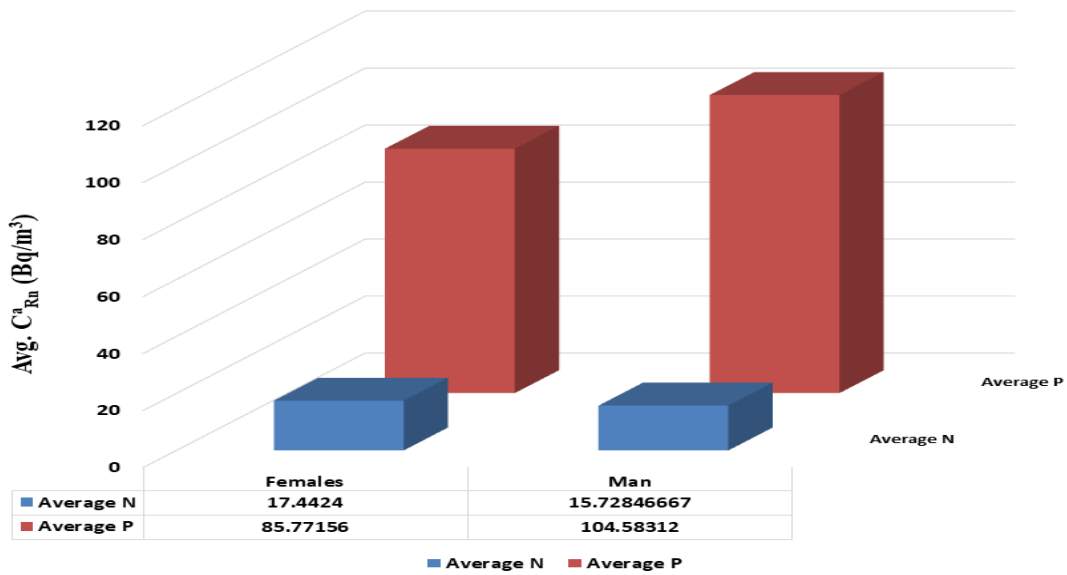


Figure 4.29. The average of radon in air space concentration for lung cancer patients and healthy for two groups.

The average uranium concentration in the healthy female was 1.371 ppm greater than the average of a healthy male, while the highest concentration in the patient male was 8.224 ppm, as in Table 4.22 and Figure 4.30.

Table 4.22. The average uranium concentration for lung cancer patients and healthy for two groups.

Cont. U(ppm)		
	Females	Male
Average N	1.371	1.237
Average P	6.745	8.224

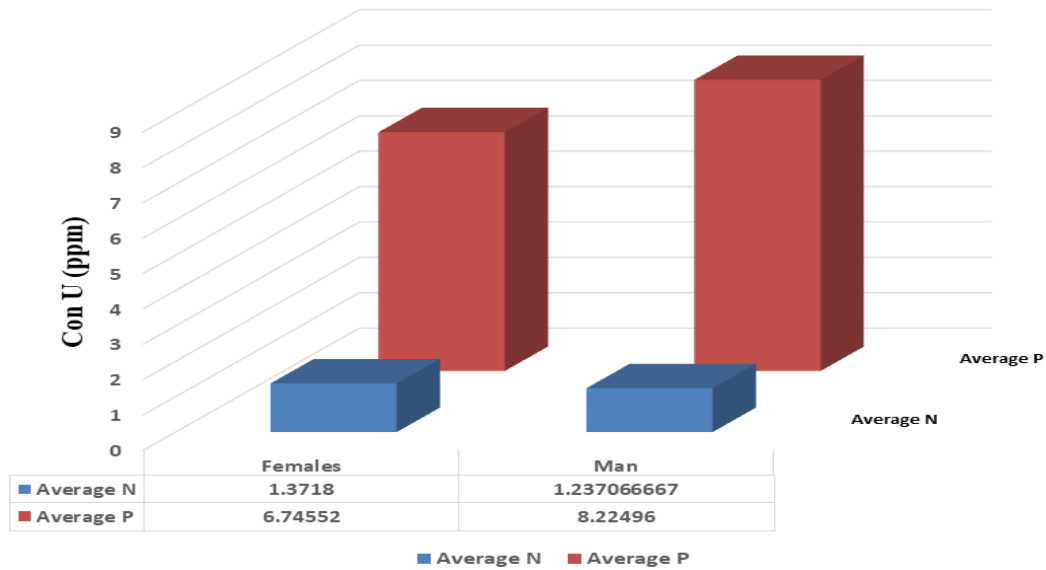


Figure 4.30. The average uranium concentration for lung cancer patients and health for two groups.

In Table 4.23, by comparing our results, we can see that the values are similar to some studies but not to others, which is normal due to differences in the geology of the area of residence, the type of food consumed, the use of nutritional supplements or therapeutic supplements, as well as the nature of people's work, all of which cause changes in element concentrations.

Table 4.23. Comparison between radon and uranium concentrations for blood samples of the present study with the other studies.

No.	Country/region	$^{222}\text{Rn}$ Bq/m <sup>3</sup>	$^{238}\text{U}$ (ppm)	References
1.	Iraq/ Babylon	7.79	-----	[56]
2.	Iraq/ Karbala	64.3	0.10	[158]
3.	Malaysia	570.25	-----	[166]
4.	Iraq/Najaf	8.62-55.37	0.032-0.202	[100]
5.	Iraq/Baghdad	-----	0.07-0.22	[167]
6.	Iraq/Basra	-----	0.965-1.992	[167]
7.	Iraq /Al-Ramadi	-----	0.835-1.174	[167]
8.	UNSCEAR	200	-----	[168]
9.	ICRP	-----	0.115	[169]
10.	Iraq/ Karbala	85.77-104.58	6.745-8.224	Present study

The study's findings generally showed that all of the samples' radon levels were below the 200 Bq/m<sup>3</sup> permissible range specified in ICRP and IAEA publications [166, 170]. Additionally, the results revealed that the blood's uranium level was below the 0.115 ppm permissible limit indicated by (ICRP) [169].

#### 4.3.6 Correlation between trace elements and uranium concentrations.

The average of the four elements (zinc, copper, lead, and cadmium) for patients and healthy people of both types was compared with the Average concentration of uranium. It was noticed that the rate of uranium concentration is higher in female patients compared to healthy females. It was noticed that copper, lead, and cadmium behaves the same, and this shows that the elements are affected by biological and mechanical changes and the same behavior for these elements with uranium. Our results were consistent with several studies [171-173]. As for zinc, it was the opposite of the behavior shown in Table 4.24 and Figure 4.31.

Table 4.24. Average uranium concentrations with minerals for health and patient of female.

Concentration	Code samples	Average
Zn(µg/L)	NF	1588,83
	PF	531,54
Cu(µg/L)	NF	152,45
	PF	176,46
Pb(µg/L)	NF	8,3
	PF	10,28
Cd(µg/L)	NF	21,41
	PF	123,74
U (ppb)	NF	1.371
	PF	6.745

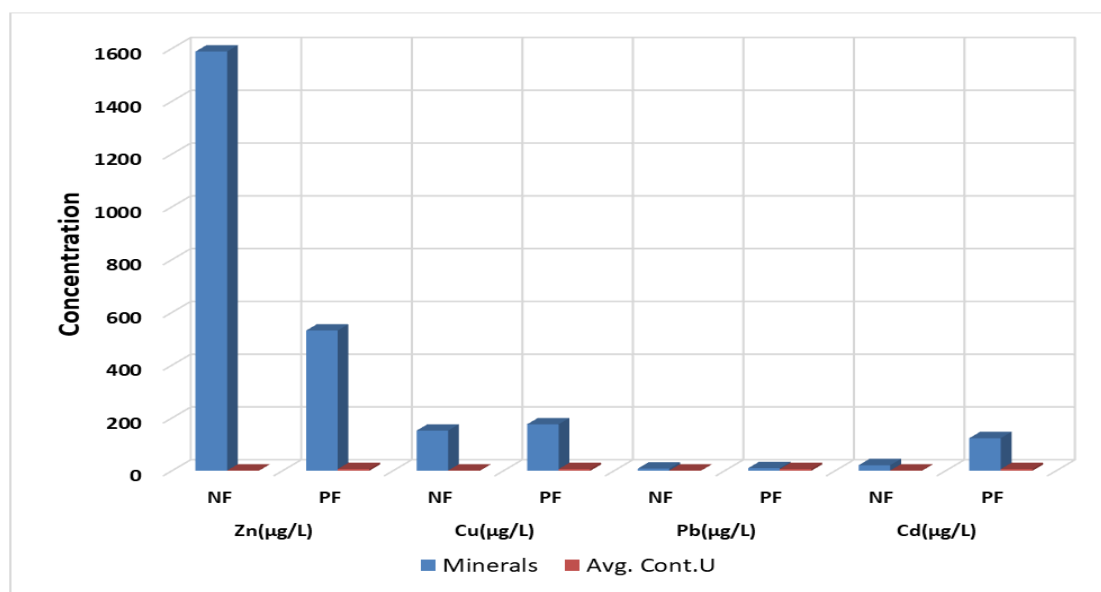


Figure 4.31. Average uranium concentrations with minerals for health and patient of female.

It was noticed that the rate of uranium concentration is higher in male patients compared to healthy males, and we have noticed that copper, lead, and cadmium exhibit the same behavior, and this shows that the elements are affected by biological and mechanical changes where the same behavior for these elements with uranium, as for zinc, it was the opposite of the behavior as seen in the Table 4.26 and Figure 4.32.

Table 4.25: Average uranium concentrations with minerals for health and patient of male.

Concentration	Code	Average
Zn (µg/L)	NM	1247.02
	PM	666.75
Cu(µg/L)	NM	155.61
	PM	218.59
Pb(µg/L)	NM	5.38
	PM	13.4
Cd(µg/L)	NM	14.02
	PM	60.87
U (ppm)	NF	1.237
	PF	8.224



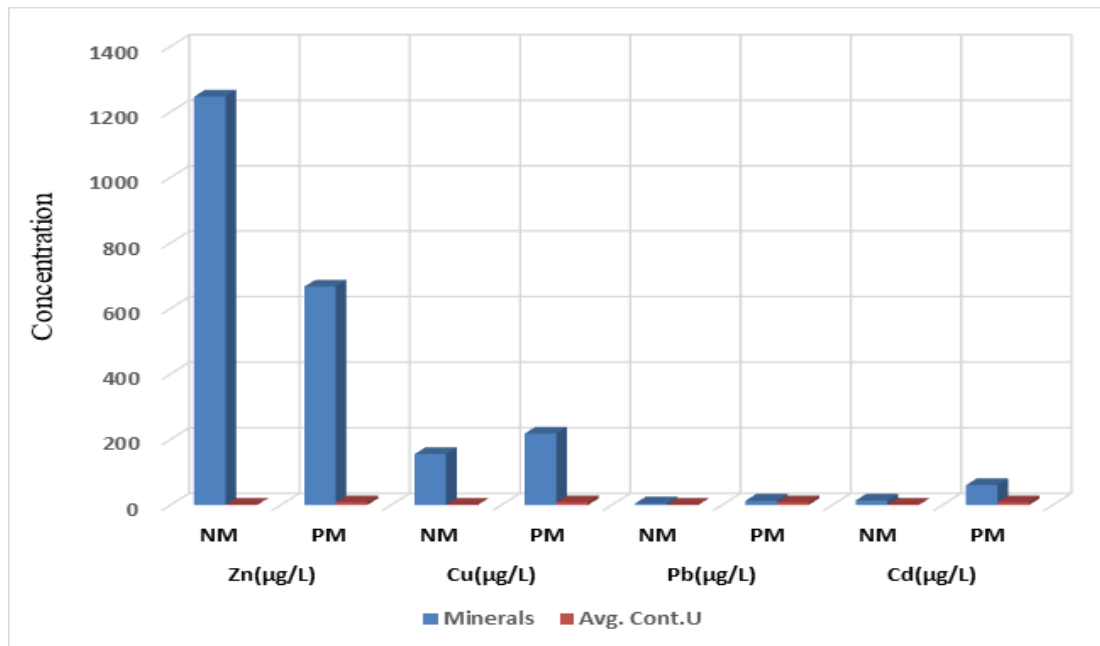


Figure 4.32. Average uranium concentrations with minerals for health and patients of male.

Previous studies reported correlations between essential and non-essential elements such as uranium, thallium, nickel, and aluminum [174, 175]. Despite their concentration within the reference values, these nonessential elements are strongly competitive with essential elements in biochemical processes [174]. A characteristic feature of heavy metals, such as lead, cadmium, uranium, and others, that increases danger is their accumulation and very slow excretion [176]. Therefore, the correlation between these elements with the essential trace elements may be due to the competition for the storage sites and the competition for the excretion routes [177, 178].

***Chapter Five***  
***Conclusions and***  
***Recommendations***



---

---

## Chapter Five Conclusion and Recommendations

### 5.1 Conclusions

The conclusions are described below based on the outcomes from the analysis of LC patients.

1. The prevalence coefficient and relationship to the number of cases, region, and age were studied. It was found that the number of male cases was higher than females.
2. The percentage of change for the studied data was also studied. Unfortunately, it was Positive that any increase in numbers and using the statistical program.
3. The Pearson coefficient has a strong positive relationship and is without statistical significance between the number of infected females and the prevalence factor for males.
4. In the chi-square test, there was no significance among the variables.
5. The  $R_1$ (lipids/proteins) ratio can effectively identify the serum of LC patients from that of healthy people.
6. The secondary architectures of proteins in malignant and normal serum were different, and the relative level of  $\alpha$ -helix was likely to be high. Some ratios can be used as markers to predict LC occurrence.
7. The serum IR spectrum may be effective in identifying LC.
8. The zinc concentration in patients was generally lower than in healthy subjects and for all samples.
9. The Copper, Lead, and Cadmium concentrations in patients were generally high than in healthy subjects and for all samples taken.
10. The findings demonstrated that healthy individuals had lower mean values of radon, radium, and uranium in their samples than LC patients.

11. The annual effective dose of radon for healthy people was lower than that for LC patients.
12. There was a positive relationship between copper, lead, and cadmium, and the high average uranium concentration.
13. There was an Inverse relationship between zinc and the high average uranium concentration.

## **5.2 Recommendations**

1. After examining the patients' conditions, we suggest a suitable building, especially for cancerous diseases.
2. Encouraging the quitting of smoking to reduce the risk of developing LC.
3. The presence of emotional support for patients and considering their psychological condition.
4. It is necessary to avoid carcinogens and hazardous chemicals at work, in addition to adhering to your employer's safety procedures.
5. Educating people with health knowledge of food and exposure to environmental toxins, such as some carcinogenic chemicals or radiation, smoking, and UV rays that cause sunburn.
6. It is necessary to exposure to fresh air and exercise daily.

## **5.3 Future studies**

1. The same physical technique is used to diagnose other diseases, such as pancreas and stomach cancer.
2. Using sputum and urine to replace serum and blood to diagnose LC is essential.
3. Using tissue instead of serum or blood to diagnose LC.
4. Using other physical techniques to diagnose LC





# **References**



## References

1. Suresh, S., Biomechanics and biophysics of cancer cells. *Acta biomaterialia*, 2007. **3**(4): p. 413-438.
2. Nie, S., Y. Xing, and G.J. Kim, and Jonathan W. Simons. *Annual Review of Biomedical Engineering*, 2007. **9**: p. 257-88.
3. Sung, H., et al., Global cancer statistics 2020: GLOBOCAN estimates of incidence and mortality worldwide for 36 cancers in 185 countries. *CA: a cancer journal for clinicians*, 2021. **71**(3): p. 209-249.
4. Lewis, P.D., et al., Evaluation of FTIR spectroscopy as a diagnostic tool for lung cancer using sputum. *BMC cancer*, 2010. **10**(1): p. 1-10.
5. Wang, X., et al., FTIR spectroscopic comparison of serum from lung cancer patients and healthy persons. *Spectrochimica Acta Part A: Molecular and Biomolecular Spectroscopy*, 2014. **122**: p. 193-197.
6. Morgensztern, D., et al., Trends in stage distribution for patients with non-small cell lung cancer: a National Cancer Database survey. *Journal of thoracic oncology*, 2010. **5**(1): p. 29-33.
7. Gunasekaran, S., et al., FTIR spectral study on jaundice blood samples before and after treatment. *Asian Journal of Chemistry*, 2010. **22**(1): p. 51.
8. Hochhegger, B., et al., PET/CT imaging in lung cancer: indications and findings. *Jornal Brasileiro de Pneumologia*, 2015. **41**: p. 264-274.
9. Latimer, K. and T. Mott, Lung cancer: diagnosis, treatment principles, and screening. *American family physician*, 2015. **91**(4): p. 250-256.

10. Frost, J.K., et al., Early lung cancer detection: results of the initial (prevalence) radiologic and cytologic screening in the Johns Hopkins study. *American Review of Respiratory Disease*, 1984. **130**(4): p. 549-554.
11. Beckles, M.A., et al., Initial evaluation of the patient with lung cancer: symptoms, signs, laboratory tests, and paraneoplastic syndromes. *Chest*, 2003. **123**(1): p. 97S-104S.
12. Krech, R.L., et al., Symptoms of lung cancer. *Palliative medicine*, 1992. **6**(4): p. 309-315.
13. Kocak, Z., et al., Challenges in defining radiation pneumonitis in patients with lung cancer. *International Journal of Radiation Oncology\* Biology\* Physics*, 2005. **62**(3): p. 635-638.
14. Travis, W.D., Pathology of lung cancer. *Clinics in chest medicine*, 2002. **23**(1): p. 65-81.
15. Conron, M., et al., Analysis of multidisciplinary lung cancer practice. *Internal medicine journal*, 2007. **37**(1): p. 18-25.
16. Akhtar, N. and J.G. Bansal, Risk factors of Lung Cancer in nonsmoker. *Current problems in cancer*, 2017. **41**(5): p. 328-339.
17. Sonke, J.-J. and J. Belderbos. Adaptive radiotherapy for lung cancer. in *Seminars in radiation oncology*. 2010. Elsevier.
18. Raez, L.E., S. Fein, and E.R. Podack, Lung cancer immunotherapy. *Clinical medicine & research*, 2005. **3**(4): p. 221-228.
19. Cabasag, C.J., et al., Ovarian cancer today and tomorrow: A global assessment by world region and Human Development Index using GLOBOCAN 2020. *International Journal of Cancer*, 2022.

20. Gupta, U.C. and S.C. Gupta, Trace element toxicity relationships to crop production and livestock and human health: implications for management. *Communications in Soil Science and Plant Analysis*, 1998. **29**(11-14): p. 1491-1522.
21. Underwood, E., Trace elements in human and animal nutrition. 2012: Elsevier.
22. Cai, L., et al., Essentiality, toxicology and chelation therapy of zinc and copper. *Current medicinal chemistry*, 2005. **12**(23): p. 2753-2763.
23. Oliver, M., Soil and human health: a review. *European Journal of soil science*, 1997. **48**(4): p. 573-592.
24. Angelova, M., et al., Copper in the human organism. *Trakia journal of sciences*, 2011. **9**(1): p. 88-98.
25. Huster, D., Wilson disease. *Best practice & research Clinical gastroenterology*, 2010. **24**(5): p. 531-539.
26. Yari, H., et al., Copper, Lead, Zinc and Cadmium levels in serum of prostate cancer patients by polarography in Iran. *Journal of Chemical and Pharmaceutical Research*, 2015. **7**(2): p. 403-408.
27. Bishak, Y.K., et al., Mechanisms of cadmium carcinogenicity in the gastrointestinal tract. *Asian Pacific Journal of Cancer Prevention*, 2015. **16**(1): p. 9-21.
28. Nielsen, F.H., Ultratrace elements in nutrition: current knowledge and speculation. *The Journal of Trace Elements in Experimental Medicine: The Official Publication of the International Society for Trace Element Research in Humans*, 1998. **11**(2-3): p. 251-274.

29. Hayat, M.T., et al., Environmental hazards of cadmium: past, present, and future, in *Cadmium toxicity and tolerance in plants*. 2019, Elsevier. p. 163-183.
30. Rattikansukha, C., et al., Health Risk Assessment of Cadmium and Mercury via Seafood Consumption in Coastal Area of Nai Thung, Nakhon Si Thammarat Province, Thailand. *Walailak Journal of Science and Technology (WJST)*, 2021. **18**(10): p. 9244 (11 pages)-9244 (11 pages).
31. Sadhra, S.S., A.D. Wheatley, and H.J. Cross, Dietary exposure to copper in the European Union and its assessment for EU regulatory risk assessment. *Science of the total environment*, 2007. **374**(2-3): p. 223-234.
32. Lead, I.I., *Environmental Health Criteria 165*. International Programme on Chemical Safety, Vol. 38. World Health Organization, 1995: p. 93-99.
33. Atkinson, S., R. Costello, and J. Donohue, Overview of global dietary calcium and magnesium intakes and allowances. *Calcium and Magnesium in Drinking-water*, 2009: p. 17.
34. Abbas Tawil, F., S. Awad Kadhim, and A. Kareem Hashim, Comparing the Cadmium, Zinc, Lead, and Copper Concentrations between Lung Cancer Patients and Healthy Iraqi Individuals. *Iranian Journal of War and Public Health*, 2022. **14**(2): p. 243-248.
35. Council, N.R., *Comparative dosimetry of radon in mines and homes*. 1991.
36. Cortina, D., I. Durán, and J. Llerena, Measurements of indoor radon concentrations in the Santiago de Compostela area. *Journal of environmental radioactivity*, 2008. **99**(10): p. 1583-1588.

37. Neves, L., S. Barbosa, and A. Pereira, Indoor radon periodicities and their physical constraints: a study in the Coimbra region (Central Portugal). *Journal of environmental radioactivity*, 2009. **100**(10): p. 896-904.
38. Abdallah, S.M., et al., Radon measurements in well and spring water in Lebanon. *Radiation measurements*, 2007. **42**(2): p. 298-303.
39. Amiri, V., M. Nakhaei, and R. Lak, Using radon-222 and radium-226 isotopes to deduce the functioning of a coastal aquifer adjacent to a hypersaline lake in NW Iran. *Journal of Asian Earth Sciences*, 2017. **147**: p. 128-147.
40. Belete, G.D. and A.M. Shiferaw, A Review of Studies on the Seasonal Variation of Indoor Radon-222 Concentration. *Oncology Reviews*, 2022: p. 1.
41. Al-Tmemi, M.B.S., Epidemiological Study of Patients with Prostate Cancer in South of Iraq. *University of Thi-Qar Journal of Science*, 2014. **4**(3): p. 72-76.
42. Khoshnaw, N., H.A. Mohammed, and D.A. Abdullah, Patterns of cancer in Kurdistan-results of eight years cancer registration in Sulaymaniyah Province-Kurdistan-Iraq. *Asian Pacific Journal of Cancer Prevention*, 2016. **16**(18): p. 8525-8531.
43. Al-Janabi, A.A.H.S., Z.H. Naseer, and T.A. Hamody, Epidemiological study of cancers in Iraq-Karbala from 2008 to 2015. *International Journal of Medical Research & Health Sciences*, 2017. **6**(1): p. 79-86.
44. Al-Abdin, O.Z. and I.Z. Al-Beeshi, Prostate cancer in the Arab population: an overview. *Saudi Medical Journal*, 2018. **39**(5): p. 453.

45. Nguyen-Nielsen, M., et al., Causes of death in men with prostate cancer: Results from the Danish Prostate Cancer Registry (DAPROCAdata). *Cancer Epidemiology*, 2019. **59**: p. 249-257.
46. Abood, R.A., K.A. Abdahmed, and S.S. Mazyed, Epidemiology of different types of cancers reported in Basra, Iraq. *Sultan Qaboos University Medical Journal*, 2020. **20**(3): p. e295.
47. M-Amen, K., et al., Cancer Statistics in Kurdistan Region of Iraq: A Tale of Two Cities. 2021.
48. Jochems, S.H., et al., Smoking and Risk of Prostate Cancer and Prostate Cancer Death: A Pooled Study. *European Urology*, 2022.
49. Sun, X., et al., Detection of lung cancer tissue by attenuated total reflection–Fourier transform infrared spectroscopy—a pilot study of 60 samples. *Journal of Surgical Research*, 2013. **179**(1): p. 33-38.
50. Ollesch, J., et al., An infrared spectroscopic blood test for non-small cell lung carcinoma and subtyping into pulmonary squamous cell carcinoma or adenocarcinoma. *Biomedical Spectroscopy and Imaging*, 2016. **5**(2): p. 129-144.
51. Cobanoglu, U., et al., Some mineral, trace element and heavy metal concentrations in lung cancer. *Asian Pacific journal of cancer prevention: APJCP*, 2010. **11**(5): p. 1383-1388.
52. Martínez-Peinado, M., et al., Serum zinc and copper concentrations and ratios in cirrhotic patients: correlation with severity index. *Nutricion hospitalaria*, 2018. **35**(3): p. 627-632.

53. Lee, S., H. Jeon, and B. Shim, Prognostic value of ferritin-to-hemoglobin ratio in patients with advanced non-small-cell lung cancer. *Journal of Cancer*, 2019. **10(7)**: p. 1717.
54. Zabłocka-Słowińska, K., et al., Serum and whole blood Cu and Zn status in predicting mortality in lung cancer patients. *Nutrients*, 2020. **13(1)**: p. 60.
55. Atiyah Essia, I., Z. Mousa Hamza, and S. Alhous, Comparison of Trace Element Concentrations in Women with Breast Cancer and Lung Cancer and Healthy Women. *Iranian Journal of War and Public Health*, 2022. **14(2)**: p. 197-201.
56. Showard, A.F. and M.S. Aswood. Measuring of Alpha particles in Blood samples of Leukemia patients in Babylon governorate, Iraq. in *Journal of physics: conference series*. 2019. IOP Publishing.
57. Shaker, F.A. and E.K. Alsabari, Measurements of radium and uranium concentrations in blood samples of lung cancer patients in Iraq. *Journal of Kufa-Physics*, 2020. **12(02)**.
58. Naji, T.F. and S.O. Hassoon. Measuring of Radon Gas Concentrations in serum samples of Lung cancer patients in Babylon governorate, Iraq. in *Journal of Physics: Conference Series*. 2021. IOP Publishing.
59. Ahmed, R.S., et al., Evaluation of uranium concentration in the blood breast cancer women with CR-39 detector. *Applied Radiation and Isotopes*, 2022. **182**: p. 110120.
60. Eroschenko, V.P. and M.S. Di Fiore, *DiFiore's atlas of histology with functional correlations*. 2013: Lippincott Williams & Wilkins.

61. Patil, A., M. Patil, and G. Birajdar, White blood cells image classification using deep learning with canonical correlation analysis. *Irbm*, 2021. **42**(5): p. 378-389.
62. Mehler, R.E., *How the circulatory system works*. 2014: John Wiley & Sons.
63. Smith, D.L. and B. Fernhall, *Advanced cardiovascular exercise physiology*. 2022: Human Kinetics.
64. Ranota, T.K., *Automation through Deep-Learning to Quantify Ventilation Defects in Lungs from High-Resolution Isotropic Hyperpolarized  $^{129}\text{Xe}$  Magnetic Resonance Imaging*. 2022.
65. Hahn, W., et al., Rules governing the creation of human tumor cells. *European Journal of Cancer*, 2001(37): p. S369.
66. Stecklein, S., et al., Breast cancer invasion and metastasis, in *Experimental Metastasis: Modeling and Analysis*. 2013, Springer. p. 27-56.
67. Bray, F., et al., Global estimates of cancer prevalence for 27 sites in the adult population in 2008. *International journal of cancer*, 2013. **132**(5): p. 1133-1145.
68. Stanton, R.E. and M.D. Newton, Normal vibrational modes of buckminsterfullerene. *The Journal of Physical Chemistry*, 1988. **92**(8): p. 2141-2145.
69. Salman, A., Beer-Sheva. 2003, Ben-Gurion University of the Negev.
70. OT\_, I.Y. and G. Fischer, LINEWIDTH OF JOSEPHSON OSCILLATIONS. *iiii!*: p. 343.
71. Lynden-Bell, D., SAO/NASA ADS (null) Abstract Service. *THE OBSERVATORY*, 1981. **101**(1040).



72. Piras, F.M., A. Rossi, and N.D. Spencer, Growth of tribological films: in situ characterization based on attenuated total reflection infrared spectroscopy. *Langmuir*, 2002. **18**(17): p. 6606-6613.
73. Urban, M.W., Surface and interface vibrational spectroscopy: relevance to adhesion. *Journal of adhesion science and technology*, 1993. **7**(1): p. 1-47.
74. Suci, P.A., J.D. Vraney, and M.W. Mittelman, Investigation of interactions between antimicrobial agents and bacterial biofilms using attenuated total reflection Fourier transform infrared spectroscopy. *Biomaterials*, 1998. **19**(4): p. 327-339.
75. Dumas, P., G.D. Sockalingum, and J. Sule-Suso, Adding synchrotron radiation to infrared microspectroscopy: what's new in biomedical applications? *Trends in biotechnology*, 2007. **25**(1): p. 40-44.
76. Baker, M.J., et al., Using Fourier transform IR spectroscopy to analyze biological materials. *Nature protocols*, 2014. **9**(8): p. 1771-1791.
77. Anand, P., et al., Cancer is a preventable disease that requires major lifestyle changes. *Pharmaceutical research*, 2008. **25**(9): p. 2097-2116.
78. Mäkinen, H., Improvement of the atomic absorption spectrometry method: Determination of calcium and magnesium from human urine. 2012.
79. Seruca, C.O.R. and C. Caldas, Genetic screening for hereditary diffuse gastric cancer. *Expert review of molecular diagnostics*, 2003. **3**(2): p. 201-215.
80. Ismail, M., et al., Alpha-decay of deformed superheavy nuclei as a probe of shell closures. *Nuclear Physics A*, 2017. **958**: p. 202-210.
81. Kuo, J., Practical aspects of hyaluronan based medical products. 2005: CRC Press.

82. Hon, Z., J. Österreicher, and L. Navrátil, Depleted uranium and its effects on humans. *Sustainability*, 2015. **7**(4): p. 4063-4077.
83. eep, K. and M. Rohit, Uranium concentration in ground water samples belonging to some areas of Western Haryana, India using fission track registration technique. *Journal of Public Health and Epidemiology*, 2011. **3**(8): p. 352-357.
84. Parent, R.A., *Comparative biology of the normal lung*. 2015: Academic Press.
85. Alebadi, S.N., S.H. Mohsen, and H.A. Abdulridha, A practical study to calculate alpha emission in human teeth through CR-39 track detector from Diyala, Iraq. *Drug Invention Today*, 2019. **11**(12): p. 1-5.
86. Magill, J. and J. Galy, *Radioactivity-Radionuclides-Radiation: Including the Universal Nuclide Chart on CD-ROM*. 2005: Springer.
87. Knoll, G.F., *Radiation detection and measurement*. 2010: John Wiley & Sons.
88. Maher, K. and W. Contributors, *Basic physics of nuclear medicine*. 2006: Libronomia Company.
89. Abubakar, A., et al., Assessment of indoor ionizing radiation profile in radiology department FMC Asaba Delta State Nigeria. *Internafional Organizafion of Scienfific Research (IOSR) Journal of Dental and Medical Sciences*, 16 (1): 98, 2017. **101**.
90. Fleischer, R., P. Price, and R. Walker, *Solid-state track detectors: applications to nuclear science and geophysics*. *Annual Review of Nuclear Science*, 1965. **15**(1): p. 1-28.

91. Algrifi, M.A. and T.M. Salman, Measurements of boron concentration from rivers in northern Basrah Governorate using SSNTDs. *Water Supply*, 2022. **22**(4): p. 4584-4593.
92. Back, A.R., E2/M1 ratio of the N to Delta transition in a modified Skyrme model. 1997: University of Kentucky.
93. Hamed, N., Measurement of radon concentration in soil at North Gaza. 2005.
94. Al-Baidhani, M.A., Determination of the radioactivity in soil and water in Baghdad, Karbala and Basrah samples. Sc Thesis, 2006.
95. Al-Nuzal, S.M., Environmental impact of radionuclides and inorganic chemicals from Al-Qaim fertilizers complex, Iraq. *Iraqi Bulletin of Geology and Mining*, 2017(7): p. 93-111.
96. Amis Jr, E.S., et al., American College of Radiology white paper on radiation dose in medicine. *Journal of the american college of radiology*, 2007. **4**(5): p. 272-284.
97. Salih, N.F., M.S. Jaafar, and A.A. Battawy, Assessment the Effects of Alpha Particles on Women's Urine using CR-39 NTDs. *Assessment*, 2014. **6**(12).
98. Dowsett, D., *Radiological sciences dictionary: keywords, names and definitions*. 2009: CRC Press.
99. Kadhim, S.A., et al. Study of the difference between uranium concentrations in blood samples of healthy, newly infected and women who took chemotherapy in Iraq, Najaf. in *AIP Conference Proceedings*. 2022. AIP Publishing LLC.
100. Abdulwahid, T.A., et al., Assessment of concentrations of alpha emitters in cancer patients blood samples. *Sylwan*, 2020. **164**(3): p. 154-164.

101. Friis, N. and P. Myers-Keith, Biosorption of uranium and lead by *Streptomyces longwoodensis*. *Biotechnology and Bioengineering*, 1986. **28**(1): p. 21-28.
102. Bulgakova, O., et al., miR-19 in blood plasma reflects lung cancer occurrence but is not specifically associated with radon exposure. *Oncology Letters*, 2018. **15**(6): p. 8816-8824.
103. Nazaroff, W., A.J. Gadgil, and C.J. Weschler, Critique of the use of deposition velocity in modeling indoor air quality. *ASTM Special Technical Publication*, 1993. **1205**: p. 81-81.
104. Durrani, S.A. and R. Ilic, *Radon Measurements By Etched Track Detectors- Applications In Radiation Protection, Earth Sciences*. 1997: World Scientific.
105. Gingrich, J.E., Radon as a geochemical exploration tool. *Journal of Geochemical Exploration*, 1984. **21**(1-3): p. 19-39.
106. Friberg, L., Air pollution and cancer-risk assessment methodology and epidemiological evidence: A preface. *Environmental Health Perspectives*, 1978. **22**: p. 43-43.
107. Duma, N., R. Santana-Davila, and J.R. Molina. Non-small cell lung cancer: epidemiology, screening, diagnosis, and treatment. in *Mayo Clinic Proceedings*. 2019. Elsevier.
108. Villanueva, J.-L.G., *Radon concentrations in air, soil, and water in a granitic area: instrumental development and measurements*. 2008, Universidad de Valladolid.
109. Appleton, J., *Radon: sources, health risks, and hazard mapping*. *Ambio*, 2007: p. 85-89.

110. Hamzah, Z.S., A.K. Hashim, and A.A. Abojassim, Assessment of Annual Effective Dose and Excess Lifetime Cancer Risk in Grain Samples Collected from Karbala Governorate, Iraq. *Iranian Journal of Science and Technology, Transactions A: Science*, 2022: p. 1-10.
111. Bala, J., Contribution of SPSS in Social Sciences Research. *International Journal of Advanced Research in Computer Science*, 2016. **7**(6).
112. Zabora, J., et al., The prevalence of psychological distress by cancer site. *Psycho-Oncology: Journal of the Psychological, Social and Behavioral Dimensions of Cancer*, 2001. **10**(1): p. 19-28.
113. Vickers, A.J., The use of percentage change from baseline as an outcome in a controlled trial is statistically inefficient: a simulation study. *BMC medical research methodology*, 2001. **1**(1): p. 1-4.
114. Akram, M.U., et al., Tumor micro-environment sensitive release of doxorubicin through chitosan based polymeric nanoparticles: An in-vitro study. *Chemosphere*, 2023. **313**: p. 137332.
115. Shi, Y., et al., Electrospinning of artemisinin-loaded core-shell fibers for inhibiting drug re-crystallization. *Journal of Biomaterials Science, Polymer Edition*, 2013. **24**(5): p. 551-564.
116. Huo, P., et al., Electrospun nanofibers of polycaprolactone/collagen as a sustained-release drug delivery system for artemisinin. *Pharmaceutics*, 2021. **13**(8): p. 1228.
117. Bel'skaya, L.V., E.A. Sarf, and D.V. Solomatin, Application of FTIR Spectroscopy for Quantitative Analysis of Blood Serum: A Preliminary Study. *Diagnostics (Basel)*, 2021. **11**(12).

118. Baltacıoğlu, E., et al., Protein carbonyl levels in serum and gingival crevicular fluid in patients with chronic periodontitis. *Archives of oral biology*, 2008. **53**(8): p. 716-722.
119. Leeman, M., et al., Proteins and antibodies in serum, plasma, and whole blood-size characterization using asymmetrical flow field-flow fractionation (AF4). *Anal Bioanal Chem*, 2018. **410**(20): p. 4867-4873.
120. Yano, K., et al., Evaluation of glycogen level in human lung carcinoma tissues by an infrared spectroscopic method. *Cancer letters*, 1996. **110**(1-2): p. 29-34.
121. Tissot, C., et al., Circulating free DNA concentration is an independent prognostic biomarker in lung cancer. *European Respiratory Journal*, 2015. **46**(6): p. 1773-1780.
122. Yano, K., et al., Direct measurement of human lung cancerous and noncancerous tissues by Fourier transform infrared microscopy: can an infrared microscope be used as a clinical tool? *Analytical biochemistry*, 2000. **287**(2): p. 218-225.
123. Rygula, A., et al., Raman spectroscopy of proteins: a review. *Journal of Raman Spectroscopy*, 2013. **44**(8): p. 1061-1076.
124. Pires, F., et al., Effect of blue light irradiation on the stability of phospholipid molecules in the presence of epigallocatechin-3-gallate. *Colloids and Surfaces B: Biointerfaces*, 2019. **177**: p. 50-57.
125. Shao, J., et al., Fourier transform Raman and Fourier transform infrared spectroscopy studies of silk fibroin. *Journal of applied polymer science*, 2005. **96**(6): p. 1999-2004.

126. Litvinov, R.I., et al., The  $\alpha$ -helix to  $\beta$ -sheet transition in stretched and compressed hydrated fibrin clots. *Biophysical journal*, 2012. **103**(5): p. 1020-1027.
127. Lee, Y.H., et al., Serum concentrations of trace elements zinc, copper, selenium, and manganese in critically ill patients. *Biological trace element research*, 2019. **188**(2): p. 316-325.
128. Lossow, K., M. Schwarz, and A.P. Kipp, Are trace element concentrations suitable biomarkers for the diagnosis of cancer? *Redox Biology*, 2021. **42**: p. 101900.
129. Muñiz, C.S., et al., Reference values for trace and ultratrace elements in human serum determined by double-focusing ICP-MS. *Biological trace element research*, 2001. **82**(1): p. 259-272.
130. Zhang, X. and Q. Yang, Association between serum copper levels and lung cancer risk: A meta-analysis. *Journal of International Medical Research*, 2018. **46**(12): p. 4863-4873.
131. Wang, Y., et al., Association between serum zinc levels and lung cancer: a meta-analysis of observational studies. *World journal of surgical oncology*, 2019. **17**(1): p. 1-8.
132. Zabłocka-Słowińska, K., et al., Serum and whole blood Zn, Cu and Mn profiles and their relation to redox status in lung cancer patients. *Journal of Trace Elements in Medicine and Biology*, 2018. **45**: p. 78-84.
133. Wang, Y., et al., Association between serum zinc levels and lung cancer: a meta-analysis of observational studies. *World Journal of Surgical Oncology*, 2019. **17**(1): p. 78.

134. Schwartz, M.K., Role of trace elements in cancer. *Cancer research*, 1975. **35**(11\_Part\_2): p. 3481-3487.
135. Aguirre, J.D. and V.C. Culotta, Battles with iron: manganese in oxidative stress protection. *Journal of Biological Chemistry*, 2012. **287**(17): p. 13541-13548.
136. Grattan, B.J. and H.C. Freake, Zinc and cancer: implications for LIV-1 in breast cancer. *Nutrients*, 2012. **4**(7): p. 648-675.
137. Gómez, N., et al., Zinc: What is your role in lung cancer. *Nutr Defic*, 2016: p. 47-53.
138. Naji, T.F. and S.O. Hassoon. Assessment of levels lead, cadmium and copper in serum of patients with lung cancer compared with healthy peoples in Babil government. in *AIP Conference Proceedings*. 2022. AIP Publishing LLC.
139. Boffetta, P., E. Merler, and H. Vainio, Carcinogenicity of mercury and mercury compounds. *Scand J Work Environ Health*, 1993. **19**(1): p. 1-7.
140. Verougstraete, V., D. Lison, and P. Hotz, Cadmium, lung and prostate cancer: a systematic review of recent epidemiological data. *Journal of Toxicology and Environmental Health, Part B*, 2003. **6**(3): p. 227-256.
141. Adams, S.V., M.N. Passarelli, and P.A. Newcomb, Cadmium exposure and cancer mortality in the Third National Health and Nutrition Examination Survey cohort. *Occupational and environmental medicine*, 2012. **69**(2): p. 153-156.
142. Sorahan, T. and N. Esmen, Lung cancer mortality in UK nickel-cadmium battery workers, 1947–2000. *Occupational and environmental medicine*, 2004. **61**(2): p. 108-116.



143. Beveridge, R., et al., Lung cancer risk associated with occupational exposure to nickel, chromium VI, and cadmium in two population-based case-control studies in Montreal. *American journal of industrial medicine*, 2010. **53**(5): p. 476-485.
144. Lener, M.R., et al., Blood cadmium levels as a marker for early lung cancer detection. *Journal of Trace Elements in Medicine and Biology*, 2021. **64**: p. 126682.
145. Xie, S. and Y. Chen, Analysis of 64 cases of lung cancer with trace elements copper and zinc. *Shanxi Med J*, 2000. **29**(2): p. 83-4.
146. Ying, Z. and X. Li, Relationship of serum trace elements to lung cancer. *Studies of Trace Elements and Health*, 2000. **17**(3): p. 15-17.
147. REN, Q., Significance of determination of serum zinc, copper and copper/zinc ratio on evaluating diagnosis, therapeutic effect, and prognosis of lung cancer. *Guangdong Weiliang Yuansu Kexue*, 2000. **7**: p. 19-22.
148. Jin, Z., L. Qian, and G. Dong, Measurement and analysis of serum copper, zinc and magnesium in patients with lung cancer and gastric cancer. *Shaanxi Med J*, 2001. **30**(3): p. 165-166.
149. Zowczak, M., et al., Oxidase activity of ceruloplasmin and concentrations of copper and zinc in serum of cancer patients. *Journal of trace elements in medicine and biology*, 2001. **15**(2-3): p. 193-196.
150. Chen, H.-F., et al., A meta-analysis of association between serum iron levels and lung cancer risk. *Cellular and Molecular Biology*, 2018. **64**(13): p. 33-37.
151. Jin, Y., et al., Combined effects of serum trace metals and polymorphisms of CYP1A1 or GSTM1 on non-small cell lung cancer: A hospital based case-control study in China. *Cancer epidemiology*, 2011. **35**(2): p. 182-187.

152. Alshebly, S.A.K., et al. Serum levels of lead, cadmium and silver in patients with breast cancer compared with healthy females in Iraq. in AIP Conference Proceedings. 2019. AIP Publishing LLC.
153. Wu, H.-D.I., et al., Differentiation of serum levels of trace elements in normal and malignant breast patients. *Biological trace element research*, 2006. **113**(1): p. 9-18.
154. Emre, O., et al., Plasma concentrations of some trace element and heavy metals in patients with metastatic colon cancer. *Journal of cancer therapy*, 2013. **4**(06): p. 1085.
155. DEMİR, D.Ç., Determining the Levels of Some Trace Elements and Heavy Metals (Cu, Mn, Mg, Fe, Zn, CO, Pb and CD) in the Cancers of Lip and Oral Cavity. 2021.
156. Mahmood, M.H., et al., Multivariate Investigation of Toxic and Essential Metals in the Serum from Various Types and Stages of Colorectal Cancer Patients. *Biological Trace Element Research*, 2022. **200**(1): p. 31-48.
157. Marouf, B., Association between serum heavy metals level and cancer incidence in darbandikhan and Kalar Area, Kurdistan Region, Iraq. *Nigerian journal of clinical practice*, 2018. **21**(6): p. 766-771.
158. Mohsen, A.A.H. and A.A. Abojassim, Determination of alpha particles levels in blood samples of cancer patients at Karbala Governorate, Iraq. *Iranian Journal of Medical Physics*, 2019. **16**(1): p. 41-47.
159. Naji, T.F., et al., Measurement of Radon Gas Concentrations in Blood of Cancer Patients Using Solid State Nuclear Track Detectors (CR-39). *International Journal of Health Sciences, (III)*: p. 8367-8372.

160. Travis, L.B., et al., Lung cancer following chemotherapy and radiotherapy for Hodgkin's disease. *Journal of the National Cancer Institute*, 2002. **94**(3): p. 182-192.
161. McCunney, R.J. and J. Li, Radiation risks in lung cancer screening programs. *Chest*, 2014. **145**(3): p. 618-624.
162. Rubino, C., et al., Radiation dose, chemotherapy and risk of lung cancer after breast cancer treatment. *Breast cancer research and treatment*, 2002. **75**(1): p. 15-24.
163. Zablotska, L.B., R.S.D. Lane, and K. Randhawa, Association between exposures to radon and  $\gamma$ -ray radiation and histologic type of lung cancer in Eldorado uranium mining and milling workers from Canada. *Cancer*, 2022. **128**(17): p. 3204-3216.
164. Al-Zoughool, M. and D. Krewski, Health effects of radon: a review of the literature. *International journal of radiation biology*, 2009. **85**(1): p. 57-69.
165. Frank, L., E. Christodoulou, and E.A. Kazerooni. Radiation risk of lung cancer screening. in *Seminars in respiratory and critical care medicine*. 2013. Thieme Medical Publishers.
166. Salih, N.F., Z.M. Jafri, and M.S. Aswood, Measurement of radon concentration in blood and urine samples collected from female cancer patients using RAD7. *Journal of Radiation research and applied sciences*, 2016. **9**(3): p. 332-336.
167. Hassan, S., Determination of Uranium concentration in human blood samples in some governorate of Iraq by using CR-39 track detector. M. Phy. Thesis, Al-Nahrain University, Iraq, 2006.

168. Salih, N.F., et al., The Effects of Alpha Emitters on Powder Blood for Women's Infertility in Kurdistan–Iraq. *International Journal of Scientific and Research Publications*, 2013. **57**.
169. Hassan, S., Determination of uranium concentration in human blood in some Governorates of Iraq. Sc. Al-Nahrain University, 2006.
170. Salih, N., Impact of Alpha Emitters on Uterus. Blood, Urine and Hormones of Infertile Woman of Iraqi Kurdistan (Doctoral dissertation, Universiti Sains Malaysia), 2014.
171. Lar, U.A., Trace elements and health: an environmental risk in Nigeria. *Earth Science*, 2013. **2**(3): p. 66-72.
172. Jones, R.L., Soil uranium, basement radon and lung cancer in Illinois, USA. *Environmental Geochemistry and Health*, 1995. **17**(1): p. 21-24.
173. Ahmed, R.S. and R.S. Mohammed, Assessment of uranium concentration in blood of Iraqi females diagnosed with breast cancer. *Radiation and Environmental Biophysics*, 2021. **60**(1): p. 193-201.
174. Zeneli, L., A. Sekovanić, and N. Daci, Chronic exposure to aluminum, nickel, thallium and uranium and their relationship with essential elements in human whole blood and blood serum. *Journal of Environmental Science and Health, Part A*, 2015. **50**(6): p. 540-546.
175. Xu, Y., et al., Association between urinary metals levels and metabolic phenotypes in overweight and obese individuals. *Chemosphere*, 2020. **254**: p. 126763.
176. Husainov, D.R., et al., Modifying action of heavy metal salts on anti-inflammatory aspirin action. *Health*, 2010. **2**(6): p. 630-633.

177. Harduin, J., P. Royer, and J. Piechowski, Uptake and urinary excretion of uranium after oral administration in man. *Radiation protection dosimetry*, 1994. **53**(1-4): p. 245-248.
178. Ogawa, K., et al., Decreasing undesirable absorbed radiation to the intestine after administration of radium-223 dichloride for treatment of bone metastases. *Scientific Reports*, 2020. **10**(1): p. 1-8.

## الخلاصة:

يعد سرطان الرئة من أخطر أنواع السرطانات في العالم. يساهم التشخيص المبكر للمرض في تحسين العلاج. ترتبط العديد من العوامل الوراثية والبيئية والمهنية بحدوث هذا المرض. تهدف الدراسة الحالية إلى استخدام البيانات السريرية لمرضى سرطان الرئة جنبًا إلى جنب مع المعايير الطيفية والمعايير الكيميائية الحيوية للاستخدام المحتمل كمؤشرات حيوية تشخيصية لمرض سرطان الرئة. تتكون الدراسة الحالية من تحليل إحصائي وتجارب عملية على مرضى سرطان الرئة. تم جمع التقارير الطبية للمريض والأمصال للتحليل الفيزيائي والكيميائي باستخدام تقنيات التحليل الطيفي المختلفة. شارك في الدراسة مائة وسبعون مريضاً بسرطان الرئة و90 من الأصحاء. تم تحليل الأمصال المنفصلة من جميع العينات باستخدام تقنيات التحليل الطيفي المختلفة، بما في ذلك التحليل الطيفي للأشعة تحت الحمراء لتحويل فورييه (ATR-FTIR)، والتحليل الطيفي للامتصاص الذري (AAS)، وكاشف المسار النووي للحالة الصلبة (SSNTD). أظهرت نتائج الدراسة الإحصائية أن أعلى نسبة انتشار لسرطان الرئة سجلت في منطقة الهند بنسبة 66.16% وأدنى قيمة في منطقة الخيرات عند 16.04%. أعلى القيم للنسب المئوية لجميع الحالات كانت في وسط المدينة (51.3%) والأدنى في منطقة الحسينية (13.1%)، وارتفع عدد مرضى سرطان الرئة إلى 298، بمعدل 44.04 حالة لكل 100,000 نسمة، مما يدل على خطورة حالة سرطان الرئة في مدينة كربلاء. أظهرت تحليلات FTIR للمصل أن قمم امتصاص مرضى سرطان الرئة أكبر من قمم امتصاص الأشخاص الأصحاء. بالإضافة إلى ذلك، وجد أن بعض المجموعات الوظيفية فقدت من طيف المرضى، بالإضافة إلى تحولات في أطياف المرضى أكثر من أطياف الأشخاص الأصحاء، والتي يمكن استخدامها في التشخيص المبكر للأمراض. أظهرت نتائج التحليل الطيفي لـ AAS وجود زنك مصل أعلى من الإناث الأصحاء (1247.02 جزء في البليون) وأدنى مستوى في مجموعة الإناث من المرضى (531.54 جزء في البليون). كان النحاس في الدم أعلى في مجموعة الذكور المريض (218.59 جزء في البليون) والأدنى في مجموعة الإناث الأصحاء (152.45 جزء في البليون). أعلى مستويات الرصاص في المرضى الذكور (13.40 جزء في البليون) والأدنى عند الذكور الأصحاء (5.38 جزء في البليون). كان مصل الكاديوم هو الأعلى في المرضى الإناث (123.74 جزء في البليون) وأقل قيمة مسجلة في الذكور الأصحاء (14.02 جزء في البليون). أفادت نتائج تقنية SSNTD أن الإشعاع الذي تم الحصول عليه من غاز الرادون في العينات كان أعلى في مرضى سرطان الرئة منه في الضوابط.

كانت مستويات اليورانيوم والراديوم والرادون المحسوبة في مرضى سرطان الرئة أعلى منها في المجموعة الضابطة. من نتائج المعلمات المقاسة والبيانات السريرية، يمكن استنتاج أن الطرق الطيفية والتغيرات الكيميائية الحيوية في المصل قد تشخص سرطان الرئة.



جامعة كربلاء  
كلية العلوم  
قسم الفيزياء

## الفحص الإشعاعي والسمي للعينات البيولوجية لمرضى سرطان الرئة

رسالة

مقدمة إلى مجلس كلية العلوم في جامعة كربلاء وهي جزء من متطلبات نيل درجة الدكتوراه في الفلسفة  
في علوم الفيزياء  
من قبل الطالبة  
فرقان عباس علوان

بإشراف

أ.د. عبد الستار كريم هاشم

أ.د. شيماء عواد كاظم